

**Temperature reconstructions for the Eastern Indian  
Ocean based on organic-geochemical proxies**

**(U<sup>K'</sup><sub>37</sub> and TEX<sub>86</sub>)**

**Dissertation**

Zur Erlangung des Doktorgrades  
der Naturwissenschaften  
-Dr.rer.nat.-

Am Fachbereich Geowissenschaften  
der Universität Bremen

Vorgelegt von

**Wenwen Chen**

Bremen, December 2015

Gutachter:

Prof. Dr. Gesine Mollenhauer

Prof. Dr. Heiko Pälike



## Erklärung / Declaration

Name: Wenwen Chen

Adresse: Room 501, Unit 3, Building 18, No.618 Huishui Road, Donglitaoyuan  
Licang District, Qingdao, Shandong Province, China

Hiermit versichere ich, das ich

1. die Arbeit ohne unerlaubte fremde Hilfe angefertigt habe,
2. keine anderen als die mir von mir angegebenen Quellen  
und Hilfsmittel benutzt habe und
3. die den benutzten Werken wörtlich oder inhaltlich entnommenen Stellen  
als solche kenntlich gemacht habe.

Bremen, den 11. March 2016

---

Wenwen Chen



**Tag des öffentlichen Promotionskolloquiums:**

11. March 2016

**Mitglieder der Kommission:**

**Gutachter der Dissertation**

Prof. Dr. Gesine Mollenhauer

Prof. Dr. Heiko Pälke

**Prüfer**

Prof. Gerhard Bohrmann

Dr. Mahyar Mohtadi

**Weitere Mitglieder des Prüfungsausschusses**

Dr. Florence Schubotz

Thorsten Riedel



## Abstract

Sea surface temperature (SST) is very important for studies of the Earth's climate system owing to the linkages between SST and various climatic processes. A reliable estimation of past SSTs is one of the main goals for paleoclimatologists to improve our understanding of oceanic and atmospheric dynamics and their connection to the global climate. Furthermore, the tropical SSTs play a key role for rapid climatic changes, because large amounts of heat and water vapor were transported from the tropics to the high latitudes. Warm SSTs at low latitude result in more evaporation and could thus induce increased ice sheet size and decreased temperatures at northern high latitudes. Establishing SST evolution in the tropics is crucial for understanding the mechanisms behind abrupt climate changes in the past.

In this thesis, the main objectives are to evaluate the applicability of the  $U_{37}^K$  (alkenone unsaturation index) and  $TEX_{86}^H$  (tetraether index of glycerol dialkyl glycerol tetraether with 86 carbon atoms) in the tropical Indian Ocean as well as to investigate their control mechanisms for reconstructing temperatures in the past. All studies presented herein are based on 36 surface sediments, a sediment trap covering an annual cycle and a gravity core in the eastern Indian Ocean.

To assess the applicability, surface sediment samples from the Indonesian continental margin off west Sumatra, south of Java, and off the Lesser Sunda Islands are measured. In the non-upwelling regions, the results show that the  $U_{37}^K$  temperature estimates are up to 2 °C lower than World Ocean Atlas 2009 (WOA09) during the entire year, likely due to the reduced sensitivity of the  $U_{37}^K$  proxy beyond 28 °C. However, the temperatures based on  $TEX_{86}^H$  are consistent with mean annual temperatures from the WOA09. In the upwelling areas, the  $U_{37}^K$ -based temperature estimates reflect the SST during the upwelling season, whereas the  $TEX_{86}^H$ -based temperature estimates are up to 2 °C lower than  $U_{37}^K$ -based temperature estimates suggesting GDGT export from greater and colder water depths around 40-50 m.

In the following work, an annual time series sediment trap study was conducted in the central upwelling region off south of Java. A pronounced seasonality of alkenone

flux is observed, whereas GDGT flux displayed a weaker seasonality in comparison. The calculated flux-weighted average  $U^{K'}_{37}$ -based temperature estimate is similar to the SE monsoon SST rather than mean annual SST. The average is based on those samples only that permitted a reliable SST estimate, i.e., mainly the samples from the SE monsoon period. On the other hand, the flux-weighted average temperature based on the  $TEX^H_{86}$  is consistent with mean annual temperature at 50 m depth, indicating  $TEX^H_{86}$ -temperatures reflect the mean annual subsurface temperature instead of the surface temperature. These observations support the findings concluded in the surface sediment samples study.

Based on results from sediment trap and surface sediment samples, the application of the two SST indices on samples from a gravity core is in order to investigate the climatic evolution covering the past 22,000 years off south of Java. In this study, the temperature reconstruction suggest a 3-4 °C cooling during the last glacial maximum (LGM) compared to modern conditions. The results also show that the  $TEX^H_{86}$  temperature estimates are up to 2 °C warmer than SST- $U^{K'}_{37}$  during the last 22ka except during the LGM and during the late Holocene. The differences between the two SST indices are paralleled by *G. bulloides* percentages as a proxy for upwelling intensity, implying that the offset between two temperature proxies could be considered as the potential for reconstructing the upwelling intensity in the study area. In addition, the initial timing for the deglacial warming of GDGT temperature estimates started at ~18 ka, whereas the lowest  $U^{K'}_{37}$  temperature estimates appeared in the middle of the Younger Dryas period (YD, ca. 12 ka) and the late Heinrich Stadial 1 period (HS1, ca. 15 ka). Our records reveal that the seasonal SSTs and mean annual subsurface temperatures were closely linked to climate changes occurring in both hemispheres, respectively. Thus, the combination of  $U^{K'}_{37}$  and  $TEX^H_{86}$  records and their difference give the complementary feedbacks on sea-water temperature developments in the past evolution in the tropical eastern Indian Ocean.

### Kurzfassung

Die Erfassung und Rekonstruktion von Meeresoberflächentemperaturen (sea surface temperatures - SSTs) sind sehr wichtig für Untersuchungen des Erdklimasystems, da sie mit unzähligen klimatischen Prozessen gekoppelt sind. Eine zuverlässige Abschätzung von SSTs der Vergangenheit ist ein Hauptziel von Paläoklimatologen, um damit unser Verständnis der ozeanischen und atmosphärischen Dynamik sowie deren Kopplung an das globale Klima zu verbessern. Darüber hinaus spielen tropische SSTs eine Schlüsselrolle für abrupte Klimaänderungen, da hier große Mengen an Wärme und Wasserdampf von den Tropen in die hohen Breiten transportiert werden. Wärmere SSTs in den niedrigen Breiten führen zu einer verstärkten Verdunstung und dies kann zu einem verstärktem Wachstum der Eisschilde und damit zu einer Verringerung der Temperaturen in den höheren Breiten führen. Das Verständnis der SST-Entwicklung in den Tropen ist deshalb entscheidend, um die Mechanismen hinter abrupten Klimaveränderungen der Vergangenheit zu verstehen.

Die Hauptziele der vorliegenden Arbeit sind zum einen die Anwendbarkeit des  $U'_{37}$  (alkenone unsaturated index) und des  $TEX^H_{86}$  (tetraether index of glycerol dialkyl glycerol tetraether with 86 carbon atoms) im tropischen Indischen Ozean zu evaluieren und zum anderen ihre Kontrollmechanismen zu untersuchen, um die Meeresoberflächentemperaturen der Vergangenheit zu rekonstruieren. Die hier präsentierten Studien basieren auf Ergebnissen von 36 Oberflächensedimenten, einer Sedimentfalle, die einen kompletten Jahreszyklus abdeckt sowie eines Schwerelots aus dem östlichen Indischen Ozean.

Um die Anwendbarkeit beurteilen zu können, wurden Oberflächensedimentproben vom indonesischen Kontinentalrand vor West-Sumatra, südlich von Java und vor der Küste der Kleinen Sunda-Inseln analysiert. In den Nicht-Auftriebsregionen sind die Werte der  $U'_{37}$ -Temperaturrekonstruktion für den gesamten Jahresverlauf bis zu 2°C geringer als im World Ocean Atlas 2009 (WOA09) angegeben, was wahrscheinlich an der verminderten Empfindlichkeit des  $U'_{37}$ -Proxy oberhalb von

28°C liegt. Die Temperaturrekonstruktion basierend auf dem  $\text{TEX}_{86}^{\text{H}}$ -Proxy spiegeln jedoch die mittlere Jahrestemperatur des WOA09 wider. In Regionen mit Tiefenwasserauftrieb spiegeln die  $U_{37}^{\text{K}}$ -basierten Temperaturrekonstruktionen die SSTs während der Auftriebssaison wider, wohingegen die  $\text{TEX}_{86}^{\text{H}}$ -basierten Temperaturrekonstruktionen bis zu 2°C kälter sind als  $U_{37}^{\text{K}}$ -basierten Temperaturen, was darauf hinweist, dass GDGTs aus tieferen und kälteren Wassertiefen von circa 40-50m exportiert werden.

In der vorliegenden Arbeit wurde eine Sedimentfallenstudie, die eine Zeitserie von einem Jahr umfasst, durchgeführt. Für diesen Zeitraum konnte eine starke Saisonalität der Alkenonflüsse festgestellt werden, während die GDGT-Flüsse im Vergleich eine schwächere Saisonalität zeigten. Der berechnete und Fluss-gewichtete Durchschnittswert der  $U_{37}^{\text{K}}$ -basierten Temperaturabschätzung ist eher vergleichbar mit den Werten der Südost-Monsun SSTs anstatt mit der mittleren Jahrestemperaturen. Der Durchschnittswert beruht nur auf Proben, für die eine zuverlässige SST-Abschätzung möglich war und diese stammen größtenteils aus Zeit des Südost-Monsuns. Der  $\text{TEX}_{86}^{\text{H}}$ -basierte Durchschnittswert dagegen stimmt mit der Jahresmitteltemperatur in 50m Wassertiefe überein, was darauf hindeutet, dass die  $\text{TEX}_{86}^{\text{H}}$ -basierte Temperaturen eher die mittlere Jahrestemperatur unterhalb der Wasseroberfläche als die Meeresoberflächentemperaturen widerspiegeln. Diese Beobachtungen unterstützen die Ergebnisse der Oberflächensedimentanalysen.

Basierend auf den Ergebnissen der Sedimentfallenproben und der Oberflächensedimente, wurde die zwei SST-Proxies an Proben aus einem Schwerelotkern südlich von Java angewendet, um die dort die klimatische Entwicklung während der letzten 22 000 Jahre zu rekonstruieren. In dieser Studie deuten die Temperaturrekonstruktionen auf eine 3-4°C Abkühlung während des letzten glazialen Maximums (LGM) im Vergleich zu modernen Bedingungen hin. Die Ergebnisse zeigen auch, dass die  $\text{TEX}_{86}^{\text{H}}$ -basierte Temperaturenschätzungen während der letzten 22 000 Jahre bis zu 2°C wärmer als die  $U_{37}^{\text{K}}$ -basierten Temperaturabschätzung sind, mit der

Ausnahme des Zeitraums des LGMs und Spätholozäns. Die Unterschiede zwischen den beiden SST-Proxies gehen einher mit unterschiedlichen prozentualen Anteilen von *G. bulloides*, welche als Anzeiger für die Intensität des Tiefenwasserauftriebs gelten. Das deutet darauf hin, dass man den Unterschied zwischen den beiden Temperatur-Proxies im Untersuchungsgebiet potenziell für die Rekonstruktion der Auftriebsintensität verwenden könnte. Darüber hinaus zeigen die GDGT-basierten Temperaturschätzungen eine deglaziale Erwärmung seit ungefähr 18 000 Jahren vor heute (v.h.). Im Gegensatz dazu gibt es in den Alkenondaten ( $U_{37}^K$ ) zwei Phasen starker Abkühlung während der deglazialen Erwärmung, d.h. in der Mitte der Jüngerer Dryas (YD, ca. 12 000 Jahre v.h.) und im späten Heinrich Stadial 1 (HS1, ca. 15 000 Jahre v.h.). Unsere Daten zeigen damit, dass die saisonalen SSTs sowie die Temperaturen der tieferen Wassersäule sehr eng mit den deglazialen Klimaveränderungen auf beiden Hemisphären gekoppelt sind. Die Kombination der  $U_{37}^K$ - und  $TEX_{86}^H$ -Daten und ihrer Unterschiede erlaubt es uns deshalb Rückschlüsse über die vergangene Meereswassertemperaturentwicklung im tropischen Indischen Ozean zu ziehen.

**List of Abbreviations**

AIM	Australian-Indonesian Monsoon
AMS	Accelerator Mass Spectrometry
BIT	Branched and Isoprenoid Tetraether
ECC	Equatorial Counter Current
ENSO	El Niño-Southern Oscillation
GDGTs	glycerol dialkyl glycerol tetraethers
IOD	Indian Ocean Dipole
HS1	Heinrich Stadial 1
IPWP	Indo-Pacific Warm Pool
ITCZ	Intertropical Convergence Zone
ITF	Indonesian Throughflow
Ka	thousand years before present
Kyr	thousand years
LC	Leeuwin Current
LSI	Lesser Sunda Islands
ma SST	mean annual SST
NECC	North Equatorial Counter Current
NW monsoon	northwest monsoon
OM	organic matter
SE monsoon	southeast monsoon
SEC	South Equatorial Current
SJC	South Java Current
SST	Sea Surface Temperature in degree centigrade (°C)
Temp	Temperature
TOC	total organic carbon
YD	Younger Dryas interval

# TABLE OF CONTENTS

<b>Abstract</b> .....	I
<b>Kurzfassung</b> .....	III
<b>List of Abbreviations</b> .....	VI
<b>Chapter 1 Introduction</b> .....	1
1.1. General Introduction.....	1
1.1.1. Global Climate and sea surface temperature (SST).....	1
1.1.2. Reconstruction of past SST.....	3
1.1.3. Organic-geochemical Proxies.....	4
1.2. Study Area.....	14
1.2.1. Regional oceanographic setting.....	14
1.2.2. Sediment Records in Eastern Indian Ocean.....	18
1.3. Objectives of this thesis.....	20
1.4. Thesis Outline.....	21
1.5. Contributions to publications.....	22
1.6. References.....	24
<b>Chapter 2 Study Material and Methods</b> .....	37
2.1. Study Material.....	37
2.2. Methods.....	37
2.3. References.....	40
<b>Chapter 3</b> <b>Organic-geochemical proxies of sea surface temperature in surface sediments of the tropical Eastern Indian Ocean</b> .....	42
<b>Chapter 4</b> <b>Concentrations and abundance ratios of long-chain alkenones and glycerol dialkyl glycerol tetraethers in sinking particles south of Java</b> .....	87
<b>Chapter 5</b> <b>Sea surface and subsurface temperature variations in the upwelling area of the eastern Indian Ocean during the last 22,000 years</b> .....	122
<b>Chapter 6 Conclusions and Outlook</b> .....	149
6.1. Summary and Conclusions.....	149
6.2. Outlook.....	151
6.3. References.....	153
<b>Acknowledgements</b> .....	154

## Chapter 1 Introduction

### 1.1. General Introduction

#### 1.1.1. Global climate and sea surface temperature (SST)

The Earth's climate is a complex, interactive system consisting of the atmosphere, the hydrosphere, the cryosphere, the land surface, and the biosphere. Climate is driven or influenced by various external forcing mechanisms, the most important of which is the sun (Fig. 1.1.). The atmospheric component of the climate system obviously characterizes climate. Climate is often defined as long term "average weather" of temperature, precipitation and wind, ranging from months to millions of years (IPCC, 2001). The hydrosphere is consisted of all surface and subterranean water bodies; both fresh water, including rivers, lakes and aquifers, and saline water of the oceans and seas. The ocean covers approximately 71 percent of the Earth's surface and contains 97 percent of the planet's water. The atmosphere and oceans are interdependent and the two are strongly coupled through complex feedback loops. For instance, ocean currents are related to atmospheric wind patterns while air temperatures influence sea surface temperature (SST). Oceans and lakes play an integral role in the Earth's climate due to their capacity to store and redistribute large amounts of heat before it is released to the atmosphere or radiated back into space (e.g., Rahmstorf, 2002; Thurman and Trujilo, 1999). In addition, the ocean participates in biogeochemical cycles and exchanges gases with the atmosphere, influencing its greenhouse gas content. Warming of the climate system is unequivocal in the past two decades, as is evident from the observation of increases in global average air and ocean temperatures due to the presence of greenhouse gases, i.e., water vapor and carbon dioxide, caused by human activities (IPCC, 2007). Moreover, SST variations can influence evaporation as well as controlling the water cycle and precipitation patterns (Henderson, 2002). Thus, SST can be linked to various climatic processes and is therefore important for studies of the Earth's climate system. A reliable estimation of past SSTs is one of the main goals for

paleoclimatologists to improve our understanding of oceanic and atmospheric dynamics and their links with global climate.

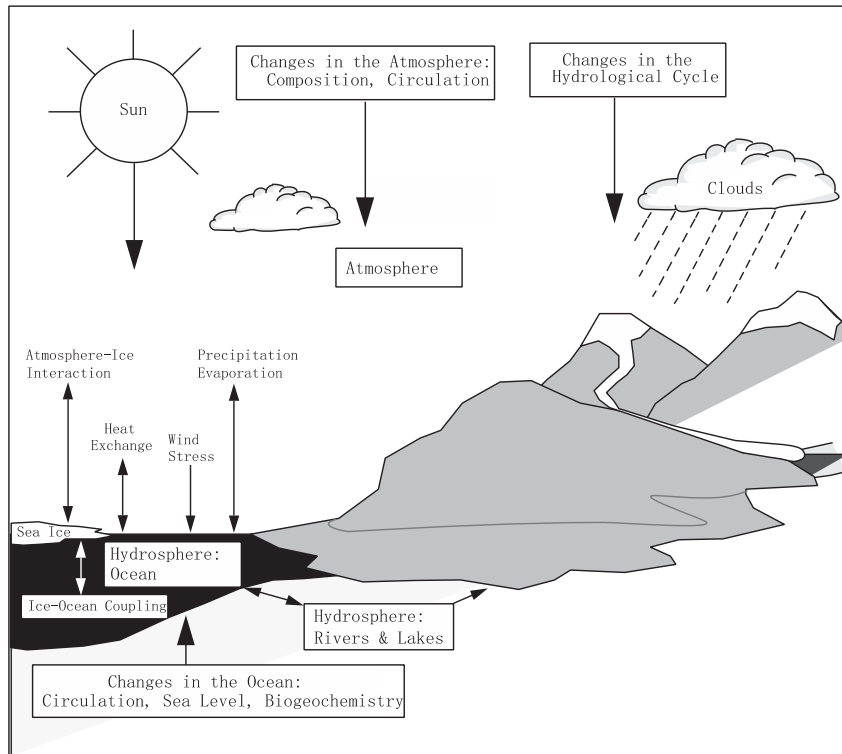


Fig. 1.1. Schematic view of the components of the global climate system (bold), their processes and interactions (arrows). Figure is after IPCC report (2001).

The best way to determine past SST is via instrumental temperature records (e.g., Oldfield and Thompson, 2004; Peterson and Vose, 1997). Climatologists rely heavily on instrumental records because these records represent direct measurements at exact points in space and time, and they have been collected at over 100,000 locations in the past two centuries (Peterson and Vose, 1997). However, these instrumental data are subject to temporal inhomogeneities and spatially too inconsistent to capture short-term processes. Therefore, instrumental records cannot provide complete pictures of past long-term SST changes. Climate and environmental reconstructions rely on proxy records, which potentially provide evidence for long-term climatic changes prior to the existence of instrumental or historical documentary records. A paleoclimatic proxy is a local record that is interpreted using chemical, physical and biological principles to

represent some combination of climate-related variation back in time (IPCC, 2001). Paleoclimatic reconstruction methods have improved greatly in the past decades. Proxy records are complicated by the presence of “noise” in which climate information is embedded, and a variety of possible uncertainties of the underlying climate information (e.g., Bradley, 1999; IPCC, 2001). The field of paleoclimatology depends heavily on careful calibration and cross-verification between proxy records from independent sources in order to build confidence in inferences about past climate (IPCC, 2007). To this end, accurate proxy records are essential to understand the past climate trends.

### **1.1.2. Reconstruction of past SST**

A series of SST proxies have been proposed. These proxies are found mostly in marine sediments and can be divided into proxies based on inorganic and organic (lipid biomarkers) fossils.

Commonly used inorganic temperature indicators made use of faunal assemblages, stable isotope fractionation of oxygen ( $\delta^{18}\text{O}$ ), elementary composition (Mg/Ca) in planktonic foraminifera, and the  $\delta^{18}\text{O}$  and Sr/Ca composition in corals (e.g., Barrows and Juggins, 2005; Beck et al., 1992; Emiliani, 1995; Nuernberg, 1995).

On the other hand, organic geochemical proxies are based on ratios of biomarkers. Biomarkers (biological markers) are molecular fossils, meaning that these compound originated from living former organisms, which are complex organic compounds composed of carbon, hydrogen, and other elements (Peters et al., 2005 and reference therein). Over the past 50 years, hundreds of biomarkers have been identified in oceans, and sediments, ancient rocks and oils, soils and coals, and in individual fossils (Gaines et al., 2008). Biomarkers are useful for climate research because their complex structures reveal more information about their origins than other compounds and they can provide information on climate history and help us to understand what causes climate to change. In general, numerous of lipid biomarkers for have been introduced in the past two decades, such as terrestrial vegetation proxy, paleotemperature proxy, paleosalinity proxy.

Since the 1980s, ratios of unsaturated alkenones have been developed as temperature proxies. These molecular proxies are increasingly being utilized to reconstruct past SSTs. Comparison with inorganic geochemistry temperature proxies, these lipid biomarkers SST proxies have their own advantages. They are not directly influenced by the chemistry of ocean water as well as occur over wide oceans and are not restricted to specific settings like e.g., corals. Although the molecular proxies have different limitations, they still can provide reliable information of past SSTs (Table 1.1.). Therefore, this thesis is based on two proxies derived from lipids that are widespread in the global ocean.

Table 1.1. Main paleotemperature proxies based on lipid biomarkers.

Proxy	Source organisms	Limitations/Uncertainties	References
$U_{37}^K$ (Alkenone unsaturation ratio)	Haptophytes	i) seasonality and depth of habitat ii) uncertainty about species composition iii) preferential degradation of $C_{37:2}$ iv) influence of nutrient input and light limitation v) lateral redistribution of sediment	Benthienand Müller, 2000 Brassell et al., 1986 Gong and Hollander, 1999 Prah et al., 2003 Prah et al., 2005
TEX <sub>86</sub> (TetraEther index of GDGTs with 86 carbons)	Marine Thaumarchaeota	i) seasonality and depth of habitat ii) uncertainty about species iii) riverine terrestrial input may bias TEX <sub>86</sub>	Herfort et al., 2006 Hopmans et al., 2004 Schouten et al., 2002 Weijers et al., 2006

### 1.1.3. Organic-geochemical Proxies

#### 1.1.3.1. Alkenone Paleothermometry

Alkenone unsaturation index is one of the most commonly used biomarker-based proxies for paleoceanographic reconstruction. It is based on a series of  $C_{37}$ - $C_{39}$  di-, tri- and tetra-unsaturated methyl and ethyl ketones (long-chain alkenones). The alkenones were first discovered in deep-sea sediments from the Walvis Ridge (Boon et al., 1978), and their structures were later identified by De Leeuw et al. (1980). The alkenones are now known to occur in globally distributed marine sediments (Fig. 1.2.). A study from

Volkman et al. (1980) reported that alkenones were found in the marine coccolithophorid *Emiliania huxleyi*. Subsequently, the alkenones have been identified in other coccolithophorid source e.g., *Gephyrocapsa oceanica* (e.g., Conte et al., 1998; Marlowe et al., 1984).

Brassell et al. (1986) introduced  $U_{37}^K$  index as a SST proxy. They applied the index on a sediment core and found that the alkenone unsaturation record showed similar downcore trends with those of the  $\delta^{18}O$  records. Originally, the  $U_{37}^K$  index reflected the proportions of the di-, tri- and tetra-unsaturated ketones with 37 carbon atoms, expressed as:

$$U_{37}^K = \frac{(C_{37:2} - C_{37:4})}{(C_{37:2} + C_{37:3} + C_{37:4})}$$

$C_{37:2}$ ,  $C_{37:3}$  and  $C_{37:4}$  represent concentrations of di-, tri- and tetra-unsaturated ketones, respectively.

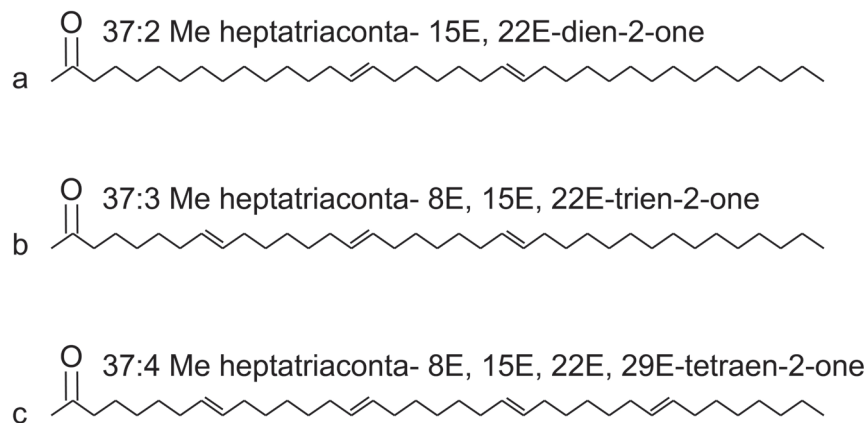


Fig. 1.2. Molecular structures of (a)  $C_{37:2}$  alkenone; (b)  $C_{37:3}$  alkenone; (c)  $C_{37:4}$  alkenone.

Subsequent work found that the  $C_{37:4}$  ketone has no empirical benefit to the paleotemperature equation because it was rarely detected in the sediments unless the temperature was lower than 10 °C (Prahl and Wakeham, 1987; Fig. 1.3.).

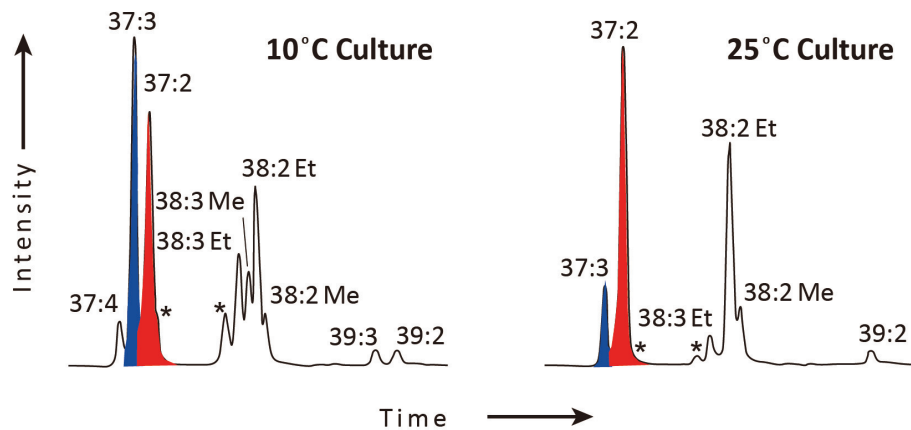


Fig. 1.3. Gas chromatograms of the long-chain, unsaturated ketone composition measured in cultures of *E. huxleyi* grown at 10 °C and 25 °C. Individual compounds are identified by carbon chain length: number of double bonds. Methyl ketones have C<sub>37</sub> and C<sub>38</sub> chain lengths; ethyl ketones have C<sub>38</sub> and C<sub>39</sub> chain lengths. Overlapping methyl (Me) and ethyl (Et) ketones with C<sub>38</sub> chain lengths are indicated. Methyl and ethyl ester of a di-unsaturated C<sub>36</sub> fatty acid are identified by the peak marked with an asterisk. The blue and red peaks represent C<sub>37:2</sub> and C<sub>37:3</sub>, respectively. This figure is modified after Prah and Wakeham, 1987.

Thus, Prah and Wakeham. (1987) re-defined the  $U_{37}^{K'}$  index as:

$$U_{37}^{K'} = \frac{(C_{37:2})}{(C_{37:2} + C_{37:3})}$$

Prah and Wakeham (1987) and Prah et al. (1988) proposed the first calibration of the alkenone unsaturated index to growth temperature using laboratory cultures of a single strain of *E. huxleyi*. Their initial samples of suspended particulate materials showed that this calibration reproduced temperatures in the northeast Pacific Ocean. The equation of  $U_{37}^{K'}$  indicates that the index values can vary between 0 and 1, roughly corresponding to 0 °C and 28 °C. Subsequently, a number of calibrations have been developed based on global core-top sediments, confirming that the  $U_{37}^{K'}$  values reflect mean annual (ma) SSTs (e.g., Conte et al., 2006; Müller et al., 1998). Additionally, these alkenone producers are sunlight dependent and thus they are limited to the upper euphotic zone reflecting near-surface ocean temperatures. However, a series of regional

calibrations of  $U_{37}^K$  showed convergence with the global core-top temperature calibration (e.g., Conte et al., 1998; 2001; 2006; Müller et al., 1998; Sawada et al., 1996; Ternois et al., 1997; Volkman et al., 1995). As with any paleoceanographic proxy, inherent uncertainties that might affect the accuracy of proxy estimates should be evaluated. These proxy uncertainties arise due to genetic, diagenetic factors, physiological, and ecological. The genetic composition of haptophytes might influence alkenone-derived temperatures, even though its affect on paleotemperature records are still under debatable (Conte et al., 1998).  $U_{37}^K$  estimated temperatures can be warm-biased due to the selective degradation of  $C_{37:3}$  (e.g., Hoefs et al., 1998; Gong and Hollander, 1999). Furthermore, radiocarbon compositions of alkenones have been used to refine age estimates of marine sediments, and in some cases, long-distance transport of alkenones by currents has been implied (e.g., Benthien and Müller, 2000; Mollenhauer et al., 2007, 2008; Ohkouchi et al., 2002). Some environmental factors that could potentially affect the unsaturation ratio of alkenones include light limitation (causing warmer SST estimates) and nutrient limitation (causing lower SST estimates) (Prah et al., 2003). Additionally, ecological concerns stem from observations related to the depth of maximum alkenone production and seasonal blooming of coccolithophores. For example, in sediment traps, alkenone concentrations showed that the highest abundance occurred not at the sea surface but in the surface mixed-layer in the North Atlantic (Conte et al., 2001) and in the Pacific (Ohkouchi et al., 1999). Some studies based on surface sediments and suspended particulates in the water column suggest that the alkenone producers are inferred to occur seasonally, it is conceivable that the alkenone signals should rather correspond to the season of maximum production, which will depend on the location (Rosell-Melé and Prah, 2013). For instance, SST- $U_{37}^K$  values appear lower than mean annual SSTs, which are attributed to the predominant production and export of alkenones during winter and spring in the Mediterranean Sea (Leider et al., 2010). Thus,  $U_{37}^K$ -derived temperature estimates reflect seasonal temperatures instead of the mean annual in some regions (e.g., Popp et al., 2006; Sikes and Volkman, 1993, Sikes et al., 1997).

### 1.1.3.2. TEX<sub>86</sub> paleotemperature proxy

Archaea are one of the three domains of single-celled microorganisms, which can be subdivided into Crenarchaeota (Marine “Group I”, latter renamed as Thaumarchaeota; Brochier-Armanet et al., 2008) and Euryarchaeota (Marine “Group II”) (Fig. 1.4.). In the 1980s, biphytanyl (C<sub>40</sub>) isoprenoid hydrocarbon chains of archaea were discovered in sedimentary systems (see review in Pearson et al., 2013). The lipids of archaea consist of GDGTs, short for *sn*-2, 3-di-*O*-biphytanyl diglycerol tetraethers. The archaea were previously thought to exist only in extreme environments, such as those with high salinity or high temperature. However, subsequent studies based on more advanced molecular biological techniques and lipid analyses suggest they can thrive in marine and terrestrial aquatic environments, sediments and soils (e.g., Schouten et al., 2002). Thaumarchaeota appear to be one of the dominant forms of pelagic picoplankton in the oceans, making up approximately 40% of all cells throughout the water column (e.g., Delong et al., 1992; Karner et al., 2001; Murray et al., 1998).

Early on, studies found that the number of cyclopentane rings in GDGTs of hyperthermophilic archaea varied with temperature increases (e.g., Delong et al., 1988; DeRose and Gambacorta, 1988; Gliozzi et al., 1983; Uda et al., 2001). Subsequently, a study demonstrated that the “cold” Thaumarchaeota were found abundantly in the marine water column, which can biosynthesize similar GDGTs as found in hyperthermophilic archaea (Schouten et al., 2000; Sinninghe Damsté et al., 2002a). Thaumarchaeota biosynthesize different structure of GDGTs, including GDGT-0 to GDGT-3 (the numbers denote internal cyclopentyl rings), crenarchaeol (containing four cyclopentyl rings and a cyclohexyl ring) and small quantities of a crenarchaeol regioisomer (e.g., Schouten et al., 2000; Sinninghe Damsté et al., 2002a) (Fig. 1.5.).

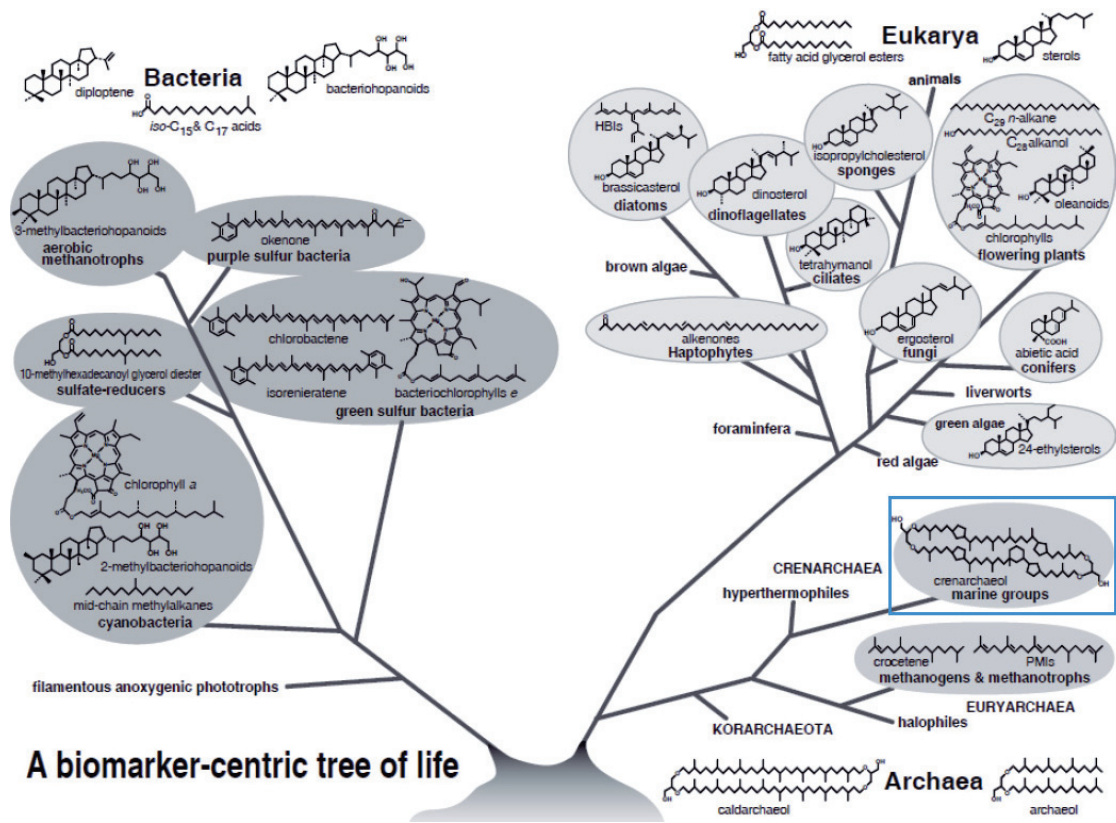


Fig. 1.4. Types of biomarkers and their precursors in the three domains of life. This picture is taken from Gaines et al. (2008).

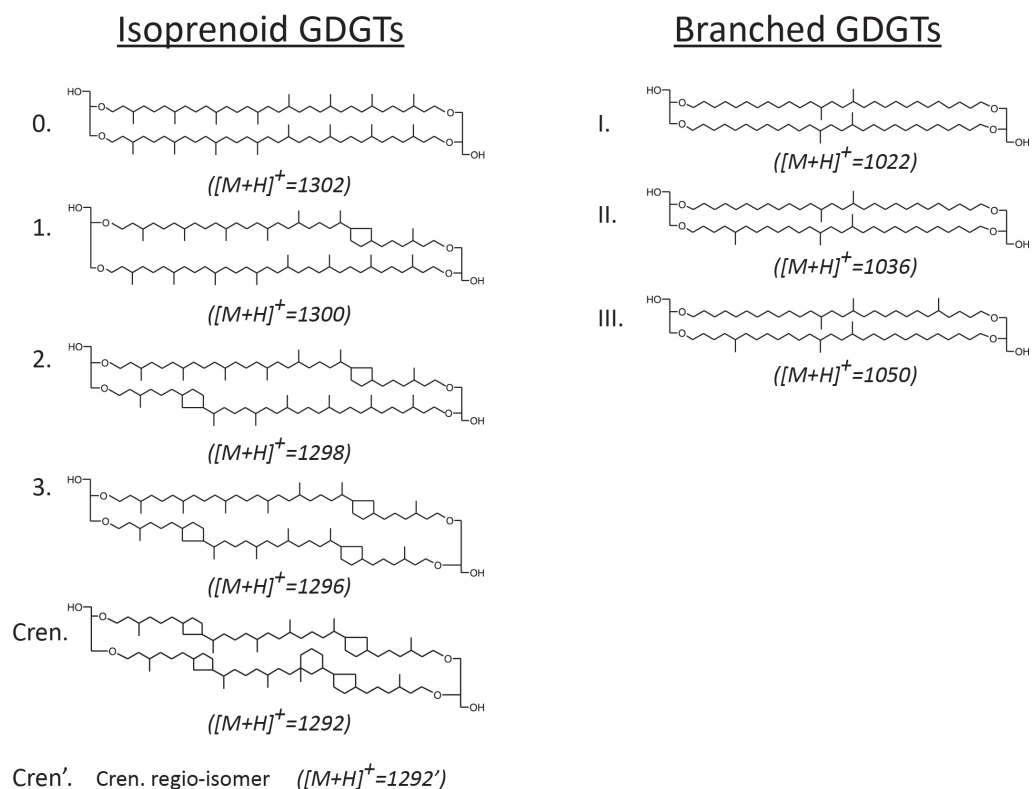


Fig. 1.5. Structures of isoprenoid (left) and branched (right) GDGTs. Numbers in italics with the structures of GDGTs indicate the masses of the  $[M+H]^+$  ions of the GDGTs. This picture is modified after Schouten et al., (2009). Cren=Crenarchaeol.

Based on a positive relationship between temperature and the number of cyclopentyl or cyclohexyl rings in GDGTs, Schouten et al. (2002) proposed a temperature proxy named  $TEX_{86}$  (TetraEther indeX of tetraether consisting 86 carbon atoms). The  $TEX_{86}$  is defined as Eq. (1).

$$TEX_{86} = \frac{[GDGT-2] + [GDGT-3] + [Cren']}{[GDGT-1] + [GDGT-2] + [GDGT-3] + [Cren']} \quad \text{Eq.(1)}$$

where GDGT-1, GDGT-2, and GDGT-3 indicate GDGTs containing 1, 2, and 3 cyclopentane moieties, respectively and Cren' the crenarchaeol regio-isomer.

Schouten et al. (2002) developed their calibration based on 44 surface sediment from 15 locations, and suggested that  $TEX_{86}$  derived temperatures correspond well with

ma SST. More recently, the original proxy has been refined further into  $\text{TEX}_{86}^{\text{H}}$  (Eq. (2)) and  $\text{TEX}_{86}^{\text{L}}$  (Eq. (3)) by Kim et al (2010) for environments with temperatures higher and lower than 15 °C, respectively.

$$\text{TEX}_{86}^{\text{H}} = \log(\text{TEX}_{86}) \text{ Eq.(2)}$$

$$\text{TEX}_{86}^{\text{L}} = \log\left(\frac{[\text{GDGT-2}]}{[\text{GDGT-1}] + [\text{GDGT-2}] + [\text{GDGT-3}]}\right) \text{ Eq.(3)}$$

Studies of the  $\Delta^{14}\text{C}$  value of crenarchaeol in surface sediments suggested that the GDGTs are less affected by long-distance lateral transport than the alkenones (e.g., Mollenhauer et al., 2007, 2008). Therefore, GDGT-based proxies are likely primarily influenced by local conditions. Likewise, the effects of changing redox conditions on the  $\text{TEX}_{86}$  are minor (e.g., Huguet et al., 2009; Kim et al., 2009; Sinninghe Damsté, 2002b).

In the past ten years, the  $\text{TEX}_{86}$  paleothermometer has been applied on suspended particulate matter (SPM), surface sediments, and ancient sedimentary archives, e.g., late Cretaceous spanning extreme events such as Paleocene-Eocene Thermal Maximum (PETM) and Eocene-Oligocene (E-O) boundary (e.g., Huguet et al., 2006; Lee et al., 2008; Leider et al., 2010; Schouten et al., 2012; see review in Schouten et al., 2013). However, these applications show offsets between the temperature records derived from  $\text{TEX}_{86}$  and those of in-situ temperatures or based on other paleotemperature proxies. A better understanding of the physiology and ecology of marine archaea may help to reconcile these offsets. It is well known that Thaumarchaeota are distributed throughout the entire water column, and can reside in deeper waters (Karner et al., 2001). Although  $\text{TEX}_{86}$  values correlate well to mean annual surface temperature in some settings, several recent studies suggested that  $\text{TEX}_{86}$  does not reflect SST, but rather reflect temperature at deeper water depth (between 40 m and 150 m) based on surface sediments, sinking particles and SPM (e.g., Basse et al., 2014; Chen et al., 2014; Huguet et al., 2007; Lee et al., 2008; Lopes dos Santos et al., 2010; Xing et al., 2015). In addition, Lengger et al. (2012) found decreasing  $\text{TEX}_{86}$  values for surface sediments with depth in the Arabian Sea, may potentially be due to a larger addition of GDGTs produced in

deeper and colder waters to the surface-derived GDGTs. Other studies have shown that TEX<sub>86</sub> derived temperatures may be biased from mean annual due to seasonal growth of Thaumarchaeota, e.g., towards summer temperature in the eastern Mediterranean (Leider et al., 2010) and the South China Sea (Jia et al., 2012), or towards winter temperature in the southern North Sea (Herfort et al., 2006). Furthermore, there are other factors that require additional caution in interpreting TEX<sub>86</sub>-derived temperatures, such as the competition for nutrients between crenarchaeota and other phytoplankton including alkenone producers (e.g., Rommerskirchen et al., 2011; Wuchter et al., 2006), nutrient availability (e.g., Turich et al., 2007), or terrestrial OM input (Hopmans et al., 2004; Weijers et al., 2006, more details see below 1.1.3.3). In addition, pelagic Group II Euryarchaeota could bias the interpretation of TEX<sub>86</sub> derived temperatures towards cooler temperature due to the isoprenoid GDGTs can be synthesized by Eucyarchaeota in upper water column (e.g., Turich et al., 2007; Wang et al., 2015).

### 1.1.3.3. Terrestrial Organic Matter Proxy (BIT index)

Branched GDGTs, a group of membrane lipids has been unambiguously identified by NMR to be derived from anaerobic soil bacteria containing branched instead of isoprenoid alkyl chains (Sinninghe Damsté et al., 2000). Branched GDGTs have been found in lacustrine sediments (Power et al., 2004), peat (Sinninghe Damsté et al., 2000), soil (Weijers et al., 2006), and in some ocean margin sediments (Hopmans et al., 2004). Branched GDGTs differ from the archaeal tetraether lipids, comprising two C<sub>28</sub> carbon chains bearing two or three methyl and zero to two cyclopentane moieties each.

Hopmans et al., (2004) presented the Branched and Isoprenoid Tetraether (BIT) index, based on the relative abundance of branched GDGTs and defined as follows:

$$\text{BIT} = \frac{([\text{GDGT-I}] + [\text{GDGT-II}] + [\text{GDGT-III}])}{([\text{GDGT-I}] + [\text{GDGT-II}] + [\text{GDGT-III}] + [\text{Crenarchaeol}])}$$

The roman numerals refer to the GDGTs indicated in Fig. 1.5. The roman numerals indicate GDGTs without cyclic components in the structure.

The BIT index serves as a proxy for the relative abundance of terrestrial OM input to coastal marine sediments. The definition dictates that the BIT index values reach 0 for open marine sediments, and 1 for soils and peats, and variable for marine and lake sediments (Hopmans et al., 2004) (Fig. 1.6.). This index is a proxy for the relative abundance of fluvial-transported soil OM vs. marine OM, which is different from general terrestrial organic proxies (such as  $\delta^{13}\text{C}_{\text{org}}$ , C/N, or odd carbon number *n*-alkanes). This may be caused by a lack of soils in the other sources or only a minor amount of branched GDGTs is carried by aeolian transport, which is more susceptible to oxic degradation than e.g., *n*-alkanes (see review in Schouten et al., 2013).

Weijers et al. (2006) found that high terrestrial OM input can potentially bias the  $\text{TEX}_{86}$  values as terrestrial-derived GDGTs can also contain GDGT1-3. In order to account for this effect, the BIT index should be quantified. The temperature deviations of +1 °C, which is the analytical error of the  $\text{TEX}_{86}$ , correspond to BIT index values of 0.2-0.3, whereas the temperature deviation >2 °C is reached at a BIT index of 0.4.

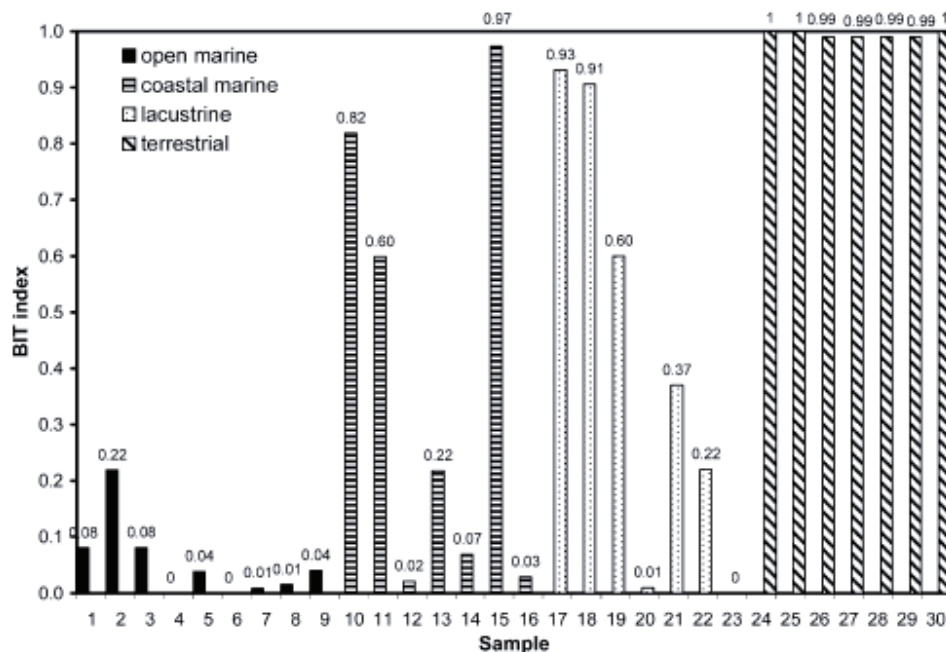


Fig. 1.6. Bars represent the BIT index analyzed in Holocene sediments from a range of environments. Data points are from 30 different locations, detailed in Hopmans et al., 2004.

## **1.2. Study Area**

### **1.2.1. Regional oceanographic setting**

The Indonesian archipelago, also known as the “Maritime Continent”, lies between latitudes 11°S and 6°N, and longitudes 95°E and 141°E, among the Indian Ocean and Pacific Ocean and the continents of Asia and Australia (Fig. 1.7.). It consists of 17,508 islands. The main islands are the Greater Sunda Islands (such as Borneo, Java and Sumatra), the Lesser Sunda Islands (also called Nusa Tenggara, a series of islands from Lombok to Timor; Fig. 1.7.).

The Indonesian region is a climate-sensitive location and part of the Indo-Pacific Warm Pool (IPWP), which plays a fundamental role in regulating the global climate changes by providing the main source of heat and water vapor transported to the high latitudes. Small SST changes can result in significant changes in the hydrological systems in this region (e.g., Neale and Slingo, 2003). The hydrography of the region is complex, i.e. it is influenced by Australian-Indonesian Monsoon (AIM), seasonal migration of the Intertropical Convergence Zone (ITCZ), and variable occurrence of El Niño-Southern Oscillation (ENSO) and Indian Ocean Dipole (IOD) on inter-annual timescales.

Because of the monsoonal circulation and seasonal migration of the ITCZ over this region, it displays contrasting seasonal characteristics. During austral summer (from January to March), strong rainfall with over 30 cm per month (Murgese et al., 2008) and huge river run-off to the ocean occur because the southerly position of the ITCZ, which brings a lot of moisture over from SE Asian and Indonesian Seas (Gordon, 2005). In contrast, during austral winter (from June to September), the SE monsoon caused by the high-pressure belt of the southern hemisphere and is relatively dry and cool when reaching Indonesia. It gathers moisture from the Indonesian and SE Asian Seas before meeting the northerly position of ITCZ and introducing heavy precipitation over the SE Asian mainland.

During the NW monsoon, the predominant wind is directed towards Asia mainland, which forces the South Java Current (SJC), originated from the Equatorial Counter Current (ECC), to move southeastward to meet the Leeuwin Current (LC), which carries warm and saline water transported from the eastern part of the Indonesian Archipelago (e.g., Tapper, 2002; Tomczak and Godfrey, 1994). The mixture of SJC and LC feeds the South Equatorial Current (SEC) that moves westward at  $\sim 15^{\circ}\text{S}$  (Fig. 1.7.). In contrast, during the SE monsoon period, the SJC takes an opposite direction flowing northwestward and joins the SEC with a reduced contribution to the LC. Advection of fresher Java Sea water through the Sunda Strait and runoff from Sumatra and Java are responsible for the low-salinity “tongue” in the SJC with salinities as low as 32‰. During the SE monsoon season, the strongest westward SJC occurs along the southern coast of Java, inducing an upwelling and shoaling of the thermocline (Susanto et al., 2001; Tomczak and Godfrey, 1994).

During the SE monsoon, alongshore winds induce coastal upwelling off Java and Sumatra. Upwelling generally starts in June and migrates westwards to the equator. It reaches a maximum in July and August and reduces at the end of October (Susanto et al., 2001). The upwelling is characterized by a small SST depression and high chlorophyll-a concentration, whereas a uniform SST distribution and relatively low chlorophyll-a concentration prevail during the non-upwelling season. In general, the mean SST is over  $28^{\circ}\text{C}$  in the Indonesian region. Seasonal SSTs vary between  $29^{\circ}\text{C}$  in austral summer and  $26^{\circ}\text{C}$  in austral winter off southwest Java. The relatively small temperature difference is typical for this upwelling system, in contrast to other tropical upwelling system, such as off Angola (SST drops by  $\sim 7^{\circ}\text{C}$ ) and Peru (SST drops by  $\sim 5^{\circ}\text{C}$ ), off Oman (SST drops by more than  $8^{\circ}\text{C}$ ) (e.g., Hastenrath and Lamb, 1979; Du et al., 2005; Boyer et al., 2006). Previous studies suggested two mechanisms, in terms of internal and external factors, to explain the small SST depression. One is the barrier layer, representing an intermediate layer that separates the base of the mixed layer from the top of the thermocline (Lukas and Lindstrom, 1991). The enhanced stratification caused by the large rainfall and runoff sustains a shallow mixed layer. However, a thick barrier layer

prevents deeper and more salinity water from below to reach the mixed layer (Sprintall and Tomczak, 1992; Qu et al., 2005).

The other key factor is the Indonesian Throughflow (ITF), a low-latitude inter-ocean pathway, which connects the upper water of the Pacific Ocean and the Indian Ocean. The ITF enters the Indian Ocean in response to the sea level height difference due to the wind system. Today, the ITF transports an annual average  $\sim 16$  SV ( $1 \text{ SV} \equiv 10^6 \text{ m}^3 \text{ s}^{-1}$ ) of warm, low-salinity water from the Pacific into the eastern Indian Ocean (e.g., Gordon and Fine, 1996; You and Tomczak, 1993). North Pacific thermocline and intermediate water masses contribute the throughflow water. Two main branches of the ITF enter the Indian Ocean through the Makassar Strait: the smaller one is known as the Lombok Strait (1.7 SV), while the larger ones can be divided into two passages that include the Timor Strait (4.3 SV) and the Ombai Strait (4.5 SV). During the upwelling period, the difference in sea level between Java and Australia is the largest, implying the maximum strength in the ITF (Tomczak and Godfrey, 1994). The Java upwelling system is counterbalanced by the increases in the ITF (e.g., Godfrey, 1996). The ITF flowing through the Lombok Strait also neutralizes a significant SST depression off Java at the same time.

Additionally, a few studies suggested that the hydrology in this region is strongly associated with the ENSO and the IOD (e.g. Ashok et al., 2001; Du et al., 2008; Halkides et al., 2006; Qu and Meyer, 2005; Saji et al., 1999; Susanto et al., 2001; Webster et al., 1999). During the El Niño periods and positive IOD events, enhanced upwelling with higher primary productivity and decreased SST of up to 4 °C are observed. During strong El Niño periods, such as in 1997/98, anomalous winds induced a relatively stronger upwelling along the coast off Java with enhanced productivity as well as extended in time up to three months (e.g. Susanto et al., 2001; 2006). Conversely, reduced upwelling intensity, enhanced precipitation, and a uniformly high SST occurred during La Niña periods and negative IOD events.

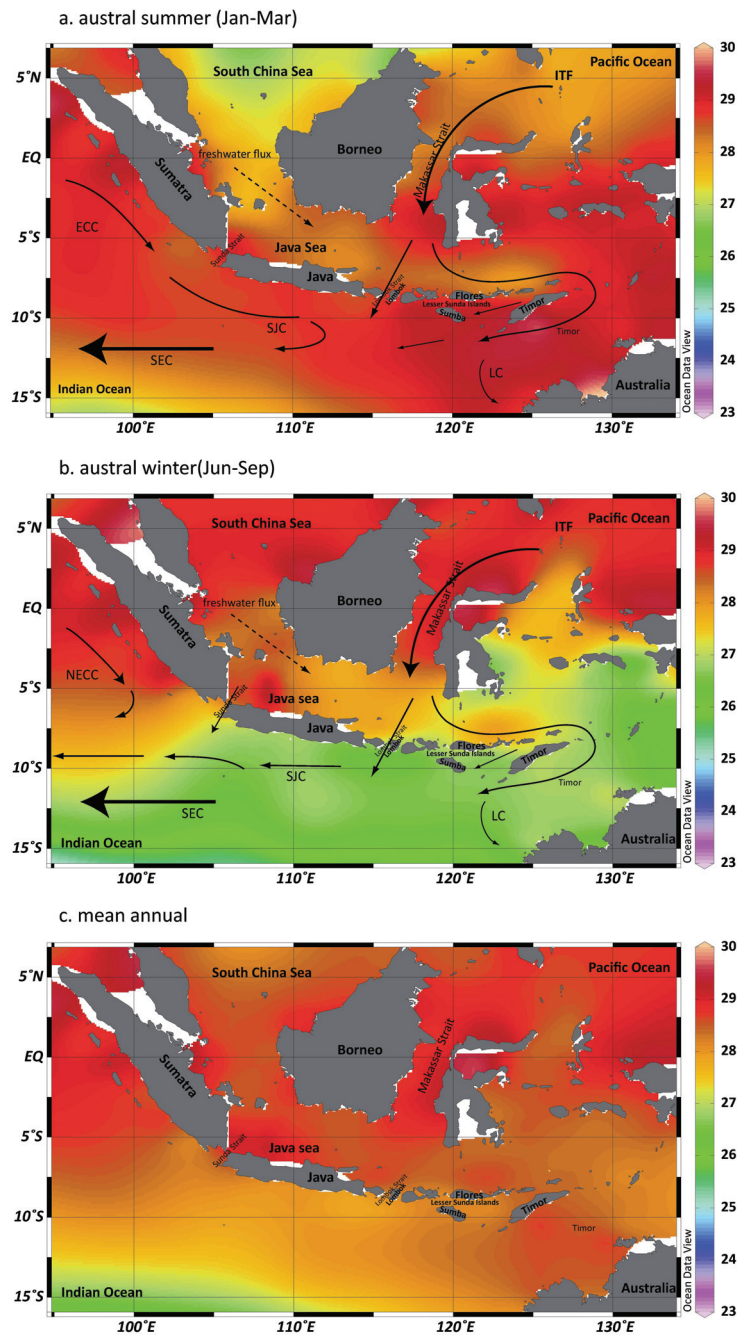


Fig. 1.7. Sea surface temperature in the tropical Eastern Indian Ocean for a) austral summer monsoon season; b) austral winter monsoon season; c) mean annual. (from WOA 2009, Locarnini et al., 2010), solid arrows indicate oceanographic surface currents: SJC: South Java Current; ECC: Equatorial Counter Current; SEC: South Equatorial Current; NECC: North Equatorial Counter Current; ITF: Indonesian Throughflow; LC: Leeuwin Current.

### 1.2.2. Sediment Records in Eastern Indian Ocean

Since the early 1980s our knowledge of the paleoceanography of the Indo-Pacific region has grown exponentially. Paleoceanographic reconstructions suggest that glacial-interglacial climate changes in the Indonesian Archipelago are dominated by the AIM.

Many quantitative proxy methods have been applied in and around Indonesian Archipelago to reconstruct glacial-interglacial SST variations (Fig. 1.8.). Published SST records indicate that uniform postglacial SSTs increased in the entire eastern Indian Ocean. For example, deglacial warming of  $\sim 3.0$  °C in the Timor Sea,  $\sim 2.3$  °C in Sulu Sea,  $\sim 2.8$  °C on the Ontong Java Plateau,  $\sim 2.7$  °C in the SW Sumatra,  $\sim 3.0$  °C in the northern and central Sumatra, and  $\sim 3.3$  °C in the Makassar (Table 1.2., references therein). The synchronous initial warming at both the surface and intermediate water depths during the early deglaciation corresponds to that in other southern mid- to high-latitude SSTs and the deglacial rise in global CO<sub>2</sub> levels (e.g., Lamy et al., 2007; Loulergue et al., 2007). However, the previously published paleo SST studies show distinct amplitudes among SST records derived from different proxies in this region, likely due to differences in the production seasonality and the depth habitat of the source organisms. For example, SST estimates based on Mg/Ca on foraminifera reveal a  $\sim 2.7$  °C increase in the SW Sumatra, whereas SST increases by  $\sim 1.7$ - $2$  °C according to alkenone-based estimates in the SW Sumatra (Table 1.2.). Therefore, multi-proxy reconstructions of SST from the same sediments are needed for a better understanding of paleotemperature changes in this region.

Furthermore, numerous of paleo-monsoon studies suggest a weaker austral winter monsoon and a stronger austral summer monsoon during the LGM (e.g., Wang et al., 2005). By using *Globigerina bulloides* percentages as a proxy for austral winter monsoon and upwelling intensity, Mohtadi et al. (2011) found the strongest austral winter monsoon during the early Holocene and stronger upwelling during HS1 and YD. In addition, Lückge et al. (2009) demonstrated that the enhanced marine paleoproductivity was directly related to strengthening of coastal upwelling during

periods of increased boreal summer insolation and was associated with the SE monsoon strength with a precessional cyclicity. On the other hand, peaks in abundance of coccolithophores, *Umbellosphaera irregularis* and the ratio of EhuxGeric (combined record of *E.huxleyi* and *G.ericsonii*) to *Gephyrocapsa oceanica* as well as distinct minima of TOC and *G.oceanica* abundance, reveal a weaker upwelling and oligotrophic conditions during every 20,000 to 25,000 years in the past 300 kyrs (Andruleit et al., 2008). Likewise, diatom paleoproductivity was higher during interglacials, primarily due to the input of lithogenics and nutrients following the rise in sea level after full glacial conditions, as well as the boreal summer insolation forcing (Romero et al., 2012).

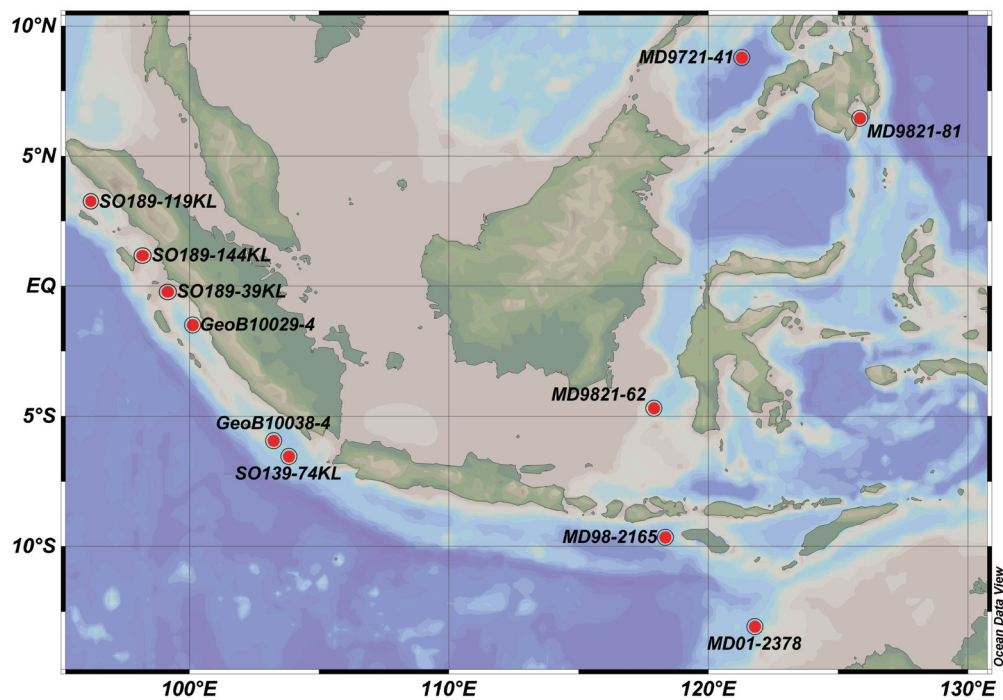


Fig. 1.8. Overview of the locations of previously published paleoceanographic records in and around the Indonesian Archipelago.

Table 1.2. Overview of the past SST reconstruction studies in and around the Indonesian Archipelago.

Stations	Type of Proxy	LGM-Holocene	References
MD01-2378	Mg/Ca SST	3.2 °C	Xu et al., 2008
GeoB10038-4	Mg/Ca SST	2.3 °C	Mohtadi et al., 2010a,b
	Alkenone-based SST	2 °C	
GeoB10029-4	Mg/Ca SST	2.7 °C	Mohtadi et al., 2010b
SO139-74KL	Alkenone-based SST	1.7 °C	Lückge et al., 2009
SO189-119KL SO189-144KL SO189-39KL	Mg/Ca SST	3.0 °C	Mohtadi et al., 2014
MD98-2165	Mg/Ca SST	3.0 °C	Levi et al., 2007
MD9821-62	Mg/Ca SST	3.3 °C	Visser et al., 2003
MD9721-41	Mg/Ca SST	2.3 °C	Rosenthal et al., 2003
MD9821-81	Mg/Ca SST	2.0 °C	Stott et al., 2002
Ontong Java Plateau	Mg/Ca SST	2.8 °C	Lea et al., 2000

### 1.3. Objectives of this thesis

Since the two organic-geochemical proxies were developed, the exact meaning of temperatures derived from alkenones and GDGTs are still under debate. The mainly open questions are: 1) the seasonal production of alkenones and GDGTs and 2) export and the water depth of their habitats. Furthermore, the tropical SSTs play a key role for rapid climatic changes during the last deglacial terminations. The aim of this thesis is to evaluate the distribution and application of the two SST proxies in the eastern Indian Ocean region against today's environmental conditions to improve the understanding of past climate variations as well as to investigate the hydrological evolution in the eastern Indian Ocean to shed light on potentially mechanisms behind past climate changes in the tropics.

The key objectives of this thesis are:

i). To evaluate the controlling factors of  $U_{37}^K$ - and  $TEX_{86}$ -derived SST estimates in the upwelling and non-upwelling areas of the eastern Indian Ocean.

ii). To investigate when and how the alkenone and GDGT signals produced in the water column are transport to the surface sediments.

iii). To study the evolution of sea-surface temperature over the time intervals of climate change (last deglaciation, Holocene) and to determine what affects the different SST proxies during the past 22,000 years in the eastern Indian Ocean as well as to illustrate what controls the climate changes in the tropics.

#### **1.4. Thesis Outline**

The main objectives of this thesis, as proposed in Section 1.3, are addressed in three first-author manuscripts, presented as Chapter 3 to 5. Chapter 2 is an overview of the materials and methods used in this study.

#### **Chapter 3. Organic-geochemical proxies of sea surface temperature in surface sediments of the tropical Eastern Indian Ocean**

Wenwen Chen, Mahyar Mohtadi, Enno Schefuß, Gesine Mollenhauer

In this chapter, we reconstruct SSTs using  $U_{37}^K$  and  $TEX_{86}^H$  in 36 surface sediment samples from the Indonesian continental margin off west Sumatra, south of Java and the Lesser Sunda Islands. The assessment of the suitability of  $U_{37}^K$  and  $TEX_{86}^H$  is based on two approaches, i) comparing the proxy data to modern SSTs (WOA 2009); and ii) evaluating the difference between the two indices used. We investigate the applicability of these two indices in the upwelling and non-upwelling areas of the Indonesian region, taking into consideration preferential degradation, lateral transport and other potential biases.

#### **Chapter 4. Concentrations and abundance ratios of long-chain alkenones and glycerol dialkyl glycerol tetraethers in sinking particles south off Java**

Wenwen Chen, Mahyar Mohtadi, Enno Schefuß, Gesine Mollenhauer

To investigate the seasonal production of alkenones and GDGTs as well as the depth of production of GDGTs in the water column, we present results from a one-year sediment trap (12.2001-11.2002) in the upwelling area south of Java. In this study, a series of published data including total flux as well as flux of lithogenic, opal, carbonate and organic carbon are involved. Our results provide important information to interpret alkenone- and GDGT-based temperature signals in the sediments for the past SST reconstruction.

#### **Chapter 5. Sea surface and subsurface temperature variations in the upwelling area of the eastern Indian Ocean during the last 22,000 years**

Wenwen Chen, Mahyar Mohtadi, Enno Schefuß, Gesine Mollenhauer

This study addresses the evolution of hydrological changes in the eastern Indian Ocean of the past 22,000 years. This is conducted on a sediment core in the central upwelling area off south Java. In this study, two organic-geochemical SST proxies ( $U^{K'}_{37}$  and  $TEX^{H}_{86}$ ) are applied. In comparison of the difference between the two proxies and *G. bulloides* percentages suggests that the difference in temperatures is tied to upwelling intensity. We also determine what controls the contrasting cooling and warming trends registered in the two temperature proxies during the abrupt climate events.

#### **1.5. Contributions to publications**

This thesis includes the complete versions of three manuscripts as first-author publications (chapter 3-5). Chapter 3 is an already published manuscript. Chapter 4 includes a submitted manuscript. Chapter 5 is a draft of a manuscript.

**Chapter 3 Organic-geochemical proxies of sea surface temperature in surface sediments of the tropical Eastern Indian Ocean**

Wenwen Chen, Mahyar Mohtadi, Enno Schefuß, Gesine Mollenhauer

In this chapter, extraction of 36 samples, lipids fraction purification and analysis were performed by Wenwen Chen. Wenwen Chen wrote this manuscript with input from all co-authors. Published in *Deep-Sea Research I*, vol. 88, page 17-24, doi:10.1016/j.dsr.2014.03.005.

**Chapter 4 Concentrations and abundance ratios of long-chain alkenones and glycerol dialkyl glycerol tetraethers in sinking particles south off Java**

Wenwen Chen, Mahyar Mohtadi, Enno Schefuß, Gesine Mollenhauer

In this chapter, extraction of 21 samples, lipids fraction purification and analysis were performed by Wenwen Chen. Wenwen Chen wrote this manuscript with input from all co-authors. This manuscript has been submitted to *Deep-Sea Research I*. This chapter includes the revised manuscript based on reviewers' comments.

**Chapter 5 Sea surface and subsurface temperature variations in the upwelling area of the eastern Indian Ocean during the last 22,000 years**

Wenwen Chen, Mahyar Mohtadi, Enno Schefuß, Gesine Mollenhauer

In this chapter, extraction of 154 samples, lipids fraction purification and analysis were performed by Wenwen Chen. Wenwen Chen wrote this manuscript with input from all co-authors. The manuscript is in the form of a draft for submission to *Earth and Planetary Science Letters*.

## 1.6. References

- Andruleit, H., Lückge, A., Wiedicke, M., Stäger, S., 2008. Late Quaternary development of the Java upwelling system (eastern Indian Ocean) as revealed by coccolithophores. *Marine Micropaleontology*, 69(1), 3-15.
- Ashok, K., Guan, Z., Yamagata, T., 2001. Impact of the Indian Ocean dipole on the relationship between the Indian monsoon rainfall and ENSO. *Geophysical Research Letter*, 28(23), 4499-4502.
- Barrows, T.T., Juggins, S., 2005. Sea-surface temperature around the Australian margin and Indian Ocean during the Last Glacial Maximum. *Quaternary Science Reviews*, 24, 1017-1047.
- Basse, A., Zhu, C., Versteegh, G.J.M., Fischer, G., Hinrichs, K.-U., Mollenhauer, G., 2014. Distribution of intact and core tetraether lipids in water column profiles of suspended particulate matter off Cape Blanc, NW Africa. *Organic Geochemistry*, 72, 1-13.
- Beck, J.W., Edwards, R.L., Ito, E., Taylor, F.W., Recy, J., Rougerie, F., Joannot, P., Henin, C., 1992. Sea-Surface Temperature from Coral Skeletal Strontium/Calcium Ratios. *Science*, 257, 644-647.
- Benthien, A., Müller, P.J., 2000. Anomalously low alkenone temperatures caused by lateral particle and sediment transport in the Malvinas Current region, western Argentine Basin. *Deep-Sea Research I*, 47, 2369-2393.
- Boon, J.J., van der Meer, F.W., Schuyl, P.J.W., de Leeuw, J.W., Schenck, P.A., Burlingame, A.L., 1978. Organic geochemical analysis of core samples from site 362 Walvis Ridge, DSDP Leg 40. In Bolli, H.M., and Ryan, W.B.F. (Hrsg.) *Initial Reports of the Deep Sea Drilling Project*, vols. 38, 39, 40, and 41, Supplement, Walvis Ridge DSDP Leg 40. Washington, DC: U.S. Government Printing Office, pp. 627–637.
- Boyer, T.P., Antonov, J.I., Garcia, H.E., Johnson, D.R., Locarnini, R.A., Mishonov, A.V., Pitcher, M.T., Baranova, O.K., Smolyar I.V., 2006, *World Ocean Database 2005 [DVD]*, NOAA Atlas NESDIS, vol. 60, edited by S. Levitus, 190 pp., U.S. Govt. Print. Off, Washington, D. C.

- Bradley, R.S., 1999. Paleoclimatology: reconstructing climates of the Quaternary (Vol. 68). Access online via Elsevier.
- Brassell, S.C., Eglinton G., Marlowe, I.T., Plaumann U., Sarnthein, M., 1986. Molecular stratigraphy: A new tool for climatic assessment. *Nature*, 320,129-133.
- Brochier-Armanet, C., Boussau, B., Gribaldo, S., Forterre, P., 2008. Mesophilic Crenarchaeota: Proposal for a third archaeal phylum, the Thaumarchaeota. *Nature Reviews Microbiology*, 6, 245-252.
- Chen, Wenwen., Mohtadi, M., Schefuß, E., Mollenhauer, G., 2014. Organic-geochemical proxies of sea surface temperature in surface sediments of the tropical Eastern Indian Ocean. *Deep-Sea Research I*, 88, 17-29.
- Conte, M.H., Thompson, A., Lesley, D., Harris, R.P., 1998. Genetic and physiological influences on the alkenone / alkenoate versus growth temperature relationship in *Emiliana huxleyi* and *Gephyrocapsa oceanica*. *Geochimica et Cosmochimica Acta*, 62, 51–68.
- Conte, M.H., Weber, J.C., King, L.L., Wakeham, S.G., 2001. The alkenone temperature signal in western North Atlantic surface waters. *Geochimica et Cosmochimica Acta*, 65, 4275-4287.
- Conte, M.H., Sicre, M.-A., Rühlemann, C., Weber, J.C., Schulte, S., Schulz-Bull, D., Blanz, T., 2006. Global temperature calibration of the alkenone unsaturation index ( $U_{37}^{K'}$ ) in surface waters and comparison with surface sediments. *Geochemistry Geophysics Geosystem*, 7, Q02005.
- De Leeuw J.W., Meer F.W.V.D., Rijpstra W.I.C., Schenck P.A., 1980. On the occurrence and structural identification of long chain unsaturated alkenones and hydrocarbons in sediments. In: *Advances in organic geochemistry 1979*, A. G. Douglas and J. R. Maxwell, editors, Pergamon Press, Oxford, pp. 211-217.
- DeLong, E.F., King, L.L., Massana, R., Cittone, H., Murray, A., Schleper, C., Wakeham, S.G., 1988. Dibiphytanyl ether lipids in nonthermophilic Crenarchaeotes. *Applied and Environmental Microbiology*, 64, 1133-1138.

- DeLong, E.F., 1992. Archaea in coastal marine environments. *Proceedings of the National Academy Science*, 89, 5685-5689.
- DeRose, M., Gambacorta, A., 1988. The lipids of archaeobacteria. *Progress in Lipid Research*, 27, 153-175.
- Du, Y., Qu, T., Meyers, G., Masumoto, Y., Sasaki, H., 2005. Seasonal heat budget in the mixed layer of the southeastern tropical Indian Ocean in a high-resolution ocean general circulation model. *Journal of Geophysical Research*, 110, C04012, doi: 10.1029/2004JC002845.
- Du, Y., Qu, T., Meyers, G., 2008. Interannual Variability of Sea Surface Temperature off Java and Sumatra in a Global GCM. *Journal of Climate*, 21(11), 2451-2465, doi:10.1175/2007JCLI1753.1.
- Emiliani, C., 1955. Pleistocene temperatures. *Journal of Geology*, 63, 538-578.
- Gaines, S.M., Eglinton, G., Rullkotter, J., 2008. *Echoes of Life: What Fossil Molecules Reveal about Earth History*. Oxford University Press.
- Gliozzi, A., Paoli, G., De Rosa, M., Gambacorta, A., 1983. Effect of isoprenoid cyclization on the transition temperature of lipids in thermophilic archae bacteria. *Biochimica et Biophysica Acta-Biomembranes*, 735, 234-242.
- Gong, C., Hollander, D.J., 1999. Evidence for differential degradation of alkenone under contrasting bottom water oxygen conditions: implication for paleotemperature reconstruction. *Geochimica et Cosmochimica Acta*, 63, 405-411.
- Gordon, A.L., Fine, R.A., 1996. Pathways of water between the Pacific and Indian oceans in the Indonesian seas. *Nature*, 379, 146-149.
- Gordon, A.L., 2005. Oceanography of the Indonesian seas and their throughflow. *Oceanography*, 18 (4), 15-27.
- Godfrey, J.S., 1996. The effect of the Indonesian Throughflow on ocean circulation and heat exchange with the atmosphere: A review. *Journal of Geophysical Research*, 101(C5), 12,217-12,237.

- Halkides, D.J., Han, W., Webster, P.J., 2006. Effects of the seasonal cycle on the development and termination of the Indian Ocean Zonal Dipole Mode. *Journal of Geophysical Research*, 111, C12017, doi: 10.1029/2005JC003247.
- Hastenrath, S., Lamb, P.J., 1979. Climatic atlas of the Indian Ocean, Part I: Surface climate and atmospheric circulation. Wisconsin University Press.
- Herbert, T.D., 2003. AlkenonePaleotemperature Determinations. In: *Treatise on Geochemistry*, pp. 391-432. Pergamon, Oxford.
- Henderson, G.M., 2002. New oceanic proxies for paleoclimate. *Earth and Planetary Science Letters*, 203, 1-13.
- Herfort, L., Schouten, S., Boon, J.P., Sinninghe Damsté, J.S., 2006. Application of the TEX<sub>86</sub> temperature proxy in the southern North Sea. *Organic Geochemistry*, 37, 1715-1726.
- Hoefs, M.J.L., Klein-Breteler G.J.M., Schouten, S., Grossi, V., de Leeuw, J.W. Sinninghe Damsté, J.S., 1998. Postdepositional oxic degradation of alkenones: implications for the measurement of palaeo sea surface temperatures. *Paleoceanography*, 13, 42-49.
- Hopmans, E.C., Weijers, J.W.H., Schefuß, E., Herfort, L., Sinninghe Damsté, J.S., Schouten, S., 2004. A novel proxy for terrestrial organic matter in sediments based on branched and isoprenoid tetraether lipids. *Earth and Planetary Science Letters*, 224, 107-116.
- Huguet, C., Kim, J.H., Sinninghe Damsté, J.S., Schouten, S., 2006. Reconstruction of sea surface temperature variations in the Arabian Sea over the last 23 kyr using organic proxies (TEX<sub>86</sub> and U<sup>K</sup><sub>37</sub>). *Paleoceanography*, 21(3).
- Huguet, C., Schimmelmann, A., Thunell, R., Lourens, L.J., Sinninghe Damsté J. S., Schouten, S., 2007. A study of the TEX<sub>86</sub> paleothermometer in the water column and sediments of the Santa Barbara Basin, California. *Paleoceanography*, 22, PA3202.

- Huguet, C., Kim, J.-H., de Lange, G.J., Sinninghe-Damsté, J.S., Schouten, S., 2009. Effects of long term oxic degradation on the  $U^{K'_{37}}$ ,  $TEX_{86}$  and BIT organic proxies. *Organic Geochemistry*, 40, 1188-1194.
- IPCC, 2001. *Climate Change 2001: The science basis. Contribution of working group I to the third assessment report of the intergovernmental panel on climate change* (eds. Houghton, J.T., Ding, Y., Griggs, D.J., Noguer, M., van der Linden, P.J., Dai, X., Maskell, K., Johnson, C.A.) New York: Cambridge University Press.
- IPCC, 2007. *Climate Change 2007: The physical science basis. Contribution of working group I to the fourth assessment report of the intergovernmental panel on climate change* (eds. Solomon, S., Qin, D., Manning, M., Chen, Z., Marquis, M., Averyt, K. B., Tignor, M., and Miller, H. L.) New York: Cambridge University Press.
- Jia, Guodong, Zhang, Jie, Chen, Jianfeng, Peng, Ping'an, Zhang, Chuanlun L., 2012. Archaeatetraether lipids record subsurface water temperature in the South China Sea. *Organic Geochemistry*, 50, 68-77.
- Karner, M.B., DeLong, E.F., Karl, D.M., 2001. Archaeal dominance in the mesopelagic zone of the Pacific Ocean. *Nature*, 409, 507-510.
- Kim, J.-H., Huguet, C., Zonneveld, K.A.F., Versteegh, G.J.M., Roeder, W., Sinninghe Damsté, J.S., Schouten, S., 2009. An experimental field study to test the stability of lipids used for the  $TEX_{86}$  and palaeothermometers. *Geochimica et Cosmochimica Acta*, 73, 2888-2898.
- Kim J.-H., van der Meer, J., Schouten, S., Helmke, P., Willmott, V., Sangiorgi, F., Koç, N., Hopmans, E.C., Sinninghe Damsté, J.S., 2010. New indices and calibrations derived from the distribution of crenarchaeal isoprenoid tetraether lipids: Implications for past sea surface temperature reconstructions. *Geochimica et Cosmochimica Acta*, 74, 4639-4654.
- Lamy, F., Kaiser, J., Arz, H.W., Hebbeln, D., Ninnemann, U., Timm, O., Timmermann, A., Toggweiler, J.R., 2007. Modulation of the bipolar seesaw in the Southeast Pacific during Termination 1. *Earth and Planetary Science Letters*, 259 (3-4), 400-413.

- Lee, K.E., Kim, J.-H., Wilke, I., Helmke, P., Schouten, S., 2008. A study of the alkenones, TEX<sub>86</sub>, and planktonic foraminifera in the Benguela Upwelling System: Implication for past sea surface temperature estimates. *Geochemistry Geophysics Geosystem*, 9, Q10019.
- Leider, A., Hinrichs, K.-U., Mollenhauer, G., Versteegh, G.J.M., 2010. Core-top calibration of the lipid-based U<sup>K</sup><sub>37</sub> and TEX<sub>86</sub> temperature proxies on the southern Italian shelf (SW Adriatic Sea, Gulf of Taranto). *Earth and Planetary Science Letters*, 300, 112-124.
- Lengger, S.K., Hopmans, E.C., Reichert, G.-J., Nierop, K.G.J., Sinninghe Damsté, J.S., Schouten, S., 2012. Intact polar and core glycerol dibiphytanyl glycerol tetraether lipids in the Arabian Sea oxygen minimum zone. Part II: Selective preservation and degradation in sediments and consequences for the TEX<sub>86</sub>. *Geochimica et Cosmochimica Acta*, 98, 244-258.
- Levi, C., Labeyrie, L., Bassinot, F., Guichard, F.O., Cortijo, E., Waelbroeck, C., Caillon, N., Duprat, J., de Garidel-Thoron, T., Elderfield, H., 2007. Low-latitude hydrological cycle and rapid climate changes during the last deglaciation. *Geochemistry Geophysics Geosystem*, 8, Q05N12.
- Locarnini, R. A., A. V. Mishonov, J. I. Antonov, T. P. Boyer, H. E. Garcia, O. K. Baranova, M.M. Zweng, and D. R. Johnson, 2010. *World Ocean Atlas 2009, Volume 1: Temperature*. S. Levitus, Ed., NOAA Atlas NESDIS 68, U.S. Government Printing Office, Washington, D.C., 184 pp.
- Lopes dos Santos, R.A., Prange, M., Castaneda, I. S., Schefuß, E., Mulitza, S., Schulz, M., Niedermeyer, E.A., SinningheDamsté, J.S., Schouten S., 2010. Glacial-interglacial variability in Atlantic Meridional Overturning Circulation and thermocline adjustment in the tropical North Atlantic. *Earth and Planet Science Letters*, 300, 407-414.
- Loulergue, L., Parrenin, F., Blunier, T., Barnola, J.-M., Spahni, R., Schilt, A., Raisbeck, G., Chappellaz, J., 2007. New constraints on the gas age-ice age difference along the EPICA ice cores, 0-50 kyr. *Climate of the Past*, 3, pp. 527-540.

- Lukas, R., Lindstrom, E., 1991. The mixed layer of the western equatorial Pacific Ocean. *Journal of Geophysical Research*, 96, 3343-3358.
- Lückge, A., Mohtadi, M., Rühlemann, C., Scheeder, G., Vink, A., Reinhardt, L., Wiedicke, M., 2009. Monsoon versus ocean circulation controls on paleoenvironmental conditions off southern Sumatra during the past 300,000 years. *Paleoceanography*, 24, PA1208.
- Marlowe, I.T., Brassell, S.C., Eglinton, G., Green, J.C., 1984. Long chain unsaturated ketones and esters in living algae and marine sediments. *Organic Geochemistry*, 6, 135-141.
- Mohtadi, M., Lückge, A., Steinke, S., Groeneveld, J., Hebbeln, D., Westphal, N., 2010a. Late Pleistocene surface and thermocline conditions of the eastern tropical Indian Ocean. *Quaternary Science Reviews* 29, 887-896.
- Mohtadi, M., Steinke, S., Lückge, A., Groeneveld, J., Hathorne, E.C., 2010b. Glacial to Holocene surface hydrography of the tropical eastern Indian Ocean. *Earth and Planetary Science Letters*, 292, 89-97.
- Mohtadi, M., Oppo, D.W., Steinke, S., Stuut, J.B.W., De Pol-Holz, R., Hebbeln, D., Lückge, A., 2011. Glacial to Holocene swings of the Australian-Indonesian monsoon. *Nature Geoscience*, 4(8), 540-544.
- Mohtadi, M., Prange, M., Oppo, D.W., De Pol-Holz, R., Merkel, U., Zhang, X., Steinke, S., Lückge, A., 2014. North Atlantic forcing of tropical Indian Ocean climate. *Nature*, 509, 76-80.
- Mollenhauer, G., Inthorn, M., Vogt, T., Zabel, M., Sinninghe-Damsté, J.S., Eglinton, T.I., 2007. Aging of marine organic matter during cross-shelf lateral transport in the Benguela upwelling system revealed by compound-specific radiocarbon dating. *Geochemistry Geophysics Geosystem*, 8, Q09004, doi:10.1029/2007GC001603.
- Mollenhauer, G., Eglinton, T.I., Hopmans, E.C., Sinninghe-Damsté, J.S., 2008. A radiocarbon-based assessment of the preservation characteristics of crenarchaeol and alkenones from continental margin sediments. *Organic Geochemistry*, 39, 1039-1045.

- Müller, P.J., Kirst, G., Ruhland, G., Von Storch, I., Rosell-Melé, A., 1998. Calibration of the alkenone paleotemperature index  $U_{37}^K$  based on core-tops from the eastern South Atlantic and the global ocean (60°N-60°S). *Geochimica et Cosmochimica Acta*, 62, 1757-1772.
- Murgese, D.S., De Deckker, P., Spooner, M.I., Young, M., 2008. A 35,000 years records of changes in the eastern Indian Ocean offshore Sumatra. *Palaeogeography, Palaeoclimatology, Palaeoecology*, 265, 195-213.
- Murray, A.E., Preston, C.M., Massana, R., Taylor, L.T., Blakis, A., Wu, K. and De Long, E.F., 1998. Seasonal and spatial variability of bacterial and archaeal assemblages in the coastal waters near Anvers Island, Antarctica. *Applied and Environmental Microbiology*, 64, 2585-2595.
- Neale, R., Slingo, J., 2003. The maritime continent and its role in the global climate: A GCM study. *Journal of Climate* 16(5), 834-848.
- Nuernberg, D., 1995. Magnesium in tests of *Neogloboquadrina pachyderma* sinistral from high northern and southern latitudes. *The Journal of Foraminiferal Research*, 25, 350-368.
- Ohkouchi, N., Kawamura, K., Kawahata, H., Okada, H., 1999. Depth ranges of alkenone production in the central Pacific Ocean. *Global Biogeochemical Cycles*, 13, 695-704.
- Ohkouchi, N., Eglinton, T.I., Keigwin, L.D., Hayes, J.M., 2002. Spatial and temporal offsets between proxy records in a sediment drift. *Science*, 298, 1224-1227.
- Oldfield, F., Thompson, R., 2004. Archives and Proxies along the PEP III Transect. In: *Past Climate Variability through Europe and Africa* (eds. Battarbee, R.W., Gasse, F., Stickley, C.E.). Springer Netherlands, pp. 7-29.
- Pearson, A., Ingalls, A.E., 2013. Assessing the use of archaeal lipids as marine environmental proxies. *Annual Review of Earth and Planetary Science* 41, 359-384.
- Peters, K.E., Walters, C.C., Moldowan, J.M., 2005. *The Biomarker Guide: Biomarkers and Isotopes in Petroleum Exploration and Earth History*. Cambridge University Press, New York.

- Peterson, T.C., Vose, R.S., 1997. An overview of the global historical climatology network temperature database. *Bulletin of the American Meteorological Society*, 2837-2849.
- Popp, B.N., Prah, F.G., Wallsgrave, R.J., Tanimoto, J., 2006. Seasonal patterns of alkenone production in the subtropical oligotrophic North Pacific. *Paleoceanography*, 21.
- Prah, F.G., Wakeham, S.G., 1987. Calibration of unsaturation patterns in long-chain ketone compositions for palaeotemperature assessment. *Nature*, 330, 367-369.
- Prah, F.G., Muehlhausen, L.A., Zahnle, D.L., 1988. Further evaluation of long-chain alkenones as indicators of paleoceanographic conditions. *Geochimica et Cosmochimica Acta*, 52, 2303-2310.
- Prah, F.G., Wolfe, G.V., Sparrow, M.A., 2003. Physiological impacts on alkenone paleothermometry. *Paleoceanography*, 18, PA1025.
- Prah, F.G., Popp, B.N., Karl, D.M., Sparrow, M.A., 2005. Ecology and biogeochemistry of alkenone production at Station ALOHA. *Deep-Sea Research I*, 52, 699-719.
- Qu, T., Du, Y., Strachan, J., Meyers, G., Slingo, J. M., 2005. Sea surface temperature and its variability in the Indonesian region. *Oceanography*, 18, 50-61, doi:10.5670/oceanog.2005.05.
- Qu, T., Meyers, G., 2005. Seasonal characteristics of circulation in the southeastern tropical Indian Ocean. *Journal of Physical Oceanography*, 35(2), 255-267, doi:10.1175/JPO-2682.1.
- Rahmstorf, S., 2002. Ocean circulation and climate during the past 120,000 years. *Nature*, 419, 207-214.
- Romero, O.E., Mohtadi, M., Helmke, P., Hebbeln, D., 2012. High interglacial diatom paleoproductivity in the westernmost Indo-Pacific Warm Pool during the past 130,000 years. *Paleoceanography*, 27(3).
- Rommerskirchen, F., Condon T., Mollenhauer, G., Dupont, L., Schefuss, E., 2011. Miocene to Pliocene development of surface and subsurface temperature in the Benguela Current System. *Paleoceanography*, 26, PA3216.

- Rosenthal, Y., Oppo, D.W., Linsley, B.K., 2003. The amplitude and phasing of climate change during the last deglaciation in the Sulu Sea, western equatorial Pacific. *Geophysical Research Letters*, 30(8), 1428.
- Rosell-Melé, A., Prahl, F.G., 2013. Seasonality of UK'37 temperature estimates as inferred from sediment trap data. *Quaternary Science Reviews*, 72, 128-136.
- Saji, N. H., Goswami, B. N., Vinayachandran, P. N., Yamagata, T., 1999. A dipole mode in the tropical Indian Ocean. *Nature*, 401(6751), 360-363.
- Sawada, K., Handa, N., Shiraiwa, Y., Danbara, A., Montani, S., 1996. Long-chain alkenones and alkyl alkenoates in the coastal and pelagic sediments of the northwest North Pacific, with special reference to the reconstruction of *Emiliania huxleyi* and *Gephyrocapsa oceanica* ratios. *Organic Geochemistry*, 24, 751-764.
- Schouten, S., Hopmans, E.C., Pancost, R.D., Sinninghe Damsté, J.S., 2000. Widespread occurrence of structurally diverse tetraether membrane lipids: evidence for the ubiquitous presence of low-temperature relatives of hyperthermophiles. *Proceedings of National Academy of Sciences*, 97, 14421-14426.
- Schouten, S., Hopmans, E.C., Schefuss, E., Sinninghe Damsté, J.S., 2002. Distributional variations in marine crenarchaeotal membrane lipids: a new tool for reconstructing ancient sea water temperatures? *Earth and Planetary Science Letters*, 204, 265-274.
- Schouten, S., Hopmans, E.C., van der Meer, J., Mets, A., Bard, E., Bianchi, T.S., Diefendorf, A., Escala, M., Freeman, K.H., Furukawa, Y., Huguet, C., Ingalls, A., Ménot-Combes, G., Nederbragt, A.J., Oba, M., Pearson, A., Pearson, E.J., Rosell-Melé, A., Schaeffer, P., Shah, S.R., Shanahan, T.M., Smith, R.W., Smittenberg, R., Talbot, H.M., Uchida, M., Van Mooy, B.A.S., Yamamoto, M., Zhang, Z., Sinninghe Damsté, J.S., 2009. An interlaboratory study of TEX<sub>86</sub> and BIT analysis using high-performance liquid chromatography-mass spectrometry. *Geochemistry Geophysics Geosystem*, 10, Q03012.
- Schouten, S., Pitcher, A., Hopmans, E.C., Villanueva, L., van Bleijswijk, J., Sinninghe Damsté, J.S., 2012. Intact polar and core glycerol dibiphytanyl glycerol tetraether

- lipids in the Arabian Sea oxygen minimum zone: I. Selective preservation and degradation in the water column and consequences for the TEX<sub>86</sub>. *Geochimica et Cosmochimica Acta*, 98, 228-243.
- Schouten, S., Hopmans, E.C., Sinninghe Damsté, J.S., 2013. The organic geochemistry of glycerol dialkyl glycerol tetraether lipids: A review. *Organic Geochemistry*, 54, 19-61.
- Sikes, E.L., Volkman, J.K., 1993. Calibration of alkenone unsaturation ratios ( $U_{37}^K$ ) for paleotemperature estimation in cold polar waters. *Geochimica et Cosmochimica Acta*, 57, 1883-1889.
- Sikes, E.L., Volkman, J.K., Robertson, L.G., Pichon, J.-J., 1997. Alkenones and alkenes in surface waters and sediments of the Southern Ocean: Implications for paleotemperature estimation in polar regions. *Geochimica et Cosmochimica Acta*, 61, 1495-1505.
- Sinninghe Damsté, J.S., Hopmans, E.C., Pancost, R.D., Schouten, S., Geenevasen, J.A., 2000. Newly discovered non-isoprenoid glycerol dialkyl glycerol tetraether lipids in sediments. *Chemical Communications*, 17, 1683-1684.
- Sinninghe Damsté, J.S., Schouten, S., Hopmans, E.C., van Duin, A.C.T., Geenevasen, J.A.J., 2002. Crenarchaeol: the characteristic core glycerol dibiphytanyl glycerol tetraether membrane lipid of cosmopolitan pelagic crenarchaeota. *Journal of Lipid Research*, 43, 1641-1651.
- Sinninghe Damsté, J.S., Rijpstra, W.I.C., Reichart, G.-J., 2002b. The influence of oxic degradation on the sedimentary biomarker record II. Evidence from Arabian Sea sediments. *Geochimica et Cosmochimica Acta*, 66, 2737-2754.
- Sprintall, J., Tomczak, M., 1992. Evidence of the barrier layer in the surface layer of the tropics. *Journal of Geophysical Research*, 97, 7305-7316.
- Stott, L., Poulsen, C., Lund, S., Thunell, R., 2002. Super ENSO and global climate oscillations at millennial time scales. *Science*, 297, 222-226.
- Susanto, R.D., Gordon, A.L., Zheng, Q., 2001. Upwelling along the coasts of Java and Sumatra and its relation to ENSO. *Geophysical Research Letters*, 28, 1599-1602.

- Susanto, R.D., Moore II, T.S., Marra, J., 2006. Ocean color variability in the Indonesian Seas during the SeaWiFS era. *Geochemistry, Geophysics, Geosystems*, 7, Q05021, doi:10.1029/2005GC001009.
- Tapper, N.J., 2002. Climate, climatic variability and atmospheric circulation patterns in the maritime continent region, in *Bridging Wallace's Line: The Environmental and Cultural History and Dynamics of the Southeast Asian–Australian Region*, edited by P. Kershaw et al., pp. 5-28, Catena, Reiskirchen, Germany.
- Ternois, Y., Sicre, M.A., Boireau, A., Conte, M.H., Eglinton, G., 1997. Evaluation of long chain alkenones as paleo-temperature indicators in the Mediterranean Sea. *Deep-Sea Research I*, 44, 271-286.
- Tomczak, M., Godfrey, J.S., 1994. *Regional oceanography: an introduction*. Elsevier, New York.
- Thurman, H.V., Trujillo, A., 1999. Air Sea interaction, in *Essentials of oceanography*, 6th ed. Macmillan Publishing company, a division of Macmillan, Inc. pp171-204.
- Turich, C., Freeman K. H., Bruns M. A., Conte M., Jones A. D. Wakeham S. G., 2007. Lipid of marine Archaea: Patterns and provenance in the water-column and sediments. *Geochimica et Cosmochimica Acta*, 71, 3272–3291.
- Uda, I., Sugai, A., Itoh, Y.H., Itoh, T., 2001. Variation on molecular species of polar lipids from *Thermoplasma acidophilum* depends on growth temperature. *Lipids*, 36, 103-105.
- Visser, K., Thunell, R.C., Stott, L.D., 2003. Magnitude and timing of temperature change in the Indo-Pacific warm pool during deglaciation. *Nature*, 421 (9), 152-155.
- Volkman, J.K., Eglinton, G., Corner, E.D.S., Forsberg, T.E.V., 1980. Long-chain alkenes and alkenones in the marine coccolithophorid *Emiliania huxleyi*. *Phytochemistry*, 19, 2619-2622.
- Volkman, J.K., Barrerr, S.M., Blackburn, S.I., Sikes, E.L., 1995. Alkenones in *Gephyrocapsa oceanica*: Implications for studies of paleoclimate. *Geochimica et Cosmochimica Acta*, 59, 513-520.

- Wang, J.-X., Wei, Y., Wang, P., Hong, Y., Zhang, C.L., 2015. Unusually low TEX<sub>86</sub> values in the transitional zone between Pearl River estuary and coastal South China Sea: Impact of changing archaeal community composition. *Chemical Geology*, 402, 18-29.
- Wang, P., Clemens, S., Beaufort, L., Braconnot, P., Ganssen, G., Jian, Z., Kershaw, P., Sarnthein, M., 2005. Evolution and variability of the Asian monsoon system: state of the art and outstanding issues. *Quaternary Science Reviews*, 24, 595-629.
- Webster, P. J., Moore, A.M., Loschnigg, J.P., Leben, R.R., 1999. Coupled ocean-atmosphere dynamics in the Indian Ocean during 1997-98. *Nature*, 401(6751), 356-360.
- Weijers, J.W.H., Schouten, S., Spaargaren, O.C., Sinninghe Damsté, J.S., 2006. Occurrence and distribution of tetraether membrane lipids in soil: Implications for the use of the TEX<sub>86</sub> proxy and the BIT indeed. *Organic Geochemistry*, 37, 1680-1693.
- Wuchter, C., Schouten, S., Wakeham, S.G., Sinninghe Damsté, J.S., 2006. Archaeal tetraether membrane lipid fluxes in the northeastern Pacific and the Arabian Sea: implications for TEX<sub>86</sub> paleothermometry. *Paleoceanography*, 21, PA4208.
- Xing, L., Sachs, J.P., Gao, W., Tao, S., Zhao, X., Li, L., Zhao, M., 2015. TEX<sub>86</sub> paleothermometer as an indication of bottom water temperature in the Yellow Sea. *Organic Geochemistry*, 86, 19-31.
- Xu, J., Holbourn, A., Kuhnt, W., Jian, Z., Kawamura, H., 2008. Changes in the thermocline structure of the Indonesian outflow during Terminations I and II. *Earth and Planetary Science Letters*, 273 (1-2), 152-162.
- You, Y., Tomczak, M., 1993. Thermocline circulation and ventilation in the Indian Ocean derived from water mass analysis. *Deep-Sea Research I*, 40, 13-56.

## Chapter 2 Study Material and Methods

### 2.1. Study Material

Analyses were done on marine surface sediments, a sediment core and materials collected in a sediment trap. Marine surface sediments (GeoB10008 to -69) and the gravity core (GeoB10053-7) were retrieved during PABESIA RV Sonne Cruise SO-184 in 2005 along the eastern IO (Hebbeln et al., 2005). Surface sediments represent the top 1 cm of multicore samples from 36 sites collected off west Sumatra, south Java and LSI. The materials are stored at -20 °C in the MARUM core repository and kept at this temperature until geochemical processing. Core GeoB10053-7 (8°40.56'S, 112°50.33'E, at 1372m water depth) was collected off south Java. Samples are taken every 5 cm intervals and started at 3 cm depth. The sediment trap (8°17.5'S, 108°02.0'E, at 2200m water depth) has been deployed off south Java between December 2001 and November 2012. Sampling intervals varied in general every 16 days.

Surface sediments and the gravity core ages were established by ten and nineteen accelerator mass spectrometry (AMS) <sup>14</sup>C dates on planktic foraminifera, respectively (Mohtadi et al., 2011a, b). The age determinations show that the surface sediments are modern. The gravity core covers the past ca. 22,000 years.

### 2.2. Methods

In this study, standard organic geochemical techniques were employed. All samples were freeze-dried and homogenized before being subjected to extraction using organic solvents.

#### 2.2.1. Lipid extraction

Lipid extraction was carried out following the protocol described by Müller et al. (1998) and Leider et al. (2010) (Fig. 2.1.). About 5 g sediments were extracted three times using an ultrasonic probe with methanol (MeOH), MeOH: dichloromethane (DCM) 1:1 (v:v) and DCM (25 mL each). Before extraction known amounts of C<sub>19</sub> ketone and C<sub>46</sub>

GDGT were added as internal standards. The combined extracts were washed with 50 mL deionized water. The DCM: MeOH phase was separated, dried over anhydrous sodium sulphate, and the solvent was evaporated by rotary evaporation under vacuum. The lipid extract was saponified for 2 hours at 80 °C with 300  $\mu$ L of 0.1M KOH in 90:10 MeOH/H<sub>2</sub>O, and fractionated into three polarity fractions using silica gel column chromatography. The fractions containing the alkenones and GDGTs were obtained by eluting with DCM: hexane 2:1 (v:v) and MeOH, respectively, and dried using a Silli-Therm at 50 °C under a stream of nitrogen (Fig. 2.1.).

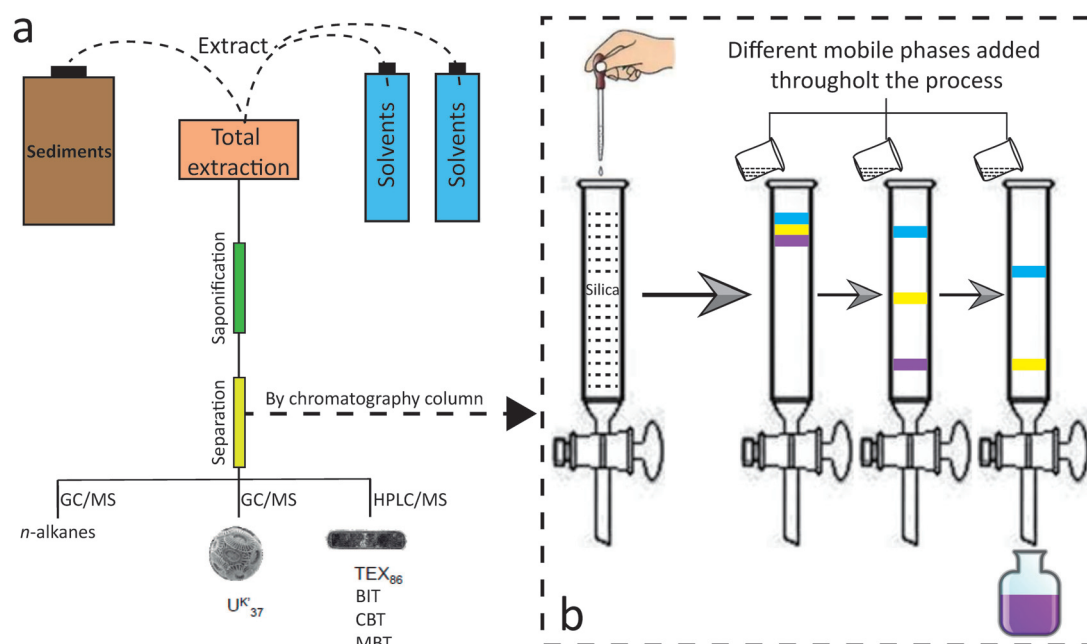


Fig. 2.1.a). Schematic view of the integrated organic geochemical lab procedures in lipid biomarker fractions; b).Schematic of silica column chromatography to separate a mixture of organic compounds into different fractions prior to analysis.

### 2.2.2. Alkenone analysis

The alkenone fraction was re-dissolved in 25  $\mu$ L MeOH: DCM 1:1 (v:v) prior to capillary gas chromatography (GC). Analyses were performed using an HP5890 series GC equipped with a flame ionization detector, using Helium as carrier gas with a constant

flow rate of 2.0 mL/min. Initial oven temperature was 60 °C, held for 1 min, subsequently increased to 150 °C at a rate of 10 °C/min, then raised to 310 °C at a rate of 4 °C/min with a total run-time of 75 min.

Peak identification of di- and tri-unsaturated C<sub>37</sub> alkenones (C<sub>37:2</sub> and C<sub>37:3</sub>) was based on retention time and comparison with parallel GC runs of extracts of a lab-internal standard sediment. Quantification was achieved by peak integration relative to the internal standard C<sub>19</sub> ketone and by assuming the same response factor as C<sub>36</sub> n-alkane measured as external standard. The instrumental precision for alkenone analysis is estimated to be ~0.15 °C based on duplicate measurements.

### **2.2.3. GDGTs analysis**

The polar fraction containing the isoprenoid and branched GDGTs was dried under a stream of nitrogen, weighed, re-dissolved in n-hexane: isopropanol 99:1 (v/v) with a concentration of 2 mg/mL (Schouten et al., 2009), and filtered using a 0.45 µm PTFE filter prior to analysis as described by Hopmans et al. (2000, 2004).

Analyses were performed as described in Leider et al. (2010) using an Agilent 1200 Series high performance liquid chromatography system with an Agilent 6210 mass spectrometer (HPLC -MS). 20 µL aliquots were injected onto an Alltech Prevail Cyano column (2.1×150 mm, 3 µm; Grace) maintained at 30 °C. GDGTs were eluted using the following gradient with solvent A (n-hexane) and solvent B (5% isopropanol in n-hexane): 80% A: 20% B for 5 min, linear gradient to 36% B in 45 min. The flow rate was 0.2 mL/min. After each analysis the column was cleaned by back-flushing with n-hexane: isopropanol 90:10 (v/v) at 0.2 mL/min for 8 min. The instrumental precision of GDGT analysis is estimated to be ~0.18 °C depended on duplicate measurements.

### 2.3. References

- Hebbeln, D., et al. 2005. Report and preliminary results of RV SONNE cruise SO-184, PABESIA, Durban (South Africa)-Cilacap (Indonesia)-Darwin (Australia), July 8th-September 13th, 2005, Rep. 246, 142 pp., Univ. Bremen, Bremen, Germany.
- Hopmans, E.C., Schouten, S., Pancost, R.D., van der Meer, M.T.J., Sinninghe Damsté, J.S., 2000. Analysis of intact tetraether lipids in archaeal cell material and sediments by high performance liquid chromatography/atmospheric pressure chemical ionization mass spectrometry. *Rapid Communications in Mass Spectrometry*, 14, 585-589.
- Hopmans, E.C., Weijers, J.W.H., Schefuß, E., Herfort, L., Sinninghe Damsté, J.S., Schouten, S., 2004. A novel proxy for terrestrial organic matter in sediments based on branched and isoprenoid tetraether lipids. *Earth and Planetary Science Letters*, 224, 107-116.
- Leider, A., Hinrichs, K.-U., Mollenhauer, G., Versteegh, G.J.M., 2010. Core-top calibration of the lipid-based  $U^{K'}_{37}$  and  $TEX_{86}$  temperature proxies on the southern Italian shelf (SW Adriatic Sea, Gulf of Taranto). *Earth and Planetary Science Letters*, 300, 112-124.
- Mohtadi, M., Oppo, D.W., Lückge, A., DePol-Holz, R., Steinke, S., Groeneveld, J., Hemme, N., Hebbeln, D., 2011a. Reconstructing the thermal structure of the upper ocean: Insights from planktic foraminifera shell chemistry and alkenones in modern sediments of the tropical eastern Indian Ocean. *Paleoceanography*, 26, PA3219.
- Mohtadi, M., Oppo, D.W., Steinke, S., Stuut, J.B.W., De Pol-Holz, R., Hebbeln, D., Lückge, A., 2011b. Glacial to Holocene swings of the Australian-Indonesian monsoon. *Nature Geoscience*, 4(8), 540-544.
- Müller, P.J., Kirst, G., Ruhland, G., von Storch, I., Rosell-Melé, A., 1998. Calibration of the alkenone paleotemperature index  $U^{K'}_{37}$  based on core-tops from the eastern South Atlantic and the global ocean (60°N–60°S). *Geochimica et Cosmochimica Acta*, 62, 1757-1772.

Schouten, S., Hopmans, E.C., van der Meer, J., Mets, A., Bard, E., Bianchi, T.S., Diefendorf, A., Escala, M., Freeman, K.H., Furukawa, Y., Huguet, C., Ingalls, A., Ménot-Combes, G., Nederbragt, A.J., Oba, M., Pearson, A., Pearson, E.J., Rosell-Melé, A., Schaeffer, P., Shah, S.R., Shanahan, T.M., Smith, R.W., Smittenberg, R., Talbot, H.M., Uchida, M., Van Mooy, B.A.S., Yamamoto, M., Zhang, Z., Sinningh-Damsté, J.S., 2009. An interlaboratory study of TEX<sub>86</sub> and BIT analysis using high performance liquid chromatography-mass spectrometry. *Geochemistry Geophysics Geosystem*, 10, Q03012.

## **Chapter 3 Organic-geochemical proxies of sea surface temperature in surface sediments of the tropical Eastern Indian Ocean**

Wenwen Chen<sup>1</sup>, Mahyar Mohtadi<sup>2</sup>, Enno Schefuß<sup>2</sup>, Gesine Mollenhauer<sup>1,2,3\*</sup>

<sup>1</sup> Department of Geosciences, University of Bremen, Bremen, Germany

<sup>2</sup> MARUM-Center for Marine Environmental Sciences, University of Bremen, Bremen, Germany

<sup>3</sup> Alfred-Wegener Institute for Polar and Marine Research, Bremerhaven Germany

\*corresponding author; gesine.mollenhauer@awi.de

Published in Deep-Sea Research I 88, 17-29 (2014)

### 3.1. Abstract

In this study we reconstruct sea surface temperatures (SSTs) using two lipid-based biomarker proxies (alkenone unsaturation index  $U_{37}^K$  and  $TEX_{86}$  index based on glycerol dibiphytanyl glycerol tetraethers) in 36 surface sediment samples from the Indonesian continental margin off west Sumatra and south of Java and the Lesser Sunda Islands. Comparison of measured temperatures (World Ocean Atlas 09) to reconstructed temperatures suggests that SST estimates based on  $U_{37}^K$  reflect the SE monsoon SST in the upwelling area south of Java and the Lesser Sunda Islands. Estimates based on  $TEX_{86}$  using the calibration for temperatures  $>20$  °C ( $TEX_{86}^H$ ) are up to 2 °C lower than  $U_{37}^K$ -based SSTs. This offset is possibly related to either one or a combination of two factors: i) the depth habitats of the source organisms; ii) different seasonal production and/ or seasonality of export associated with phytoplankton blooming triggered by primary productivity. In the non-upwelling area off west Sumatra, the alkenone-based SSTs are cooler than measured temperatures during the entire year, likely reflecting the limitation of the  $U_{37}^K$  proxy beyond 28 °C, while reconstructed temperatures based on  $TEX_{86}^H$  are consistent with mean annual SST.

### 3.2. Introduction

Accurate SST reconstructions are an important prerequisite for understanding the climate system. Two organic-geochemical proxies, namely  $U_{37}^K$  (alkenone unsaturation) and  $TEX_{86}$  (tetraether index of glycerol dibiphytanyl glycerol tetraether with 86 carbon atoms), are widely employed to reconstruct surface water temperatures in the oceans and in lakes.

Alkenones, di- and tri-unsaturated  $C_{37}$  methyl ketones, are synthesized by prymnesiophyte algae (Brassell et al., 1986). The coccolithophores *Emiliana huxleyi* and *Gephyrocapsa oceanica* are the two major source organisms of alkenones (Conte et al., 1998; Volkman et al., 1980). A range of alkenone studies in surface waters and cultures have demonstrated the close linkage between the alkenone unsaturation ratio and

growth temperatures of the precursor organisms (Conte et al., 1992, 1994; Conte and Eglinton, 1993; Marlowe, 1984; Prah et al., 1988; Volkman et al., 1995; Yamamoto et al., 2000).

For temperature estimation, the unsaturation is generally expressed as the  $U^{K'}_{37}$  ratio (Prah et al., 1987). Since its introduction in 1987, determination of alkenone unsaturation has become a widespread technique to reconstruct past SST from marine sediments. Previous calibration studies showed linear relationships between global marine core-top  $U^{K'}_{37}$  and mean annual surface water temperature (Conte et al., 1998, 2006; Müller et al., 1998). The temperature range of the calibration spans from 2 to 28 °C. Sedimentary records of  $U^{K'}_{37}$  correlate well with mean annual SST (ma SST) in the surface waters and have proven reliable and robust for reconstructing past SST changes (Herbert, 2003). However, occasionally observed deviations between global calibrations and sedimentary alkenone temperature are still contentious. Discrepancies between  $U^{K'}_{37}$  and ma SST have been explained by physical factors such as, for instance, lateral redistribution of sediments (Benthien and Müller 2000), ecological factors like export production originating from below the euphotic zone (Prah et al., 1993, 2001; Ternois et al., 1997), influence of nutrients (Versteegh et al., 2001), and the thriving of alkenone-producers in specific seasons (Popp et al., 2006). In addition, species composition (Conte et al., 1998) and differential degradation of alkenones (Conte et al., 1992; Prah et al., 1989) could also affect the temperature-estimates derived from  $U^{K'}_{37}$ .

Schouten et al. (2002) introduced another organic proxy,  $TEX_{86}$ , based on the relative distribution of glycerol dialkyl glycerol tetraethers (GDGT). These GDGTs are membrane lipids produced by marine Crenarchaeota, re-named Thaumarchaeota (Brochier-Armanet et al., 2008). The relative distribution of the GDGTs is suggested to vary with growth temperature, similar to the  $U^{K'}_{37}$  (Schouten et al., 2013b and reference therein). In the last decade, several calibration studies using core-top sediments and archaeal cultures have been conducted, and linear as well as non-linear regressions with

SST have been proposed (Liu et al., 2009; Kim et al., 2008; Schouten et al., 2002; Wuchter et al., 2006). More recently, the original proxy has been refined further into  $\text{TEX}_{86}^{\text{H}}$  and  $\text{TEX}_{86}^{\text{L}}$  by Kim et al (2010) for temperatures higher and lower than 15 °C, respectively. The  $\text{TEX}_{86}$  proxy is expected to reflect the temperature in the upper parts of the water column (Schouten et al., 2002; Wuchter et al., 2006). Although the GDGT-based proxy has already been widely used, it remains uncertain as to how well it reflects ma SST. For example, some studies suggested that  $\text{TEX}_{86}$  does not reflect SST, but rather subsurface temperature due to additional production of GDGTs below the mixed layer (Huguet et al., 2007; Lee et al., 2008; Lopes dos Santos et al., 2010). Other studies have shown that the  $\text{TEX}_{86}$  may be biased due to seasonality in growth or export of Thaumarchaeota, e.g., towards summer temperature in the eastern Mediterranean (Leider et al., 2010) and the South China Sea (Jia et al., 2012), or towards winter temperature in the southern North Sea (Herfort et al., 2006). Additionally, it has been suggested that the  $\text{TEX}_{86}$  signal reflects other temperatures than annual mean SST because Thaumarchaeota are outcompeted by and phytoplankton including alkenone producers e.g., during upwelling events, and thus thrive during seasons or at depths less favourable for phytoplankton producers (Rommerskirchen et al., 2011; Wuchter et al., 2006, Lee et al., 2008; Turich et al., 2007). Another complication arises from input of terrestrially derived isoprenoid GDGTs (Weijers et al., 2006).

Hopmans et al. (2004) proposed the Branched and Isoprenoid Tetraether (BIT) index, a proxy for the relative abundance of terrestrial soil organic matter in the marine environment, which could bias the  $\text{TEX}_{86}$  (Herfort et al., 2006). The BIT index represents the ratio between crenarchaeol and three branched GDGT lipids in marine and lacustrine sediments, and is expected to be near 1 in soils and approach 0 in deep sea sediments with negligible contribution o soil-derived terrestrial organic matter (Hopmans et al., 2004). The proxy can potentially be used to assess whether a bias of the  $\text{TEX}_{86}$  index by input of soil-derived isoprenoid GDGTs is to be expected, and cut-off values of BIT <0.3 or <0.2 have been suggested (Weijers et al., 2006; Zhu et al., 2011).

These values are not to be regarded globally reliable, as on the one hand potential impact of terrestrially derived isoprenoid GDGTs, depends not only on the relative contribution to total isoprenoid GDGTs in marine sediments but also on the relative abundance of those GDGTs that are relevant for TEX<sub>86</sub> in the soils of the source area. The latter parameter in most cases is complicated to determine. On the other hand, BIT index determinations are not directly comparable between different laboratories (Schouten et al., 2013a), which is further complicating the use of BIT.

Generally, all temperature proxies have their uncertainties. To better understand the significance of each proxy, multiple proxies have been applied to the same sediment material. Comparison of U<sup>K</sup><sub>37</sub> and TEX<sub>86</sub> data for sediments and suspended particles has been reported in several publications (e.g., Huguet et al., 2006; Jia et al., 2012; Lee et al., 2008; Leider et al., 2010; Lopes dos Santos et al., 2010; Rommerskirchen et al., 2011). These studies attributed a significant potential source of uncertainty to different seasonal production and/or depth habitats of the source organisms.

In this study, we investigate the applicability of the U<sup>K</sup><sub>37</sub> and TEX<sup>H</sup><sub>86</sub> indices in the upwelling and non-upwelling areas of the eastern tropical Indian Ocean. We present alkenone and GDGT data from 36 surface sediment samples and compare the reconstructed temperatures to temperatures from the World Ocean Atlas 2009 in order to evaluate the factors influencing these proxies in the study area.

### **3.3. Study area**

The eastern tropical Indian Ocean south of Java and the Lesser Sunda Islands (LSI) is strongly affected by the Australian-Indonesian Monsoon (AIM) system and the seasonal shifting of the Inter-Tropical Convergence Zone (ITCZ), which cause opposite seasonal characteristics at the sea surface (Tomczak & Godfrey, 1994; Webster et al., 1998). During the austral winter (Fig. 3.1b.), the ITCZ is in the Northern Hemisphere and the southeast (SE) monsoon (July – September) winds are such that the southeast trades from Australia induce dry conditions off Java and the LSI. During the austral summer

(January – March, Fig. 3.1a.), the ITCZ migrates to northern Australia and the northwest (NW) monsoon is associated with the opposite wind direction from the Indonesian Seas and Asian continent carrying warm and moist air to the region. The precipitation rates over this region during NW monsoon are among the highest in the world resulting in maximum riverine discharge (Milliman et al., 1999). During this time, the predominant winds force the South Java Current (SJC) to flow from northwest to the southeast, before turning southward to eventually join the South Equatorial Current (SEC) (Fig. 3.1a.). Advection of fresher Java Sea waters through the Sunda Strait and run-off from Sumatra and Java are responsible for the low-salinity “tongue” in the SJC (Qu et al., 2005).

During the SE monsoon (Fig. 3.1b.), the SJC and its prolongation, the SEC, flow westward along the southern coast of Java, when coastal upwelling off Java and the LSI occurs (Tomczak & Godfrey, 1994). The upwelling is associated with higher chlorophyll-a concentration (Fig. 3.1f, g.), higher salinities and SSTs that are 1-2 °C lower compared to the non-upwelling season (Gordon et al., 2005, Susanto et al., 2006). In contrast, the area off W and NW Sumatra does not show any significant seasonality in SST and precipitation and is considered a non-upwelling, ever-wet tropical region (Fig. 3.1a, b, c; Aldrian and Susanto, 2003).

The Indonesian Throughflow (ITF) connects the upper water masses of the Pacific and Indian Oceans and substantially influences the salinity and heat exchange between these oceans (Gordon and Fine, 1996). During the SE monsoon season (Fig. 3.1b.), the sea level difference between the Western Pacific and the Eastern Indian Ocean is largest, implying maximum strength in ITF (Tomczak & Godfrey, 1994). It is suggested that the Java upwelling system is counterbalanced by the ITF and, consequently, except for brief periods, fails to bring subsurface nutrients to the surface (Godfrey, 1996). In this case, the ITF branch through the Lombok Strait counteracts a significant SST depression off Java during the upwelling season.

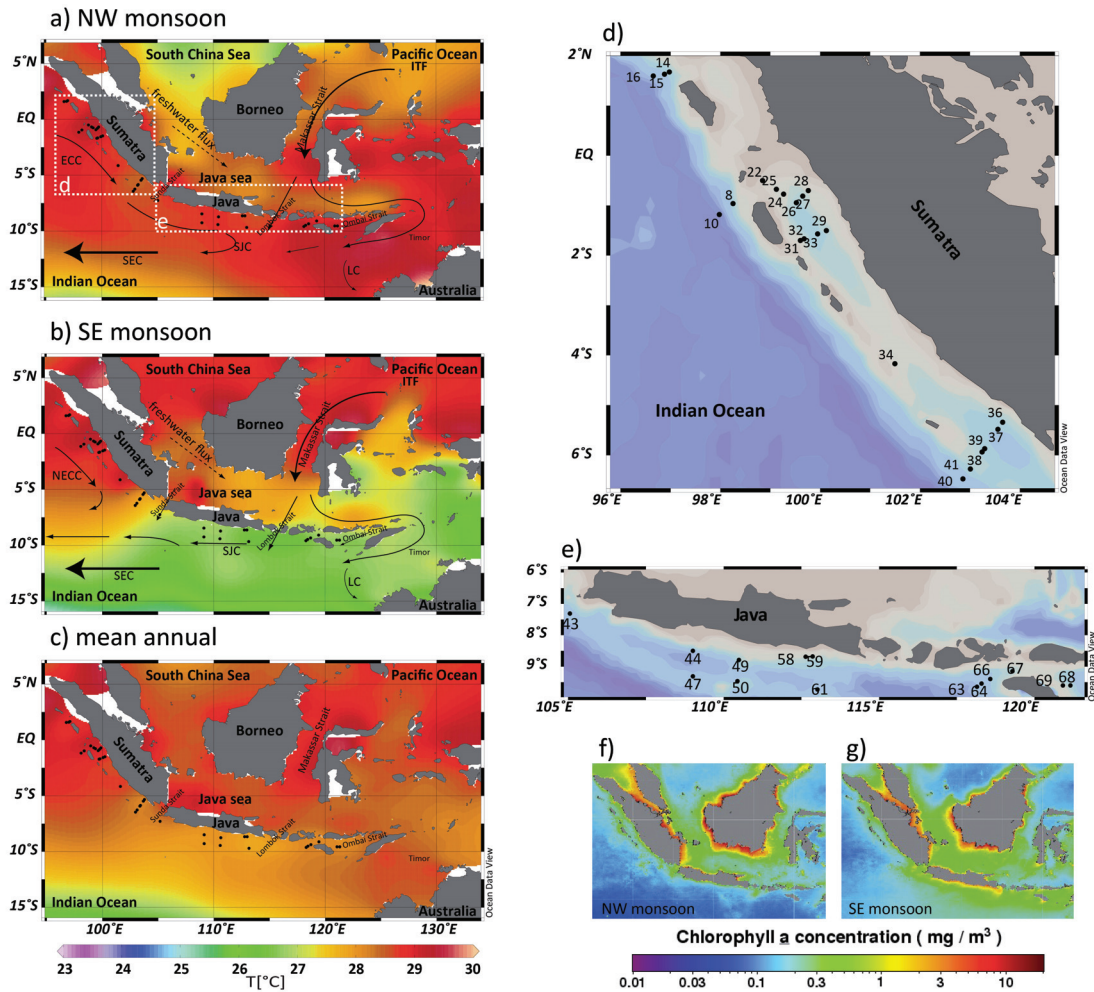


Fig. 3.1. Sea surface temperature around Java reflecting a) the NW monsoon season (white boxes mark areas presented in d) and e)); b) the SE monsoon season; c) mean annual SST (from World Ocean Atlas 2009). Black dots show the position of the core-top samples, solid arrows indicate oceanographic surface currents: SJC: South Java Current; ECC: Equatorial Counter Current; SEC: South Equatorial Current; NECC: North Equatorial Counter Current; ITF: Indonesian Throughflow; LC: Leeuwin Current. Maps d) and e) indicate the station numbers (GeoB100xx). Mean seasonal chlorophyll-a concentration ( $\text{mg} \text{m}^{-3}$ ) around Indonesia (SeaWiFs 1997-2010; <http://oceancolor.gsfc.nasa.gov/>); f) mean values during NW monsoon seasons; g) mean values during SE monsoon seasons.

### 3.4. Material and Methods

#### 3.4.1. Surface samples

In this study, we use the top 1 cm of multicore samples from 36 sites collected during PABESIA RV Sonne Cruise SO-184 in 2005 off west Sumatra and south Java and the LSI (Hebbeln et al., 2005) (Table 3.1, Fig. 3.1.).

A set of  $U_{37}^K$  temperature estimates for the same samples has been published by Mohtadi et al. (2011). Most of the data reached the upper limit of this proxy, i.e. close or above 28 °C. Six of the samples analyzed here have been included in the global GDGT core-top calibration study of Kim et al. (2010), but for reasons of consistency have been re-analyzed in this study.

Modern surface sediment ages have been confirmed at nine selected stations by accelerator mass spectrometry (AMS)  $^{14}C$  dates on planktic foraminifera (Mohtadi et al., 2011; Table. 3.1). The age determinations show that surface sediments are modern. Two samples from off Sumatra show older ages implying that sedimentation rates are lower at these locations (cores GeoB10008-4 and GeoB10016-2).

#### 3.4.2. Lipid extraction

Lipid extraction for GDGT and alkenone analyses was carried out following the protocol described by Müller et al. (1998). About 5 g of freeze-dried and homogenized samples were extracted three times using an ultrasonic probe with successively methanol (MeOH), MeOH: dichloromethane (DCM) 1:1 (v:v) and DCM (25 mL each). Before extraction known amounts of  $C_{19}$  ketone and  $C_{46}$  GDGT were added as internal standards. The combined extracts were washed with 50 mL deionized water to remove salts. The DCM: MeOH phase was separated, dried over anhydrous sodium sulphate, and the solvent was evaporated by rotary evaporation under vacuum. The lipid extract was saponified for 2 hours at 80 °C with 300  $\mu$ L of 0.1M KOH in 90:10 MeOH/H<sub>2</sub>O, and fractionated into three polarity fractions using silica gel column chromatography. The

fractions containing the alkenones and GDGTs were obtained by eluting with DCM: hexane 2:1 (v:v) and MeOH, respectively, and dried using a Silli-Therm at 50 °C under a stream of nitrogen.

### 3.4.3. Alkenone analysis and $U_{37}^K$ SST

The alkenone fraction was re-dissolved in 25  $\mu$ L MeOH: DCM 1:1 (v:v) prior to capillary gas chromatography. Analyses were performed using a HP5890 series gas chromatograph (GC) equipped with a flame ionization detector, using Helium as carrier gas with a constant flow rate of 2.0 mL/min. Initial oven temperature was 60 °C, held for 1 min, subsequently increased to 150 °C at a rate of 10 °C/min, then raised to 310 °C at a rate of 4 °C/min with a total run-time of 75 min.

Peak identification of di- and tri-unsaturated  $C_{37}$  alkenones ( $C_{37:2}$  and  $C_{37:3}$ ) was based on retention time and comparison with parallel GC runs of extracts of a lab-internal standard sediment. Quantification was achieved by peak integration relative to the internal standard  $C_{19}$  ketone and by assuming the same response factor as  $C_{38}$  *n*-alkane measured as external standard. Concentrations of di- and triunsaturated  $C_{37}$  alkenones are given as sum in  $\mu$ g/g total organic carbon (TOC). The TOC contents determined for core-tops of parallel multi-corer subcores were taken from Baumgart et al., 2010.

$U_{37}^K$  was calculated as:  $U_{37}^K = (C_{37:2}) / (C_{37:2} + C_{37:3})$ .  $U_{37}^K$  values were converted to temperature estimates by applying the calibration of Conte et al. (2006):

$$T = 29.876 \times (U_{37}^K) - 1.334$$

Table 3.1. Surface sediment data and results of alkenone and GDGT analyses.

Station [0-1cm] GeoB	Latitude	Longitude	water Depth (m)	$U^{K_{37}}$	SST- $U^{K_{37}}$ <sup>a</sup> [°C]	TEX <sub>86</sub>	Temp- TEX <sub>86</sub> <sup>b</sup> [°C]	BIT Index	Coig <sup>c</sup> (%)	Conc. Alkenone ( $\mu$ g/g <sub>roc</sub> )	Conc. GDGTs ( $\mu$ g/g <sub>roc</sub> )	<sup>14</sup> C Age <sup>d</sup> (years)	±Error (years)	Calibrated Age
10008-4	0°57.29'S	98°15.59'E	934	0.978	27.9	0.708	28.3	0.05	1.2	28.8	251.2	215	15	>1950AD
10010-1	1°10.69'S	97°58.89'E	2937	0.956	27.2	0.710	28.4	0.08	0.5	24.9	261.7	-295	50	>1950AD
10014-1	1°40.71'N	96°58.86'E	1158	0.977	27.9	0.717	28.7	0.07	1.6	38.3	369.4			
10015-1	1°37.95'N	96°53.17'E	1464	0.972	27.7	0.714	28.6	0.06	1.6	29.5	349.9			
10016-2	1°35.79'N	96°39.62'E	1900	0.963	27.4	0.720	28.9	0.06	1.2	12.9	162.2	640	20	281±20
10022-3	0°29.88'S	98°51.05'E	704	0.969	27.6	0.700	28.0	0.04	3.0	22.8	179.4	-335	15	>1950AD
10024-3	0°46.09'S	99°16.09'E	1381	0.911	25.9	0.720	28.8	0.07	1.6	21.6	231.7			
10025-3	0°40.46'S	99°7.39'E	1149	0.980	27.9	0.715	28.6	0.05	1.6	19.7	332.2			
10026-2	0°56.65'S	99°31.28'E	1641	0.986	28.1	0.705	28.2	0.04	n.d	n.d.	n.d.	-180	15	>1950AD
10027-3	0°48.53'S	99°39.18'E	875	0.957	27.3	0.707	28.3	0.06	n.d	n.d.	n.d.			
10028-4	0°41.80'S	99°45.78'E	522	0.946	26.9	0.720	28.8	0.04	2.3	27.4	410.3			
10029-3	1°29.75'S	100°7.58'E	974	0.973	27.7	0.713	28.6	0.04	2.1	11.9	240.7			
10031-3	1°41.93'S	99°36.19'E	1671	0.855	24.2	0.711	28.5	0.06	1.7	19.4	336.0			
10032-1	1°40.00'S	99°40.83'E	1758	0.974	27.8	0.706	28.3	0.07	n.d	n.d.	n.d.			
10033-5	1°33.79'S	99°57.14'E	1755	0.971	27.7	0.703	28.1	0.04	2.2	9.9	263.0			
10034-3	4°9.89'S	101°29.94'E	995	0.959	27.3	0.694	27.7	0.06	1.1	11.0	212.5			
10036-3	5°20.33'S	103°39.43'E	1502	0.974	27.8	0.697	27.9	0.22	1.1	10.5	71.2			
10037-2	5°28.83'S	103°33.56'E	2016	0.957	27.3	0.689	27.6	0.19	0.6	20.3	256.4			
10038-3	5°56.23'S	103°14.78'E	1891	0.966	27.5	0.677	27.0	0.14	0.4	15.0	58.1			
10039-3	5°52.10'S	103°17.65'E	1799	0.978	27.9	0.672	26.8	0.06	0.4	22.8	137.1			
10040-3	6°28.57'S	102°51.56'E	2605	0.953	27.1	0.673	26.9	0.04	0.5	25.2	140.8			
10041-3	6°16.44'S	103°0.51'E	1540	0.946	26.9	0.664	26.4	0.04	0.5	12.2	111.7	-325	15	>1950AD
10043-2	7°18.53'S	105°3.50'E	2170	0.875	24.8	0.714	28.6	0.07	1.0	22.0	199.7			
10044-3	8°29.99'S	109°0.98'E	3346	0.943	26.9	0.677	27.0	0.13	1.0	18.0	114.3			
10047-1	9°18.53'S	109°0.98'E	1780	0.944	26.9	0.662	26.3	0.04	1.7	6.2	57.8			
10049-5	8°47.08'S	110°29.80'E	1289	0.944	26.9	0.662	26.3	0.06	1.1	32.5	251.2			
10050-1	9°27.90'S	110°26.79'E	1221	0.847	24.0	0.663	26.4	0.02	0.4	48.8	351.9			

10058-1	8°41.03'S	112°38.25'E	1113	0.929	26.4	0.660	26.2	0.05	1.9	19.5	288.9	-295	15	>1950AD
10059-1	8°40.69'S	112°52.08'E	1370	0.936	26.6	0.651	25.9	0.05	1.5	18.8	349.3			
10061-5	9°43.75'S	113°1.45'E	2170	0.950	27.0	0.650	25.8	0.03	1.4	20.1	205.7			
10063-5	9°38.76'S	118°9.00'E	2501	0.949	27.0	0.636	25.2	0.01	1.7	16.6	457.2	-350	15	>1950AD
10064-5	9°32.36'S	118°18.03'E	2033	0.954	27.2	0.634	25.0	0.01	1.8	29.5	464.2			
10066-6	9°23.61'S	118°34.54'E	1632	0.935	26.6	0.640	25.4	0.02	2.2	16.5	207.2			
10067-5	9°8.94'S	119°17.43'E	1136	0.943	26.8	0.647	25.7	0.03	1.5	29.8	311.4			
10068-1	9°35.72'S	121°9.09'E	2011	0.945	26.9	0.651	25.9	0.02	2.0	12.8	197.4			
10069-4	9°35.70'S	120°54.95'E	1249	0.962	27.4	0.634	25.1	0.01	2.3	44.1	491.5	>modern		>1950AD

n.d.: not detected

- SST- $U_{37}^K$  calculated by applying the calibration of Conte et al. (2006).
- Temp- $TEX_{86}^H$  calculated by applying the calibration of Kim et al. (2010).
- $C_{org}$ (%) published by Baumgart et al. (2010).
- AMS  $^{14}C$  radiocarbon dates published by Mohtadi et al. (2011), expressed as conventional  $^{14}C$  ages in years BP.

#### 3.4.4. GDGT analysis and TEX<sub>86</sub> temperature

The polar fraction containing the GDGTs was dried under a stream of nitrogen, weighed, re-dissolved in *n*-hexane: isopropanol 99:1 (v/v) with a concentration of 2 mg/mL (Schouten et al., 2013a), and filtered using a 0.45 µm PTFE filter prior to analysis as described by Hopmans et al. (2000, 2004).

Analyses were performed as described in Leider et al. (2010) using an Agilent 1200 Series high performance liquid chromatography system with an Agilent 6210 mass spectrometry (HPLC -MS). 20 µL aliquots were injected onto an Alltech Prevail Cyano column (2.1×150 mm, 3 µm; Grace) maintained at 30 °C. GDGTs were eluted using the following gradient with solvent A (*n*-hexane) and solvent B (5% isopropanol in *n*-hexane): 80% A: 20% B for 5 min, linear gradient to 36% B in 45 min. The flow rate was 0.2 mL/min. After each analysis the column was cleaned by back-flushing with *n*-hexane: isopropanol 90:10 (v/v) at 0.2 mL/min for 8 min. GDGTs were identified using single ion monitoring (SIM) as described in Schouten et al., (2007).

TEX<sub>86</sub> was calculated on the basis of the relative peak areas of GDGTs as follows (Schouten et al., 2002):

$$\text{TEX}_{86} = (\text{GDGT2} + \text{GDGT3} + \text{GDGT4}') / (\text{GDGT1} + \text{GDGT2} + \text{GDGT3} + \text{GDGT4}')$$

where the numbers 1-4 indicate the number of cyclopentane rings in the isoprenoid molecules, and GDGT4' is the region-isomer of crenarchaeol. TEX<sup>H</sup><sub>86</sub> is the log-transformed original TEX<sub>86</sub> and has been introduced by Kim et al. (2010) for reconstruction of SSTs in (sub) tropical oceans (>15 °C):

$$\text{TEX}_{86}^{\text{H}} = \log(\text{TEX}_{86})$$

in which 'H' stands for high temperature regions. The TEX<sup>H</sup><sub>86</sub> values relate to temperature estimates according to the following relationship (Kim et al., 2010):

$$\text{SST} = 68.4 \times \text{TEX}_{86}^{\text{H}} + 38.6$$

GDGT concentrations were calculated from the respective peak areas relative to the peak area of the C<sub>46</sub>-GDGT used as internal standard and assuming equivalent response factors. To examine the potential influence of terrestrial GDGTs we analyzed the BIT index. The samples were analyzed in duplicate. BIT index was calculated based on the relative peak areas of branched GDGTs and crenarchaeol as defined by Hopmans et al. (2004).

#### **3.4.5. Analytical reproducibility**

To determine the analytical reproducibility of the U<sup>K</sup><sub>37</sub> and TEX<sub>86</sub> SST estimates, a series of subsamples from a homogenized batch of a standard sediment was extracted independently and measured along with the surface sediment samples. The standard deviation of the U<sup>K</sup><sub>37</sub> and TEX<sub>86</sub> SST estimates of these subsamples was 0.27 °C and 0.60 °C, respectively, and better than 20% and 10% for concentrations of alkenones and total isoprenoid GDGTs, respectively. Furthermore, the 36 surface sediment samples were measured in duplicate. The reproducibility of the U<sup>K</sup><sub>37</sub> and TEX<sub>86</sub> SST estimates was 0.15 °C and 0.18 °C, respectively.

### **3.5. Results**

#### **3.5.1. Alkenone-based temperatures**

The alkenone-based temperatures (SST-U<sup>K</sup><sub>37</sub>) range from 24.2 °C to 28.1 °C at stations off Sumatra and from 24.0 °C to 27.4 °C at upwelling stations off Java and the Lesser Sunda Islands (J-LSI; Fig. 3.2a.). The average alkenone temperature estimates is 27.3 °C and 26.6 °C off Sumatra and off J-LSI, respectively. The SST-U<sup>K</sup><sub>37</sub> is up to 2 °C lower than the satellite-based ma SST, and closely resembles SE monsoon SST (Fig. 3.3.).

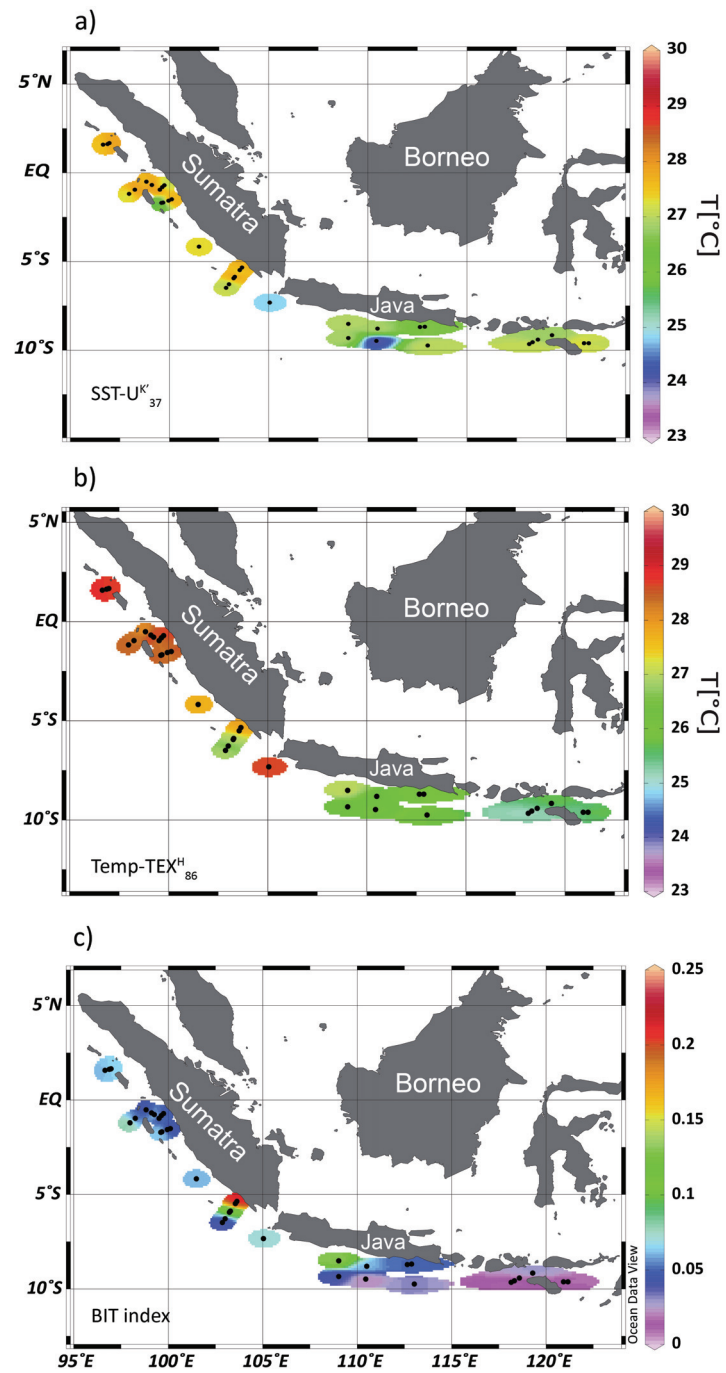


Fig. 3.2. Temperature estimates for surface sediments in the study area, a) alkenone-based temperature ( $SST-U^{K}_{37}$ , °C); b) GDGT-based temperature ( $Temp-TEX^{H}_{86}$ , °C); c) BIT index value.

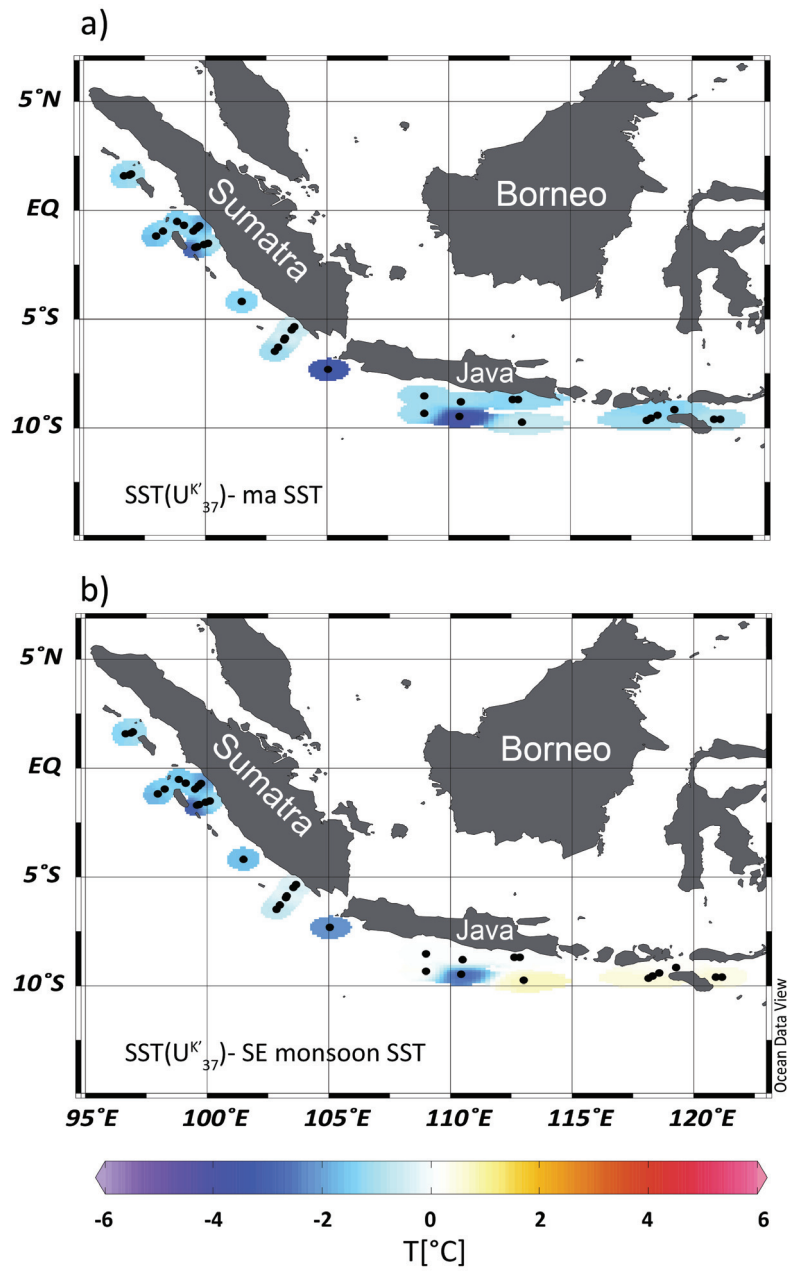


Fig. 3.3. Difference between reconstructed temperature based on  $U^K_{37}$  and seasonal satellite derived SST, a)  $U^K_{37}$  temperature estimates minus mean annual SSTs ( °C); b)  $U^K_{37}$  temperature estimates minus SE monsoon SSTs ( °C).

### 3.5.2. GDGT-based temperatures

The GDGT-based temperature estimates (Temp-TEX<sup>H</sup><sub>86</sub>) range from 26.4 °C to 28.9 °C at stations off Sumatra and from 25 °C to 28.6 °C at upwelling stations off J-LSI (Fig. 3.2b.). The average GDGT-based temperature off Sumatra (28.1 °C) is warmer than the average temperature off J-LSI (25.9 °C). There is also a decreasing trend with longitude as observed in SST-U<sup>K</sup><sub>37</sub> (Fig. 3.2a, b.). The difference between temperatures based on alkenones and GDGTs ( $\Delta T$ ) shows that Temp-TEX<sup>H</sup><sub>86</sub> is higher than SST-U<sup>K</sup><sub>37</sub> at stations in the non-upwelling area by up to 3 °C (Fig. 3.2a, b.). In contrast, Temp-TEX<sup>H</sup><sub>86</sub> is lower than SST-U<sup>K</sup><sub>37</sub> at stations in the upwelling area by up to 2 °C (Fig. 3.2a, b.). The Temp-TEX<sup>H</sup><sub>86</sub> matches the ma SST at the stations off Sumatra. As there is little or no seasonality in SST off Sumatra, Temp-TEX<sup>H</sup><sub>86</sub> is also in agreement with SE monsoon SST. Off Java, Temp-TEX<sup>H</sup><sub>86</sub> is in agreement with SE monsoon SST (Fig. 3.4, 5.). Furthermore, the Temp-TEX<sup>H</sup><sub>86</sub> is slightly colder than SE monsoon SST at the stations off LSI (Fig. 3.4b, 5.).

### 3.5.3. BIT index

Although the core-top sediments were all derived from the continental margin, they all contain low amounts of branched GDGTs, resulting in BIT values consistently below 0.30. The BIT index values show a decreasing trend from northwest to southeast. The BIT index varies between 0.01 and 0.22 with the highest values close to the Sunda Strait (Fig. 3.2c.). The lowest BIT index values are observed in the upwelling area off LSI. There is a decreasing trend from the coastal to the deeper ocean near the Sunda Strait.

### 3.5.4. Alkenone and GDGT concentrations

The bulk sedimentary concentrations of alkenones and GDGTs could be affected by the high lithogenic content in this area (Baumgart et al., 2010). To compensate for this effect, we calculated the concentrations relative to the TOC content from Baumgart et al. (2010). The total alkenone concentrations vary between 9.9 and 38.3 µg/g TOC at stations off Sumatra and between 6.2 and 48.8 µg/g TOC at stations off J-LSI (Fig. 3.6a.).

The total GDGT concentrations range from 58.1 to 410.3  $\mu\text{g/g}$  TOC at stations off Sumatra and from 57.8 to 491.5  $\mu\text{g/g}$  TOC at stations off J-LSI (Fig. 3.6b.). Crenarchaeol is the predominant GDGT, accounting for 69-75% of the total GDGTs. The GDGT concentrations cannot be regarded absolutely accurate due to the lack of an external GDGT standard which could be used to quantify the relative response factors of the  $\text{C}_{46}$  internal standard and the respective GDGTs used for the calculation of  $\text{TEX}_{86}$ .

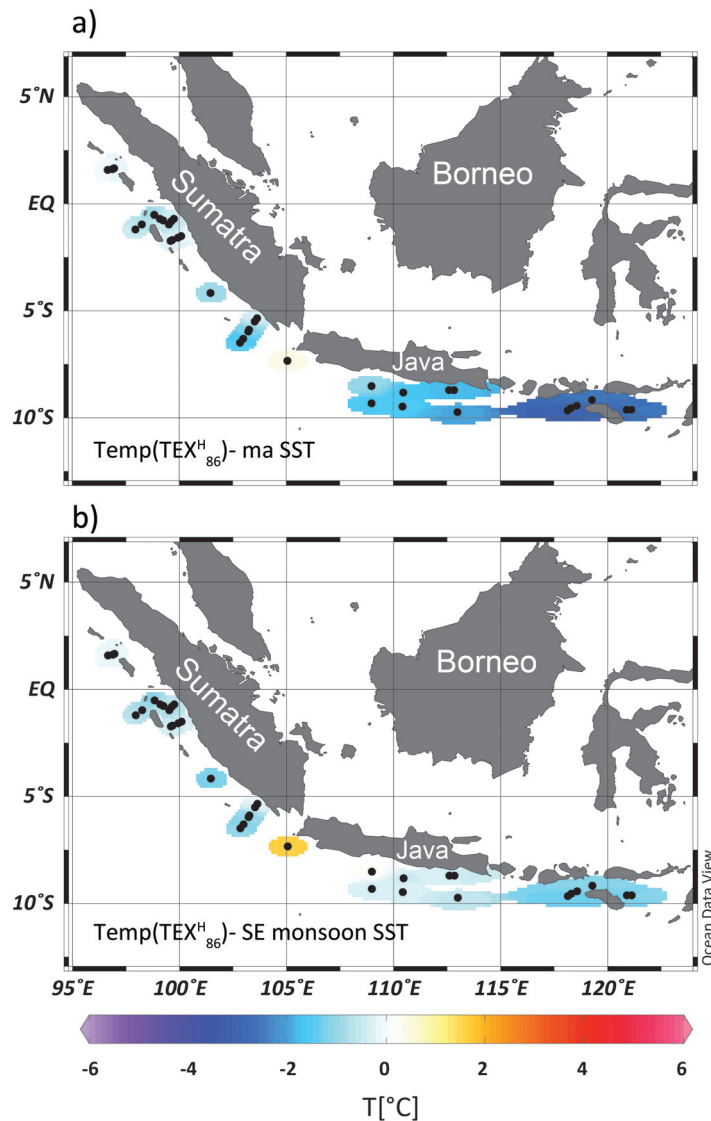


Fig. 3.4. Difference between reconstructed temperature based on  $\text{TEX}_{86}^{\text{H}}$  and seasonal satellite derived SST, a)  $\text{TEX}_{86}^{\text{H}}$  temperature estimates minus mean annual SSTs ( $^\circ\text{C}$ ); b)  $\text{TEX}_{86}^{\text{H}}$  temperature estimates minus SE monsoon SSTs ( $^\circ\text{C}$ ).

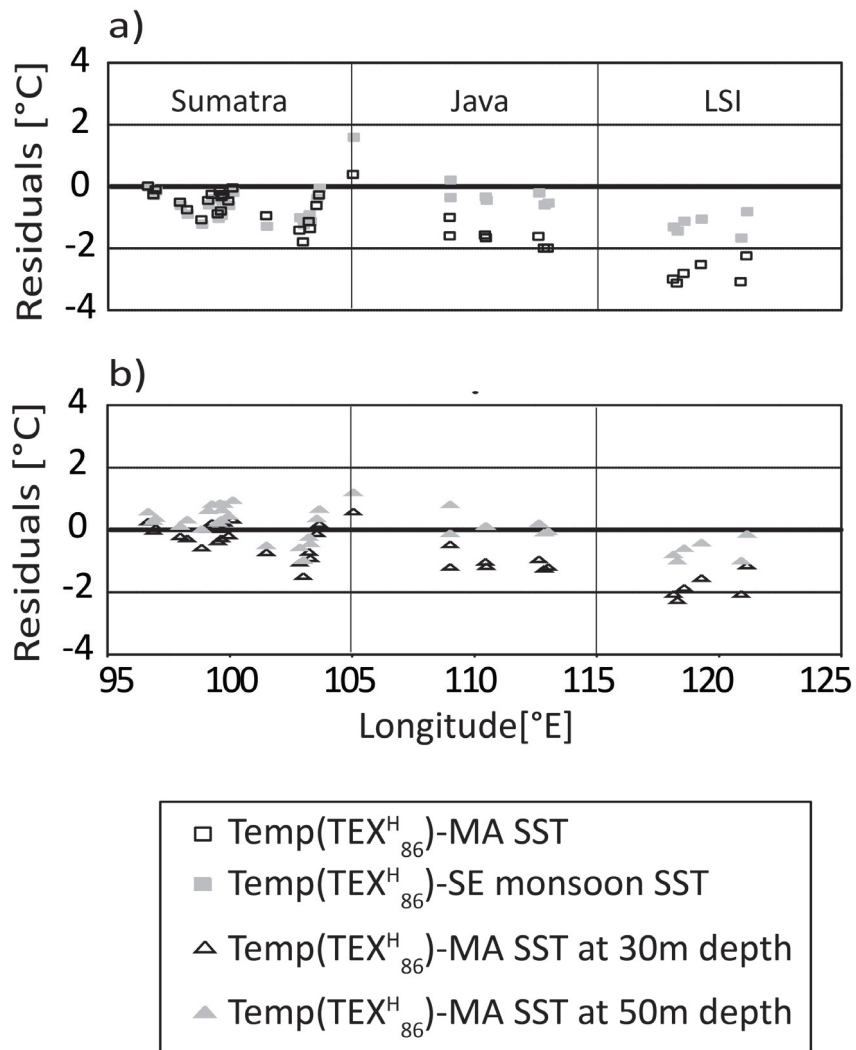


Fig. 3.5. Residuals for: a) GDGT-based temperature estimates minus mean annual SST (SE monsoon SST); b) GDGT-based temperature estimates minus mean annual SST at 30 m (50m) water depth, plotted versus longitude of the sample locations.

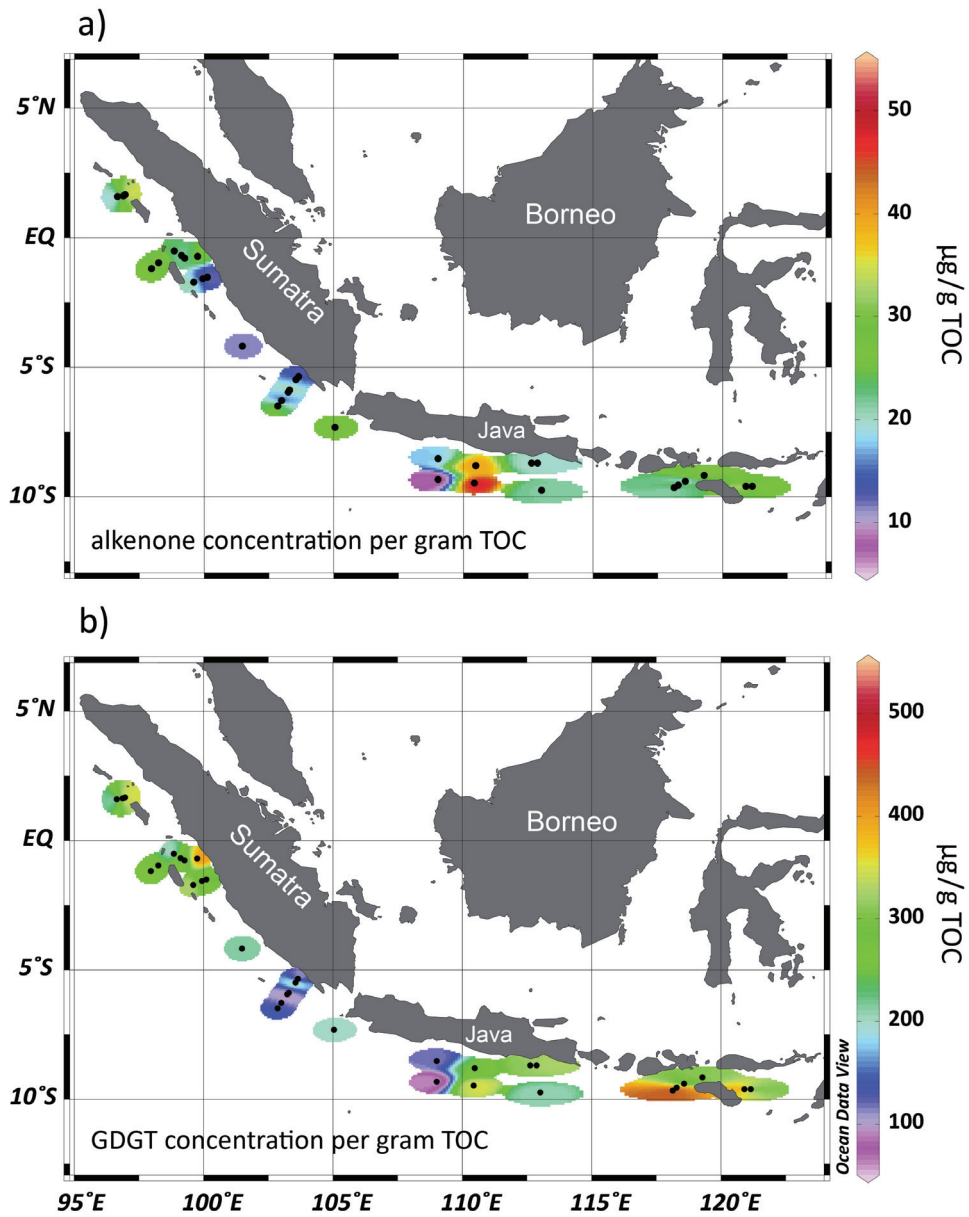


Fig. 3.6. Concentrations of a) alkenones per gram TOC ( $\mu\text{g/gTOC}$ ); b) GDGTs per gram TOC ( $\mu\text{g/gTOC}$ ) in surface sediments (TOC content published by Baumgart et al., 2010).

### 3.6. Discussion

#### 3.6.1. Temperature calibrations

We discuss temperature estimates based on the linear calibration of Conte et al. (2006) for  $U_{37}^K$  and based on the  $TEX_{86}^H$  calibration from Kim et al. (2010). These authors have demonstrated that for tropical setting like our study area, these are the best calibration for surface sediments.

The aforementioned deviations of  $TEX_{86}^H$ -based SST estimates from measured SSTs are within calibration error of the method. There is, however, a systematic pattern in deviations within our study area, which appears to be related to the prevailing oceanographic conditions. Moreover, regional calibrations for  $TEX_{86}$  (Shevenell et al., 2011) tend to display lower residuals than the global calibration. Thus we believe that the offsets we observe are significant and can be interpreted in context with the environmental conditions observed in the sub-regions of our study area.

### **3.6.2. Non-upwelling region off Sumatra**

Alkenone-derived SST estimates are by 2 °C lower than the ma SST (World Ocean Atlas 2009 (WOA); Loncarnini et al., 2010) in the non-upwelling area (Fig. 3.5.). Off Sumatra, the seasonal SST variations are small (less than 2 °C). The discrepancy between measured and reconstructed temperatures is significant in the equatorial region, as the mean standard error of temperature estimation for the calibration is 1.1 °C (Conte et al., 2006). However, the ma SST is warmer than 28 °C in this area, beyond the defined temperature range of the  $U_{37}^K$  method. Thus the alkenone-based SST estimates underestimate SST in the tropical regions with ma SST exceeding 28 °C. Our results are in agreement with previous studies (e.g., Conte et al., 1998; Mohtadi et al., 2011; Pelejero and Grimalt, 1997; Sikes and Volkman, 1993; Sonzogni et al., 1997). In order to explain this, several studies have argued that the slopes of SST- $U_{37}^K$  calibrations are non-linear or show reductions at high growth temperatures (Pelejero and Grimalt, 1997; Sikes and Volkman, 1993; Sonzogni et al., 1997). Conte et al. (1998) suggested that the cell's limited physiological adjustment to temperature via alkenone biochemistry would introduce a reduction in the slope of the relationship at high growth temperatures.

Mohtadi et al. (2011) reported up to  $\sim 1.0$  °C higher  $U_{37}^K$  SST estimates than our data for the same core top samples, with the alkenone index measurements being performed in another laboratory. The authors report that the alkenone temperature estimates correspond to modern mean annual SST rather than seasonal temperatures in the study area. However, they noted that a seasonal signal might be masked by the fact that the alkenone proxy is at its limit of temperature response. Nevertheless, a clear and strong seasonal signal in alkenone-based temperature estimates is observed in a downcore study off SW Sumatra during glacial periods (e.g., Lückge et al., 2009). Rosell-Melé et al. (2001) estimated that differences between  $U_{37}^K$  temperature estimates from the analysis of oceanic sediment samples, between any two laboratories, may be as high as 2.1 °C (at 95% confidence level) owing to analytical uncertainties. Therefore we refrain from discussing these discrepancies but rather interpret differences between data obtained in one single laboratory.

In contrast to the alkenone-derived SST estimates, Temp- $TEX_{86}^H$  agrees well with ma SSTs in the non-upwelling area (Fig. 3.4, 5.). The high SSTs in the region are well within the range of calibration of  $TEX_{86}$  and  $TEX_{86}^H$ , and our results suggest that Temp- $TEX_{86}^H$  might reflect ma SST in the non-upwelling areas in the eastern tropical Indian Ocean.

### 3.6.3. Java-Lesser Sunda Islands Upwelling System

At the upwelling sites, the  $U_{37}^K$  and  $TEX_{86}^H$  temperature estimates are up to 2 °C lower than ma SST (Fig. 3.3, 4.). The alkenone-based and GDGT-based temperatures agree better with SE monsoon SST within analytical error at the Java sites, whereas at the LSI sites SST- $U_{37}^K$  is approximately 1 °C higher and  $TEX_{86}^H$  temperature estimates are up to 2 °C lower than SE monsoon SST, respectively. We thus observe an offset between the two indices in the upwelling area off LSI, showing up to  $\sim 2$  °C warmer SST- $U_{37}^K$  than Temp- $TEX_{86}^H$ , whereas the SST- $U_{37}^K$  is equivalent to the Temp- $TEX_{86}^H$  off Java (Fig. 3.7.). Generally, reconstructed temperatures derived from alkenones and GDGTs are expected

to represent the temperatures of the upper parts of the water column, because both indices correlate well with ma SST in most settings (Kim et al., 2008; Prah1 et al., 2000; Schouten et al., 2002). Offsets between the two temperature estimates could be caused by different seasonal production of source organisms and/ or depth habitats, or processes like degradation, transport, or terrestrial input. In upwelling regions it is also conceivable that upwelled water carries with it archaeal cells originally thriving in deeper habitats and carrying the respective Temp-TEX<sub>86</sub>. Offset between SST-U<sup>K</sup><sub>37</sub> and Temp-TEX<sub>86</sub> have been found in several previous studies, particularly in upwelling settings (Huguet et al., 2006; Lee et al., 2008; Leider et al., 2010; Lopes dos Santos et al., 2010; Rommerskirchen et al., 2011).

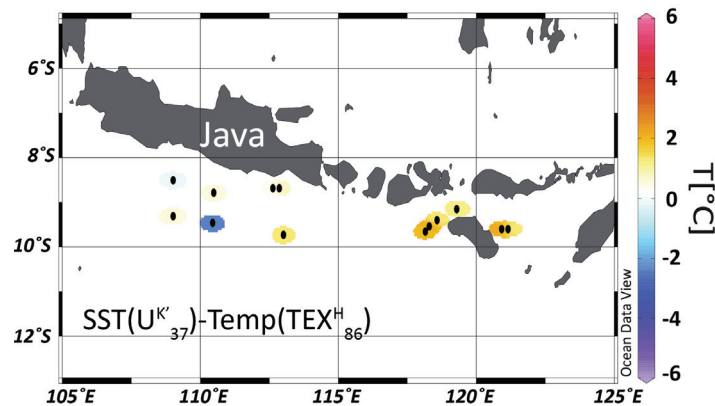


Fig. 3.7. Difference between reconstructed temperatures based on alkenones and GDGTs in the upwelling area.

### 3.6.3.1. Effect of terrestrial input, degradation and lateral transport

As described above, the BIT index can potentially be used to assess whether or not input of terrestrial isoprenoidal GDGTs could bias the TEX<sub>86</sub> and TEX<sub>86</sub> at sites with BIT index values above 0.2 or 0.3 are potentially unreliable (Weijers et al., 2006; Zhu et al., 2011). The BIT index at our sites varies between 0.01 and 0.22, suggesting a low relative soil organic matter contribution. This indicates that the TEX<sup>H</sup><sub>86</sub> is likely not strongly biased by terrigenous material at most sites. This assumption is also supported by the

low concentration of terrestrial organic matter in the study area inferred from  $\delta^{13}\text{C}$  compositions of TOC (Baumgart et al., 2010).

A preferential degradation of the tri-unsaturated alkenone relative to the di-unsaturated alkenone under oxic bottom water conditions could result in a warm bias in alkenone SST estimates (Gong and Hollander, 1999; Hoefs et al., 1998; Kim et al., 2009a). However, other studies suggest that differential degradation has a minor effect on  $U^{K'}_{37}$  temperature estimates (up to 1.2 °C) (Kim et al., 2009a; Huguet et al., 2009). On the other hand, several studies demonstrated no significant effect of differential degradation on GDGT distributions under oxic or anoxic conditions (Kim et al., 2009a; Schouten et al., 2004). In our study area, the average bottom water oxygen concentration is 2.98 mL/L off Java, which is slightly higher than 2.64 mL/L off LSI (Baumgart et al., 2010). If differential degradation played an important role, a stronger effect creating a warm bias would be expected off Java. In contrast, we observe a slightly warmer SST- $U^{K'}_{37}$  off LSI than off Java. This suggests that preferential degradation is not a significant factor for  $U^{K'}_{37}$  temperature estimates in the study area and preferential degradation can thus not account for the observed differences between temperature estimates between the sites off Java and the LSI.

Organic proxy signals in marine sediments are not always derived solely from the overlying water column but may originate also from remote regions. In particular, fine-grained particles are susceptible to resuspension and lateral advection by strong currents (e.g., Ohkouchi et al., 2002). Organic matter in marine sediments is often associated with the fine grain size fraction. Previous studies recognized that alkenone SST records are affected by laterally advected allochthonous input (e.g., Sachs and Anderson, 2003; Sicre et al., 2005). SST-  $U^{K'}_{37}$  have been found to be at odds with in situ SST in some areas due to lateral transport (Benthien and Müller, 2000; Rühlemann and Butzin, 2006). However, magnitude and direction of the deviations between alkenone-based temperatures and in situ SST caused by lateral transport depend on the SST and productivity in the source region where advected particles might originate. In our study

region, the ITF presently transports an annual average of  $\sim 16\text{SV}$  ( $1\text{SV}=10^6\text{m}^3\text{s}^{-1}$ ) of warm, low-salinity surface water from the Western Pacific Warm Pool (WPWP) and Indonesian-Malaysian archipelago in to the eastern Indian Ocean (Gordon and Fine, 1996; You and Tomczak, 1993), and thus is the likely source for advected material. The average surface temperature of the WPWP is over  $28\text{ }^\circ\text{C}$ , slightly warmer than the average SST off Java and the LSI, and the productivity is lower. Our  $\text{SST-U}_{37}^{\text{K}}$  estimates are ca.  $1.5\text{ }^\circ\text{C}$  lower than ma SST and ca.  $1\text{ }^\circ\text{C}$  higher than SE monsoon SST off LSI. If lateral advection is considered as a main cause, a source region would be required with a ma SST similar to our alkenone temperature estimates. Moreover, previous studies suggested that GDGTs are less affected by long-distance lateral transport than alkenones (Mollenhauer et al., 2007; Shah et al., 2008). Kim et al. (2009b) found that isoprenoid GDGTs are less refractory than alkenones. So, GDGT-based proxies are likely primarily influenced by local conditions and less subject to long-distance lateral transport (Kim et al., 2010). It is thus unlikely that advected alkenones, or GDGTs should dominate the signal recorded in the sediment.

### **3.6.3.2. Depth habitat of prymnesiophyte and Thaumarchaeota**

The offset between the two temperature estimates might relate to the water depth in which the source organisms live. Prymnesiophyte algae are photoautotrophic which means they live within the euphotic zone. Thaumarchaeota are distributed throughout the entire water column, and can reside in deeper waters (Karner et al., 2001). Several studies have suggested that  $\text{TEX}_{86}$  temperature estimates reflect slightly deeper waters, i.e. just below the surface mixed layer (e.g., Huguet et al., 2007; Lee et al., 2008; Lopes dos Santos et al., 2010). Huguet et al. (2007) suggested that the GDGTs were derived from a deeper and colder water mass (100-150m) instead of surface waters. Lee et al. (2008) measured  $\text{TEX}_{86}$  in suspended matter samples from surface water and roughly the upper 80 m of the water column in the Benguela upwelling system and found that the  $\text{Temp-TEX}_{86}$  was colder than in situ temperature. They supposed that the GDGT producers thriving below the mixed layer (<40 m) were

transported upward by upwelling resulting in a cold bias. The surface sediments analyzed in the same study revealed that  $\text{TEX}_{86}$  reflect deeper water (>40 m) temperature better than SST. Lopes dos Santos et al. (2010) investigated surface sediments located near the equatorial upwelling in the Atlantic Ocean and found that the  $\text{TEX}_{86}$  temperature estimates reflect subsurface temperature, likely around the thermocline, rather than SST. However, in contrast to the above studies, Schouten et al. (2012) analyzed the GDGTs in suspended particles in the water column of the Arabian Sea and observed relatively low  $\text{TEX}_{86}$  values in surface waters and an increase between 170 and 450 m depth. Basse et al. (submitted manuscript) analyzed suspended particulate matter samples and surface sediment samples off Cape Blanc (NW Africa) and found that the GDGTs transported to the sediment likely originated from approximately 60m water depth. The potential deeper depth habitat suggested for GDGT producers could thus be between 40 and 100 m.

In the upwelling area off LSI comparison between estimated temperatures based on alkenones, GDGTs and WOA 09 (Loncrnini et al., 2010) suggests that alkenone SST estimates might reflect mean annual temperature of 26.5-27.5 °C at 30 m water depth or SE monsoon temperature at 0 m depth (Fig. 3.8.). The predominant production of alkenones occurs in SE monsoon (more details discussed below). Hence, alkenones in surface sediments likely reflect SE monsoon surface temperature. In contrast, GDGT-based temperatures seem to record SE monsoon temperature at 30-50 m water depth ranging from 25-27 °C off J-LSI. Taken together, our results from the upwelling area off LSI suggest that  $\text{TEX}_{86}^{\text{H}}$  may often be more reflective of deeper waters at 30-50 m, while  $\text{U}_{37}^{\text{K}}$  correlates well to SST.

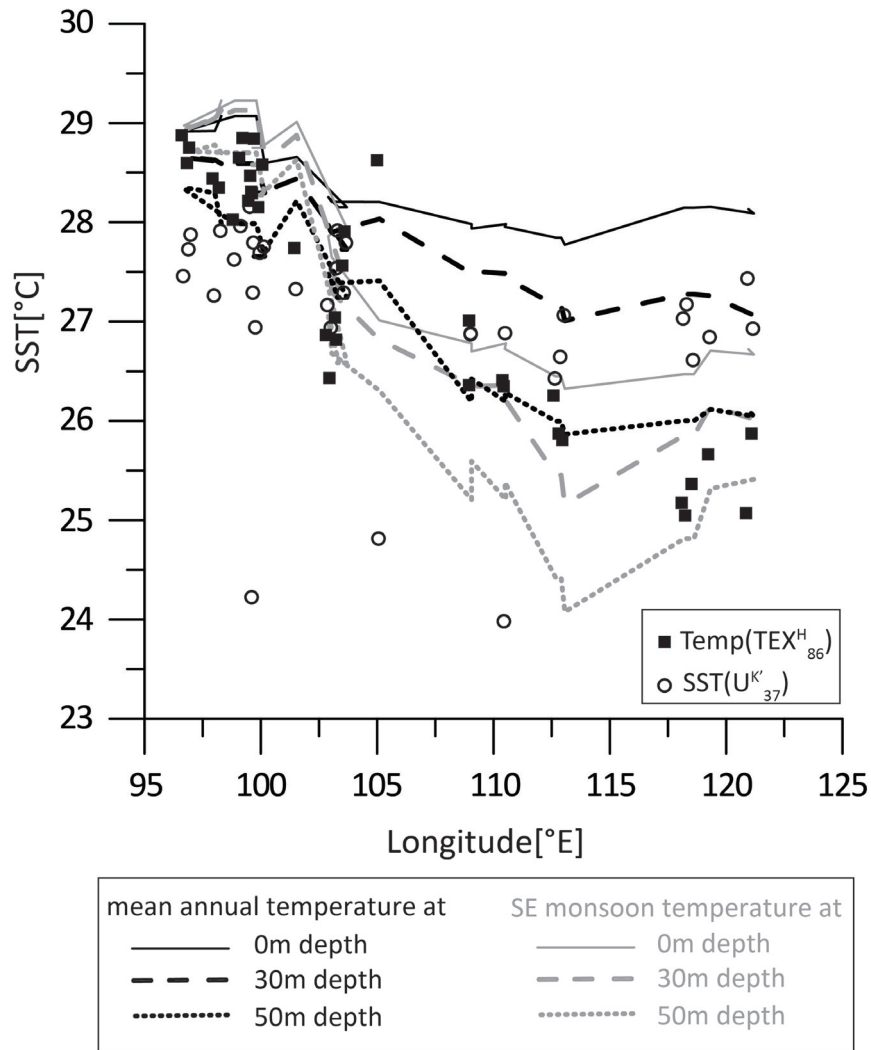


Fig. 3.8. Alkenone- and GDGT-based temperatures vs. longitude. Solid, dashed, and dotted lines indicate upper water column temperatures at 0 m, 30 m and 50 m, respectively, black for mean annual temperatures, grey for the SE monsoon season; temperatures were averaged for each depth in the study area using the WOA 09 database (Loncrnini et al., 2010).

### 3.6.3.3. Seasonal prymnesiophyte and Thaumarchaea production

SST- $U_{37}^K$  is lower than ma SST but consistent with SE monsoon SST in the upwelling area (Fig. 3.5.). Although it is generally assumed that  $U_{37}^K$  reflects ma SST, it has been reported that the abundance of prymnesiophyte algae varies throughout the

annual cycle. The lower  $U_{37}^K$  temperature could indicate that SST- $U_{37}^K$  might be biased toward the colder season if the source organisms thrive in the colder seasons. This scenario has been invoked to account for lower SST- $U_{37}^K$  than ma SST in surface sediments (e.g., Lee et al., 2008; Leider et al., 2010).

Primary production is strongly associated with upwelling dynamics and monsoon cycles along the coast of Java/Lombok Basin. Satellite derived chlorophyll-a concentration in the upwelling area displays a distinct seasonality with maxima between June and September (data from SeaWiFS between 1997 and 2010, Fig. 3.1f, g.). *E. huxleyi* and *G. oceanica* occur in high abundance during the SE monsoon season in the investigated region (Andruleit et al., 2007). Chlorophyll-a concentration and the concentration of alkenones appear higher at the stations off Java than LSI, suggesting a higher primary productivity for this region (Table, 3.1.; Fig. 3.6.). This suggests that alkenones are mainly derived from alkenone producers thriving during the SE monsoon, and that SST- $U_{37}^K$  possibly reflects SE monsoon season alkenone production in the upwelling area.

Although a strong relationship between  $TEX_{86}$  and ma SST is observed in several surface sediments studies,  $TEX_{86}$  does not necessarily reflect ma SST at each location. The abundance of Thaumarchaeota varies with seasonality (Murray et al., 1998; Pitcher et al., 2011). Besides the production of Thaumarchaeota in specific seasons, the mode of transport of GDGTs is likely another crucial process for controlling the sedimentary  $TEX_{86}$  signal. It is known that the cells of archaea are very small and neutrally buoyant and thus cannot sink by themselves (Schouten et al., 2013b and reference therein). They have to be transported by an efficient process i.e., by aggregation with phytoplankton cells and other suspended matter, in order for the GDGTs to reach the sea floor. Thus, export of the GDGT signal likely occurs primarily during the season of elevated primary productivity (Huguet et al., 2007; Wuchter et al., 2005). In the upwelling area, Temp- $TEX_{86}^H$  is more than 3 °C colder than satellite SST during the entire year except for the SE monsoon season (Fig. 3.6.). Temp- $TEX_{86}^H$  matches SE monsoon SST at sites off Java,

whereas it is slightly colder than SE monsoon SST off LSI. This could suggest that the production of planktonic archaea and/or export of their lipids to the sediments predominantly take place during the cooler seasons, leading to the hypothesis that their seasonality or at least the seasonality of their export is similar to that of the prymnesiophytes. High fluxes of GDGTs associated with high abundance of Thaumarchaeota have been observed to be seasonal (Herfort et al., 2006; Huguet et al., 2007; Wuchter et al., 2005). Wuchter et al. (2005) observed a positive correlation between chlorophyll-a and archaeal lipids in surface waters from Bermuda. At those sites, wind-induced convective mixing results in nutrient enrichment of surface waters, which promotes production during winter and possibly also the growth of planktonic archaea. In the Arabian Sea, the flux of GDGTs to the sediments was higher during the upwelling season than in the non-upwelling season (Wakeham et al., 2002). The Arabian Sea shows a similar environmental setting as our study area. Hence, we propose that off J-LSI the Temp-TEX<sup>H</sup><sub>86</sub> possibly reflects planktonic archaea production during the SE monsoon season. Our relatively cold TEX<sup>H</sup><sub>86</sub> temperature signal suggests that production of GDGTs predominantly takes place during the high productivity season related to upwelling. However, the difference between the two sub-areas of the upwelling system, i.e., off Java and the LSI, remains unexplained by a simple seasonality scenario.

#### **3.6.3.4. Timing of export production**

The offset between SST-U<sup>K'</sup><sub>37</sub> and Temp-TEX<sup>H</sup><sub>86</sub> is smaller at lower TOC sites off Java than at sites with high TOC off LSI (Baumgart et al., 2010) (Fig. 3.9a.). This suggests that the temperature offset ( $\Delta T$ ) depends on the degree of marine primary productivity in the surface water. Coincidentally, the same pattern has been observed in the Benguela upwelling system (Rommerskirchen et al., 2011). Additionally, the  $\Delta T$  correlates ( $R^2=0.59$ ,  $P<0.05$ ) with the concentration of GDGTs (Fig. 3.9b.), but shows a weaker correlation with concentration of alkenones ( $R^2=0.25$ ,  $P<0.1$ ; Fig. 3.9c.), suggesting that the offsets depend on GDGT production. We notice that the weaker correlation between  $\Delta T$  and TOC than with GDGT concentration could be explainable by other factors that influence

TOC content in sediments such as dilution by other components and diagenetic preservation (Meyers et al., 1999). However,  $\Delta T$  is negatively correlated with the BIT index ( $R^2=0.67$ ,  $P<0.001$ ; Fig. 3.9d) suggesting that off Java a small bias towards warmer Temp-TEX<sup>H</sup><sub>86</sub> might indeed be caused by input of terrigenous isoprenoid GDGTs, potentially during the wet NW monsoon season. On the other hand, several studies has pointed out that BIT index might also reflect variations in productivity of marine Thaumarchaeota rather than changes in the input of terrigenous GDGTs (e.g., Smith et al., 2012), which would be in line with higher GDGT production off LSI than off Java.

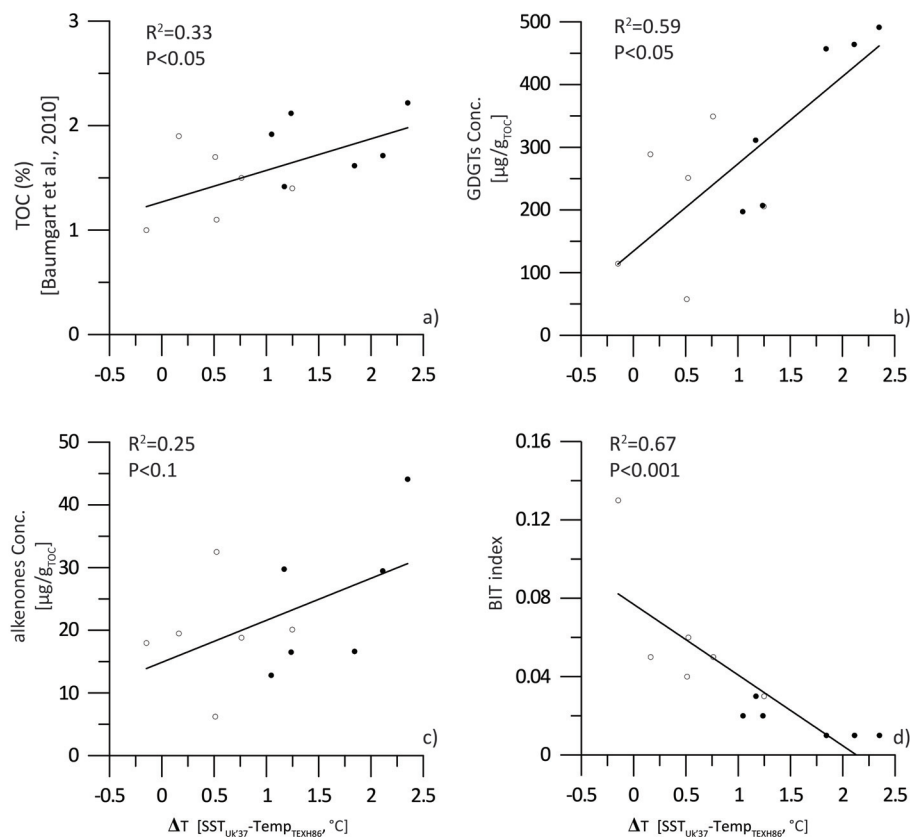


Fig. 3.9. a) TOC content published by Baumgart et al. (2010) against the offset between SST- $U_{37}^K$  and Temp-TEX<sup>H</sup><sub>86</sub> ( $\Delta T$ ); b) Concentration of GDGTs per g TOC against the  $\Delta T$ ; c) Concentration of alkenones per g TOC against  $\Delta T$ ; d) BIT index against the  $\Delta T$ . Open circles represent sites off Java, filled dots refer to sites off LSI.

The alkenone producers may not occur at maximum abundance during peak upwelling, either, but could be outcompeted by other phytoplankton. For instance, in the Arabian Sea, living diatoms typically dominate in the centre of upwelling, whereas the abundance of coccolithophores increases towards more nutrient-depleted and stratified surface water (Schiebel et al., 2004). The observation of warmer  $U^{K'}_{37}$  temperature estimates off LSI than off Java suggests that the alkenone-based temperatures may not reflect the coldest upwelling SSTs.

As detailed above, the potential seasonal bias of GDGT-based temperatures may also be caused by seasonal variation in the export of GDGTs, which may depend on the timing of export productivity, i.e. the time of highest carbon flux to the sediment, which is high during increased phytoplankton productivity (Schouten et al., 2013b and reference therein). The timing of highest particle flux could be different between the areas off Java and LSI. In contrast to the alkenones, GDGTs off LSI could be primarily exported by aggregates produced by phytoplankton during peak upwelling, the  $TEX^H_{86}$ -based temperatures might be reflective of peak upwelling conditions, which is associated with the highest export flux. During non-upwelling times, GDGTs produced in the water column might not be exported and potentially degrade, while rapid aggregation might result in selective preservation of the lipids incorporated in sinking particles. As a result, the sinking GDGTs could be dominated by material produced during this coldest time period, irrespective of whether or not Thaumarchaeota productivity is highest during this time. We suggest this scenario to be at work off LSI, while off Java, where productivity in general is higher, high vertical fluxes might prevail for a longer time period, resulting in inclusion of more GDGTs produced during warmer time periods.

Recent investigations on a sediment trap time-series off Java between 2001 and 2003 observed that fluxes of diatoms, opal and particulate organic carbon were also enhanced during the rainy and warm season during the NW monsoon, defining a secondary peak in productivity (Rixen et al., 2006; Romero et al., 2009). Elevated riverine nutrient discharges following the rainy season might play an important role in

detected fluxes and consequent additional phytoplankton blooms. Thus, the warmer Temp-TEX<sup>H</sup><sub>86</sub> off Java than off LSI could also be attributed to additional export of GDGTs occurring during the NW monsoon season and carrying a warm signal. A warm bias of Temp-TEX<sup>H</sup><sub>86</sub> during the NW monsoon season caused by supply of terrigenous isoprenoid GDGTs is regarded less likely, as the BIT index values for all stations off Java are very low ( $\leq 0.13$ , Table 3.1.). Further support for our interpretation comes from the precipitation rates on the Java and LSI. The rainfall rates derived from the Tropical Rainfall Measuring Mission (TRMM) from 1998 to 2007 show that higher rainfall rates are observed off Java than off LSI (Bissutti et al., 2012), suggesting a higher riverine discharge off Java than LSI. On the other hand, river supplied nutrients might stimulate a prymnesiophyte bloom during NW monsoon, resulting in export of alkenones carrying a warm SST signature, which could impact the sedimentary U<sup>K'</sup><sub>37</sub> values, an effect which cannot be seen in our data.

### 3.7. Conclusions

Analysis of our data set of combined U<sup>K'</sup><sub>37</sub> and TEX<sup>H</sup><sub>86</sub>-based temperature estimates off the coasts of Sumatra, Java and the Lesser Sunda Islands supports the following conclusions, partly corroborating previous findings:

1. Alkenone-based temperature estimates probably underestimate tropical SST due to the limitations of the U<sup>K'</sup><sub>37</sub> proxy at SST beyond 28 °C in the equatorial non-upwelling area off western Sumatra. In contrast, GDGT-based temperature estimates off Sumatra are in agreement with mean annual and/or SE monsoon temperatures within the upper 50 m of the water column.

2. In the upwelling region, SST-U<sup>K'</sup><sub>37</sub> matches well with SE monsoon SST, which can be attributed to predominant production of alkenones during upwelling conditions in the SE monsoon season.

Lower Temp-TEX<sub>86</sub><sup>H</sup> than mean annual SST in the upwelling areas can be explained by maximum abundance and export of Thaumarchaeota during highest upwelling-induced surface water productivity and a predominant habitat at 30-50 m water depth.

3. The offset between the temperature estimates derived from the two indices is larger in the upwelling area off LSI than off Java. This might be interpreted by either one or a combination of the following factors: Predominant export of GDGTs occurs during peak upwelling with alkenones not reflecting the peak upwelling conditions off LSI, while exported GDGTs off Java include a higher relative contribution of GDGTs produced during warmer times due to overall higher vertical particle fluxes. Moreover, off Java GDGTs carrying a warm temperature signal might be exported to the sediment following a secondary flux maximum caused by high river runoff in the NW monsoon season.

### **Acknowledgements**

The sediment samples from the eastern Indian Ocean were collected during the PABESIA Cruise with RV Sonne (SO-184). We thank the participating crews and scientists for collecting the cores used in this study. We would like to thank Ralph Kreutz and Maria Winterfeld for laboratory assistance. This study was supported by the German Bundesministerium für Bildung und Forschung (PABESIA), the Helmholtz Association through a Young Investigators Group Award to GM and the China Scholarship Council (CSC) with support to Wenwen Chen. The data presented in this study are archived in PANGAEA (<http://www.pangaea.de>). We thank Carme Huguet and two anonymous reviewers for constructive and detailed reviews that greatly helped to improve the manuscript.

### 3.8. References

- Aldrian, E., Susanto, R.D., 2003. Identification of three dominant rainfall regions within Indonesia and their relationship to sea surface temperature. *International Journal of Climatology*, 23, 1435-1452.
- Andruleit, H., 2007. Status of the Java upwelling area (Indian Ocean) during the oligotrophic northern hemisphere winter monsoon season as revealed by coccolithophores. *Marine Micropaleontology*, 64, 36-51.
- Basse, A., Zhu, C., Versteegh, G.J.M., Fischer, G., Hinrichs, K.-U., Mollenhauer, G., 2013. Implications for community structure or metabolism of marine Thaumarchaeota and the TEX<sub>86</sub> SST proxy. *Organic Geochemistry*, 72, 1-13.
- Baumgart, A., Jennerjahn, T., Mohtadi, M., Hebbeln, D., 2010. Distribution and burial of organic carbon in sediments from the Indian Ocean upwelling region off Java and Sumatra, Indonesia. *Deep-Sea Research I*, 57, 458-467.
- Benthien, A., Müller, P.J., 2000. Anomalously low alkenone temperatures caused by lateral particle and sediment transport in the Malvinas Current region, western Argentine Basin. *Deep-Sea Research I*, 47, 2369-2393.
- Biasutti, M., Yuter, S.E., Burleyson, C.D., Sobel, A.H., 2012. Very high resolution rainfall patterns measured by TRMM precipitation radar: seasonal and diurnal cycles. *Climate dynamics*, 39(1-2), 239-258.
- Brassell, S.C., Eglinton, G., Marlowe, I.T., Plaumann, U., Sarnthein, M., 1986. Molecular stratigraphy: A new tool for climatic assessment. *Nature*, 320,129-133.
- Brochier-Armanet, C., Boussau, B., Gribaldo, S., Forterre, P., 2008. Mesophilic Crenarchaeota: Proposal for a third archaeal phylum, the Thaumarchaeota. *Nature Reviews Microbiology*, 6 (3), 245-252.
- Bryden, H.L Imawaki, S., 2001. Ocean Heat Transport, Chapter 6.1, pp. 455-474 in *Ocean Circulation and Climate*, G. Siedler, J. Church and J. Gould, eds. Academic Press.
- Conte, M.H., Eglinton, G., Madueira, L.A.S., 1992. Long-chain alkenones and alkyl alkenoates as paleotemperature indicators: Their production, flux and early

- sediment diagenesis in the eastern North Atlantic. in *Advances in Organic Geochemistry 1991*, edited by C. B. Eckardt and S. R. Larter, *Organic Geochemistry*, 19, 287-298.
- Conte, M.H., Thompson A., Eglinton G. 1994. Primary production of lipid biomarker compounds by *Emiliana huxleyi*: Results from an experimental mesocosm study in Korsfjorden, southern Norway. *Sarsia*, 79, 319-332.
- Conte, M.H., Thompson, A., Lesley, D., Harris, R. P., 1998. Genetic and physiological influences on the alkenone/alkenoate versus growth temperature relationship in *Emiliana huxleyi* and *Gephyrocapsa oceanica*. *Geochimica et Cosmochimica Acta*, 62, 51-68.
- Conte, M.H., Sicre, M.-A., Rühlemann, C., Weber, J.C., Schulte, S., Schulz-Bull, D., Blanz, T., 2006. Global temperature calibration of the alkenone unsaturation index ( $U^{K'}_{37}$ ) in surface water and comparison with surface sediments. *Geochemistry Geophysics Geosystems*, 7, Q02005, doi:10.1029/2005GC001054.
- Du, Y., Qu T., Meyers G., 2008. Interannual variability of sea surface temperature off Java and Sumatra in a global GCM. *Journal of Climate*, 21(11), 2451-2465, doi:10.1175/2007JCLI1753.1.
- Epstein, B.L., D'Hondt, S., Quinn, J.G., Zhang, J., Hargraves, P.E., 1998. An effect of dissolved nutrient concentrations on alkenone-based temperature estimates. *Paleoceanography* 13(2), 122-126.
- Gong, C. Hollander D.J. 1999. Evidence for differential degradation of alkenone under contrasting bottom water oxygen conditions: implication for paleotemperature reconstruction. *Geochimica et Cosmochimica Acta*, 63, 405-411.
- Goñi, M.A., Hartz, D.M., Thunell, R.C., Tappa, E., 2001. Oceanographic considerations for the application of the alkenone-based paleotemperature  $U^{K'}_{37}$  index in the Gulf of California. *Geochimica et Cosmochimica Acta*, 65, 545-557.
- Gordon, A.L., Fine R.A., 1996. Pathways of water between the Pacific and Indian oceans in the Indonesian seas. *Nature*, 379, 146-149.

- Gordon, A.L., Susanto R.D., Field A.L., 1999. Throughflow within Makassar Strait. *Geophysical Research Letters*, 26, 3325-3328.
- Gordon, A.L., 2001. Interocean Exchange, Chapter 4.7, pp. 455-474 in *Ocean Circulation and Climate*, G. Siedler, J. Church and J. Gould, eds. Academic Press.
- Gordon, A.L., Susanto R.D., Vranes, K., 2003. Cool Indonesian throughflow as a consequence of restricted surface layer flow. *Nature*, 425, 824-828.
- Hebbeln, D., et al. 2005. Report and preliminary results of RV SONNE cruise SO-184, PABESIA, Durban (South Africa)-Cilacap (Indonesia)-Darwin (Australia), July 8th-September 13th, 2005, Rep. 246, 142 pp., Univ. Bremen, Bremen, Germany.
- Hendiarti, N., Siegel, H., Ohde, T., 2004. Investigation of different coastal processes in Indonesian water using SeaWiFS data. *Deep-Sea Research II*, 51, 85-97.
- Herbert, T.D., Schuffert, J.D., Thomas, D., Lange, C., Weinheimer, A., Peleo-Alampay, A., Herguera, J.-C., 1998. Depth and seasonality of alkenone production along the California margin inferred from a core top transect. *Paleoceanography*, 13(3), 263-271.
- Herbert, T.D., Heinrich, D.H., Karl, K.T., 2003. Alkenone paleotemperature determinations. *Treatise on Geochemistry*. Pergamon, Oxford, pp. 391-432.
- Herfort, L., Schouten S., Boon J.P., Sinninghe Damsté J.S., 2006. Application of the TEX<sub>86</sub> temperature proxy in the southern North Sea. *Organic Geochemistry*, 37, 1715-1726.
- Hirst, A.C., Godfrey, J.S., 1993. The role of Indonesian throughflow in a global ocean GCM. *Journal of Physical Oceanography*, 23, 1057-1086.
- Hoefs, M.J.L., Klein-Breteler G.J.M., Schouten S., Grossi V., de Leeuw J.W. Sinninghe Damsté J.S., 1998. Postdepositional oxic degradation of alkenones: implications for the measurement of palaeo sea surface temperatures. *Paleoceanography*, 13, 42-49.
- Hopmans, E.C., Schouten, S., Pancost, R.D., van der Meer, M.T.J., Sinninghe Damsté, J.S., 2000. Analysis of intact tetraether lipids in archaeal cell material and sediments by high performance liquid chromatography/atmospheric pressure chemical

- ionization mass spectrometry. *Rapid Communications Mass Spectrometry*, 14, 585-589.
- Hopmans, E.C., Weijers, J.W.H., Schefuß, E., Herfort, L., Sinninghe Damsté, J.S., Schouten, S., 2004. A novel proxy for terrestrial organic matter in sediments based on branched and isoprenoid tetraether lipids. *Earth and Planetary Science Letters*, 224, 107-116.
- Huguet, C., Kim, J.-H., Sinninghe Damsté, J.S., Schouten, S., 2006. Reconstruction of sea surface temperature variations in the Arabian Sea over the last 23 kyr using organic proxies (TEX<sub>86</sub> and U<sup>K</sup><sub>37</sub>), *Paleoceanography*, 21, PA3003.
- Huguet, C., Schimmelmann, A., Thunell, R., Lourens, L.J., Sinninghe Damsté, J.S., Schouten, S., 2007. A study of the TEX<sub>86</sub> paleothermometer in the water column and sediments of the Santa Barbara Basin, California. *Paleoceanography*, 22, PA3202.
- Huguet, C., Kim, J. H., de Lange, G. J., Sinninghe Damsté J. S., Schouten, S., 2009. Effects of long term oxic degradation on the U<sup>K</sup><sub>37</sub>, TEX<sub>86</sub> and BIT organic proxies. *Organic Geochemistry*, 40(12), 1188-1194.
- Jia, Guodong, Zhang, Jie, Chen, Jianfeng, Peng, Ping'an, Zhang, Chuanlun L., 2012. Archaeal tetraether lipids record subsurface water temperature in the South China Sea. *Organic Geochemistry*, 50, 68-77.
- Karner, M. B., DeLong, E.F., Karl, D.M., 2001. Archaeal dominance in the mesopelagic zone of the Pacific Ocean. *Nature*, 409, 507-510.
- Kim, J.H., Schouten, S., Hopmans, E.C., Donner, B., Sinninghe Damsté, J.S., 2008. Globalesediment core-top calibration of the TEX<sub>86</sub> paleothermometer in the ocean. *Geochimica et Cosmochimica Acta*, 72(4), 1154-1173.
- Kim, J.H., Huguet, C., Zonneveld, K.A.F., Versteegh, G.J.M., Roeder, W., Sinninghe Damsté, J. S., Schouten, S., 2009a. An experimental field study to test the stability of lipids used for the TEX<sub>86</sub> and U<sup>K</sup><sub>37</sub> palaeothermometers, *Geochimica et Cosmochimica Acta*, 73(10), 2888-2898.

- Kim J.-H., Crosta X., Michel E., Schouten S., Duprat J. Sinninghe Damsté, J.S., 2009b. Impact of lateral transport on organic proxies in the Southern Ocean. *Quaternary Research*, 71, 246-250.
- Kim, J.-H., van der Meer, J., Schouten, S., Helmke, P., Willmott, V., Sangiorgi, F., Koç, N., Hopmans, E.C., Sinninghe Damsté, J.S., 2010. New indices and calibrations derived from the distribution of crenarchaeal isoprenoid tetraether lipids: implications for past sea surface temperature reconstructions. *Geochimica et Cosmochimica Acta*, 74, 4639-4654.
- Kirst, G.J., Schneider, R.R., Müller, P.J., von Storch, I., Wefer, G., 1999. Late Quaternary temperature variability in the Benguela Current system derived from alkenones. *Quaternary Research*, 52, 92-103.
- Lee, K. E., Kim, J.-H., Wilke, I., Helmke, P., Schouten, S., 2008. A study of the alkenones, TEX<sub>86</sub>, and planktonic foraminifera in the Benguela Upwelling System: Implication for past sea surface temperature estimates. *Geochemistry Geophysics Geosystems*, 9, Q10019, doi:10.1029/2008GC002056.
- Leider, A., Hinrichs, K.-U., Mollenhauer, G., Versteegh, G.J.M., 2010. Core-top calibration of the lipid-based U<sup>K</sup><sub>37</sub> and TEX<sub>86</sub> temperature proxies on the southern Italian shelf (SW Adriatic Sea, Gulf of Taranto). *Earth and Planetary Science Letters*, 300, 112-124.
- Liu, Z., Pagani, M., Zinniker, D., DeConto, R., Huber, M., Brinkhuis, H., Shah, S.R., Leckie R.M. Pearson, A., 2009. Global cooling during the Eocene-Oligocene climate transition. *Science*, 323, 1187-1190.
- Locarnini, R.A., Mishonov, A.V., Antonov, J.I., Boyer, T.P., Garcia, H.E., Baranova, O.K., Zweng, M.M., Johnson, D.R., 2010. *World Ocean Atlas 2009, Volume 1: Temperature*. S. Levitus, Ed. NOAA Atlas NESDIS 68, U.S. Government Printing Office, Washington, D.C., 184 pp.
- Lopes dos Santos, R., Prange, M., Castaneda, I.S., Schefuß, E., Mulitza, S., Schulz, M., Niedermeyer, E.A., Sinninghe Damsté, J.S., Schouten, S., 2010. Glacial-interglacial variability in Atlantic meridional overturning circulation and thermocline

- adjustment in the tropical North Atlantic. *Earth and Planetary Science Letters*, 300, 407-414.
- Marlowe, I.T., 1984. *Lipids as palaeoclimatic indicators*, 273 pp., Ph.D thesis, Univ. of Bristol, Bristol, UK.
- Meyers, P.A., and Dooe., H. 1999. Sources, preservation, and thermal maturity of organic matter in Pliocene-Pleistocene organic-carbon-rich sediments of the western Mediterranean Sea. In: R. Zahn, M.C. Comas, A. Kraus et al., *Proceedings, Ocean Drilling Program, Scientific Results*, 161. Pages 383-390.
- Milliman, J.D., Farnsworth, K.L., Albertin, C.S., 1999. Flux and fate of fluvial sediments leaving large islands in the East Indies. *Journal of Sea Research*, 41(1-2), 97-107.
- Mohtadi, M., W. Oppo, D., Lückge, A., DePol-Holz, R., Steinke, S., Groeneveld, J., Hemme, N., Hebbeln, D., 2011. Reconstructing the thermal structure of the upper ocean: Insights from planktic foraminifera shell chemistry and alkenones in modern sediments of the tropical eastern Indian Ocean. *Paleoceanography*, 26, PA3219.
- Mollenhauer, G., Inthorn, M., Vogt, T., Zabel, M., Sinninghe Damsté, J.S., Eglinton, T.I., 2007. Aging of marine organic matter during cross-shelf lateral transport in the Benguela upwelling system revealed by compound-specific radiocarbon dating. *Geochemistry Geophysics Geosystems*, 8, Q09004, doi:10.1029/2007GC001603
- Murray, A.E., Preston, C.M., Massana, R., Taylor, L. T., Blakis, A., Wu, K., DeLong, E.F., 1998. Seasonal and spatial variability of bacterial and archaeal assemblages in the coastal waters near Anvers Island, Antarctica. *Applied and Environmental Microbiology*, 64, 2585-2595.
- Murray, A.E., Blankis, A., Massana, R., Strawzewski, S., Passow, U., Alldredge, A., DeLong, E.F., 1999. A time series assessment of planktonic archaeal variability in the Santa Barbara Channel. *Aquatic Microbial Ecology*, 20, 129-145.
- Müller, P.J., Kirst, G., Ruhland, G., von Storch, I., Rosell-Melé, A., 1998. Calibration of the alkenone paleotemperature index  $U_{37}^K$  based on core-tops from the eastern South Atlantic and the global ocean (60°N–60°S). *Geochimica et Cosmochimica Acta*, 62, 1757-1772.

- Müller, P.J., Fischer, G., 2001. A 4-year sediment trap record of alkenones from the filamentous upwelling region off Cape Blanc, NW Africa and a comparison with distributions in underlying sediments. *Deep-Sea Research I*, 48, 1877-1903.
- Ohkouchi, N., Eglinton, T.I., Keigwin, L.D., Hayes, J.M., 2002. Spatial and temporal offsets between proxy records in a sediment drift. *Science*, 298, 1224-1227.
- Pelejero, C., Grimalt, J.O., 1997. The correlation between the  $U_{37}^K$  index and sea surface temperatures in the warm boundary: The South China Sea. *Geochimica et Cosmochimica Acta*, 61, 4789-4797.
- Pitcher, A., Wuchter, C., Siedenberg, K., Schouten, S., Sinninghe Damsté, J.S., 2011. Crenarchaeol tracks winter blooms of planktonic, ammonia-oxidizing Thaumarchaeota in the coastal North Sea. *Limnology and Oceanography*, 56, 2308-2318.
- Popp, B.N., Prahl, F.G., Wallsgrove, R.J., Tanimoto, J., 2006. Seasonal patterns of alkenone production in the subtropical oligotrophic North Pacific. *Paleoceanography*, 21, PA1004.
- Potemra, J.T., Hautala, S.L., Sprintall J., 2003. Vertical structure of Indonesian throughflow in a large-scale model. *Deep-Sea Research II*, 50, 2143-2161.
- Prahl, F.G., Muehlhausen, L.A., Zahnle, D.L. 1988. Further evaluation of long-chain alkenones as indicators of paleoceanographic conditions. *Geochimica et Cosmochimica Acta*, 52, 2303-2310.
- Prahl, F.G., Muehlhausen, L.A., Lyle, M., 1989. An organic geochemical assessment of oceanographic conditions at MANOP Site C over the past 26,000 years. *Paleoceanography*, 4(5), 495-510.
- Prahl, F.G., Collier, R.B., Dymond, J., Lyle, M., Sparrow, M. A., 1993. A biomarker perspective on prymnesiophyte productivity in the northeast Pacific Ocean. *Deep-Sea Research I*, 40, 2061-2076.
- Prahl, F.G., Herbert, T., Brassell, S.C., Ohkouchi, N., Pagani, M., Repeta, D., Rosell-Melé, A., E. Sikes., 2000. Status of alkenone paleothermometer calibration: Report from Working Group 3. *Geochemistry Geophysics Geosystems*, 1, 1034.

- Prahl, F.G., Pilskalns, C.H., Sparrow, M.A., 2001. Seasonal record for alkenones in sedimentary particles from the Gulf of Maine. *Deep-Sea Research I*, 48, 515-528.
- Prahl, F.G., Popp, B.N., Karl, D.M., Sparrow, M.A., 2005. Ecology and biogeochemistry of alkenone production at Station ALOHA. *Deep-Sea Research I*, 52, 699-719.
- Prahl, F.G., Mix, A.C., Sparrow, M.A., 2006. Alkenone paleothermometry: Biological lessons from marine sediment records off western South America. *Geochimica et Cosmochimica Acta*, 70, 101-117.
- Qu, T., Meyers, G., 2005. Seasonal characteristics of circulation in the southeastern tropical Indian Ocean. *Journal of Physical Oceanography*, 35(2), 255-267.
- Rixen, T., Ittekkot, V., Herunadi, B., Wetzel, P., Maier-Reimer, E., Gaye-Haake, B., 2006. ENSO-driven carbon see saw in the Indo-Pacific. *Geophysical Research Letters*, 33, L07606, doi:10.1029/2005GL024965.
- Romero, O.E., Rixen, T., Herunadi, B., 2009. Effects of hydrographic and climate forcing on diatom production and export in the tropical southeastern Indian Ocean. *Marine Ecology Progress Series*, 384, 69-82, doi: 10.3354/meps08013.
- Rommerskirchen, F., Condon T., Mollenhauer, G., Dupont, L., Schefuss, E., 2011. Miocene to Pliocene development of surface and subsurface temperature in the Benguela Current System. *Paleoceanography*, 26, PA3216.
- Rosell-Melé, A., Bard, E., Emeis, K.-C., Müller, P. and Schneider, R., Bouloubassi, I., Epstein, B., Fahl, K., Fluegge, A., Freeman, K., Goñi, M., Güntner, U., Hartz, D., Hellebert, S., Herbert, T., Ikehara, M., Ishiwatari, R., Kawamura, K., Kenig, F., de Leeuw, J., Lehman, S., Mejanelle, L., Ohkouchi, N., Pancost, R.D., Pelejero, C., Prahl, F., Quinn, J., Rontani, J.-F., Rostek, F., Rullkötter, J., Sachs, J., Blanz, T., Sawada, K., Schulz-Bull, D., Sikes, E., Sonzogni, C., Ternois, Y., Versteegh, G., Volkman, J.K., Wakeham, S., 2001. Precision of the current methods to measure the alkenone proxy  $U_{37}^K$  and absolute alkenone abundance in sediments: Results of an interlaboratory comparison study. *Geochemistry Geophysics Geosystems*, 2, 10.1029/2000GC000141.

- Rühlemann, C., Butzin, M., 2006. Alkenone temperature anomalies in the Brazil-Malvinas Confluence area caused by lateral advection of suspended particulate material. *Geochemistry Geophysics Geosystems*, 7, 10.1029/2006GC001251.
- Sachs, J.P., Anderson, R.F., 2003. Fidelity of alkenone paleotemperatures in southern Cape Basin sediment drifts. *Paleoceanography*, 18, 1082.
- Saji, N.H., Yamagata, T., 2003. Possible impacts of Indian Ocean Dipole mode events on global climate. *Climate Research*, 25, 151-169.
- Schiebel, R., Zeltner, A., Treppke, U.F., Waniek, J.J., Bollmann, J., Rixen, T., Hemleben, C., 2004. Distribution of diatoms, coccolithophores and planktic foraminifers along a trophic gradient during SW monsoon in the Arabian Sea. *Marine Micropaleontology*, 51, 345-371.
- Schouten, S., Hopmans, E.C., Schefuss, E., Sinninghe Damsté, J.S., 2002. Distributional variations in marine crenarchaeotal membrane lipids: a new tool for reconstructing ancient sea water temperatures? *Earth and Planetary Science Letters*, 204, 265-274.
- Schouten, S., Hopmans, E.C., Sinninghe Damsté, J.S., 2004. The effect of maturity and depositional redox conditions on archaeal tetraether lipid palaeothermometry. *Organic Geochemistry*, 35(5), 567-571.
- Schouten, S., Huguet, C., Hopmans, E.C., Kienhuis, M.V.M., Sinninghe Damsté, J.S., 2007. Analytical methodology for TEX<sub>86</sub> paleothermometry by High-Performance Liquid Chromatography/Atmospheric Pressure Chemical Ionization-Mass Spectrometry. *Analytical Chemistry*, 79, 2940-2944, doi:10.1021/ac062339v.
- Schouten, S., Pitcher, A., Hopmans, E.C., Villanueva, L., van Bleijswijk, J., Sinninghe Damsté, J.S., 2012. Intact polar and core glycerol dibiphytanyl glycerol tetraether lipids in the Arabian Sea oxygen minimum zone: I. Selective preservation and degradation in the water column and consequences for the TEX<sub>86</sub>. *Geochimica et Cosmochimica Acta*, 98, 228-243.
- Schouten, S., Hopmans, E.C., Rosell-Melé, A., Pearson, A., Adam, P., Bauersachs, T., Bard, E., Bernasconi, S.M., Bianchi, T.S., Brocks, J.J., Carlson, L.T., Castañeda, I.S.,

- Derenne, S., Selver, A.D., Dutta, K., Eglinton, T., Fosse, C., Galy, V., Grice, K., Hinrichs, K.-U., Huang, Y., Huguet, A., Huguet, C., Hurley, S., Ingalls, A., Jia, G., Keely, B., Knappy, C., Kondo, M., Krishnan, S., Lincoln, S., Lipp, J., Mangelsdorf, K., Martínez-García, A., Ménot, G., Mets, A., Mollenhauer, G., Ohkouchi, N., Ossebaar, J., Pagani, M., Pancost, R.D., Pearson, E.J., Peterse, F., Reichart, G.-J., Schaeffer, P., Schmitt, G., Schwark, L., Shah, S.R., Smith, R.W., Smittenberg, R.H., Summons, R.E., Takano, Y., Talbot, H.M., Taylor, K.W.R., Tarozo, R., Uchida, M., van Dongen, B.E., Van Mooy, B.A.S., Wang, J., Warren, C., Weijers, J.W.H., Werne, J.P., Woltering, M., Xie, S., Yamamoto, M., Yang, H., Zhang, C.L., Zhang, Y., Zhao, M., Damsté, J.S.S., 2013a. An interlaboratory study of TEX<sub>86</sub> and BIT analysis of sediments, extracts, and standard mixtures. *Geochemistry, Geophysics, Geosystems*, 14 (12), 5263-5285.
- Schouten, S., Hopmans, E.C., Sinninghe Damsté, J.S., 2013b. The organic geochemistry of glycerol dialkyl glycerol tetraether lipids: A review. *Organic Geochemistry*, 54, 19-61.
- Schlitzer, R., 2012. Ocean Data View, <http://odv.awi.de>
- Shah, S. R., Mollenhauer, G., Ohkouchi, N., Eglinton, T. I., Pearson, A., 2008. Origins of archeal tetraether lipids in sediments: insights from radiocarbon analysis. *Geochimica et Cosmochimica Acta*, 72, 4577-4594.
- Shevenell, A.E., Ingalls, A.E., Domack, E.W., Kelly, C., 2011. Holocene Southern Ocean surface temperature variability west of the Antarctic Peninsula. *Nature*, 470, 250-254.
- Sicre, M.A., Labeyrie, L., Ezat, U., Duprat, J., Turon, J.L., Schmidt, S., Mazaud, A., Michel, E., 2005. Mid-latitude Southern Indian Ocean response to Northern Hemisphere Heinrich events. *Earth and Planetary Science Letters*, 240, 724-731.
- Sikes, E.L., Volkman, J.K., 1993. Calibration of alkenone unsaturation ratios ( $U'_{37}$ ) for paleotemperature estimation in cold polar waters. *Geochimica et Cosmochimica Acta*, 57, 1883-1889.

- Sikes, E.L., O'Leary T., Nodder, S.D., Volkman J.K., 2005. Alkenone temperature records and biomarker flux at the subtropical front on the Chatham Rise, SW Pacific Ocean. *Deep-Sea Research I*, 52, 721-748.
- Smith, R.W., Bianchi, T.S., Li, X., 2012. A re-evaluation of the use of branched GDGTs as terrestrial biomarkers: Implications for the BIT Index. *Geochimica et Cosmochimica Acta*, 80 (0), 14-29.
- Sonzogni, C., Bard, E., Rostek, F., Dollfus, D., Rosell-MeleH, A., Eglinton, G., 1997. Temperature and salinity effects on alkenone ratios measured in surface sediments from the Indian Ocean. *Quaternary Research*, 47, 344-355.
- Susanto, R.D., Gordon, A.L., Zheng Q., 2001. Upwelling along the coasts of Java and Sumatra and its relation to ENSO. *Geophysical Research Letters* 28, 1599-1602.
- Susanto, R.D., Moore II, T.S., Marra, J., 2006. Ocean color variability in the Indonesian Seas during the SeaWiFS era. *Geochemistry Geophysics Geosystems*, 7, Q05021 doi:10.1029/2005GC001009.
- Ternois, Y., Sicre, M.-A., Boireau, A., Conte, M.H., Eglinton, G., 1997. Evaluation of long-chain alkenones as paleo-temperature indicators in the Mediterranean Sea. *Deep-Sea Research I*, 44, 271-286.
- Tomczak, M., Godfrey, J.S., 1994. *Regional oceanography: an introduction*. Elsevier, New York.
- Turich, C., Freeman K.H., Bruns M.A., Conte M., Jones A.D. Wakeham S.G., 2007. Lipid of marine Archaea: Patterns and provenance in the water-column and sediments. *Geochimica et Cosmochimica Acta*, 71, 3272-3291, doi:10.1016/j.gca.2007.04.013.
- Verschuren, D., Sinninghe Damsté, J.S., Moernaut, J., Kristen, I., Blaauw, M., Fagot, M., Haug, G.H., 2009. Half-precessional dynamics of monsoon rainfall near the East African Equator. *Nature*, 462, 637-641.
- Versteegh, G.J.M., Riegman, R., de Leeuw, J.W., Jansen, J.H.F., 2001.  $U^{K}_{37}$  values for *Isochrysis galbana* as a function of culture temperature, light intensity and nutrient concentrations. *Organic Geochemistry*, 32, 785-794.

- Volkman, J.K., Eglinton, G., Corner, E.D.S., Forsberg, T.E.V., 1980. Long-chain alkenes and alkenones in the marine coccolithophorid *Emiliana huxleyi*. *Phytochemistry*, 19, 2619-2622.
- Volkman, J.K., Barrett S.M., Blackburn S.I., Sikes, E.L., 1995. Alkenones in *Gephyrocapsa oceanica*: Implications for studies of paleoclimate. *Geochimica et Cosmochimica Acta*, 59, 513-520.
- Wakeham, S.G., Peterson, M.L., Hedges, J.I., Lee, C., 2002. Lipid biomarker fluxes in the Arabian Sea: With a comparison to the equatorial Pacific Ocean. *Deep-Sea Research II*, 49, 2265-2301.
- Webster, P.J., Magana, V.O., Palmer, T.N., Shukla, J., Tomas, R.A., Yanai, M., Yasunari, T., 1998. Monsoons: Processes, predictability, and the prospects for prediction. *Journal of Geophysical Research: Oceans (1978-2012)*, 103(C7), 14451-14510.
- Weijers, J.W.H., Schouten, S., Spaargaren, O.C., Sinninghe Damsté, J.S., 2006. Occurrence and distribution of tetraether membrane lipids in soil: Implications for the use of the TEX<sub>86</sub> proxy and the BIT indeed. *Organic Geochemistry*, 37, 1680-1693.
- Wuchter, C., Schouten, S., Wakeham, S.G., Sinninghe Damsté, J.S., 2005. Temporal and spatial variation in tetraether membrane lipids of marine Crenarchaeota in particulate organic matter: Implications for TEX<sub>86</sub> paleothermometry. *Paleoceanography*, 20, PA3013.
- Wuchter, C., Schouten, S., Wakeham, S.G., Sinninghe Damsté, J.S., 2006. Archaeal tetraether membrane lipid fluxes in the northeastern Pacific and the Arabian Sea: implications for TEX<sub>86</sub> paleothermometry. *Paleoceanography*, 21, PA4208.
- Wyrski, K., 1961. Physical oceanography of Southeast Asian waters, NAGA Rep.2, Scripps Institution of Oceanography, University of California, San Diego, 195pp.
- Yamamoto, M., Shiraiwa, Y., Inouye, I., 2000. Physiological responses of lipids in *Emiliana huxleyi* and *Gephyrocapsa oceanica* (Haptophyceae) to growth status and their implications for alkenone paleothermometry. *Organic Geochemistry*, 31, 799-811.

You, Y., Tomczak, M., 1993. Thermocline circulation and ventilation in the Indian Ocean derived from water mass analysis. *Deep-Sea Research I*, 40, 13-56.

Zhu, C., Weijers, J.W.H., Wagner, T., Pan, J.-M., Chen, J.-F., Pancost, R.D., 2011. Sources and distributions of tetraether lipids in surface sediments across a large river-dominated continental margin. *Organic Geochemistry*, 42 (4), 376-386.

## **Chapter 4 Concentrations and abundance ratios of long-chain alkenones and glycerol dialkyl glycerol tetraethers in sinking particles south of Java**

Wenwen Chen<sup>1</sup>, Mahyar Mohtadi<sup>2</sup>, Enno Schefuß<sup>2</sup>, Gesine Mollenhauer<sup>1,2,3\*</sup>

<sup>1</sup> Department of Geosciences, University of Bremen, Bremen, Germany

<sup>2</sup> MARUM-Center for Marine Environmental Sciences, University of Bremen, Bremen, Germany

<sup>3</sup> Alfred-Wegener Institute for Polar and Marine Research, Bremerhaven Germany

\*corresponding author: [gesine.mollenhauer@awi.de](mailto:gesine.mollenhauer@awi.de)

Deep Sea Research I, in press

#### 4.1. Abstract

In this study, we obtained concentrations and abundance ratios of long-chain alkenones and glycerol dialkyl glycerol tetraethers (GDGTs) in a one-year time-series of sinking particles collected with a sediment trap moored from December 2001 to November 2002 at 2200m water depth south of Java in the eastern Indian Ocean. We investigate the seasonality of alkenone and GDGT fluxes as well as the potential habitat depth of the Thaumarchaeota producing the GDGTs entrained in sinking particles. The alkenone flux shows a pronounced seasonality and ranges from  $0.3 \mu\text{g m}^{-2} \text{d}^{-1}$  to  $8.6 \mu\text{g m}^{-2} \text{d}^{-1}$ . The highest alkenone flux is observed in late September during the Southeast monsoon, coincident with high total organic carbon fluxes as well as high net primary productivity. Flux-weighted mean temperature for the high flux period using the alkenone-based sea-surface temperature (SST) index  $U_{37}^K$  is  $26.8 \text{ }^\circ\text{C}$ , which is similar to satellite-derived Southeast (SE) monsoon SST ( $26.4 \text{ }^\circ\text{C}$ ). The GDGT flux displays a weaker seasonality than that of the alkenones. It is elevated during the SE monsoon period compared to the Northwest (NW) monsoon and intermonsoon periods (approximately 2.5 times), which is probably related to seasonal variation of the abundance of Thaumarchaeota, or to enhanced export of GDGTs by aggregation with sinking phytoplankton detritus. Flux-weighted mean temperature inferred from the GDGT-based  $\text{TEX}_{86}^H$  index is  $26.2 \text{ }^\circ\text{C}$ , which is  $1.8 \text{ }^\circ\text{C}$  lower than mean annual (ma) SST but similar to SE monsoon SST. As the time series of  $\text{TEX}_{86}^H$  temperature estimates, however, does not record strong seasonal amplitude, we infer that  $\text{TEX}_{86}^H$  reflects ma upper thermocline temperature at approximately 50 m water depth.

#### 4.2. Introduction

Two biomarker-based temperature proxies,  $U_{37}^K$  and  $\text{TEX}_{86}$ , are commonly used in paleoclimate studies (e.g., Hugué et al., 2006; Rommerskirchen et al., 2011; Wang et al., 2013).  $U_{37}^K$  quantifies the relative abundance of di- and tri-unsaturated  $\text{C}_{37}$  alkenones, which are produced by certain prymnesiophytes, including coccolithophorids *Emiliania huxleyi* and *Gephyrocapsa oceanica* (Marlowe, 1984; Prahl and Wakeham, 1987;

Volkman et al., 1980).  $\text{TEX}_{86}$  is another organic geochemical proxy suggested to reflect sea surface temperature (SST), which is based on glycerol dialkyl glycerol tetraethers (GDGTs) and defined as the abundance ratio of specific types of GDGTs with variable numbers of cyclopentane rings (Schouten et al., 2002). These compounds are synthesized as membrane lipids by the ubiquitous marine Thaumarchaeota (formerly named Crenarchaeota; Brochier-Armanet et al., 2008; Schouten et al., 2002; Sinninghe Damsté et al., 2002). Although core-top calibrations established robust correlations between  $U^{K'}_{37}$  and  $\text{TEX}_{86}$  with mean annual SST (ma SST) (e.g., Conte et al., 1998, 2006; Kim et al., 2008, 2010; Müller et al., 1998; Schouten et al., 2002), some studies have shown that deviations of both proxy temperature estimates from ma SST can be attributed to seasonal production and/or a subsurface depth habitat of the source organisms (e.g., Huguet et al., 2007; Jia et al., 2012; Kim et al., 2012; Lee et al., 2008; Leider et al., 2010; Prah et al., 2005; Rommerskirchen et al., 2011; Seki et al., 2007; Wuchter et al., 2006).

Seasonal production and flux of biomarkers has the potential to bias a proxy signal towards the seasonal of maximum production. It is debated in the literature whether or not a seasonally variable flux of alkenones results in a seasonal bias of the  $U^{K'}_{37}$  signal in sediments, or if preserved alkenones reflect mean annual conditions (e.g., Conte et al., 2006, Leduc et al., 2010, Schneider et al., 2010). For GDGTs, the ongoing debate relates not only to the season of export but also to the production depth of the lipids constituting the sedimentary  $\text{TEX}_{86}$  record (e.g., Herfort et al., 2006; Lopes dos Santos et al., 2010, Kim et al., 2012). Thaumarchaeota are known to thrive throughout the water column and are reported to occur at maximum abundance at a depth of 100-200 m (e.g., Tolar et al., 2013). Seasonality and production depth effects of alkenones and GDGTs likely depend on the different oceanic settings and thus, it is necessary to investigate their respective response in individual regions for a better interpretation of local sedimentary records.

Sediment trap studies are an excellent tool to shed light on the seasonality and depth of alkenone and GDGT production exported to the sediment. Rosell-Melé and Prah (2013) recently compiled published sediment trap time series data for alkenones from 34 sampling locations and found that the seasonality of alkenone flux varies strongly between sites and depends on the local oceanographic settings. The seasonal patterns of export production are complex, resulting from the interplay of seasonality in production and particle flux. No clear biogeographic or latitudinal pattern in alkenone flux seasonality could be deduced from the existing data set. The seasonality is not necessarily coupled to bulk export primary productivity and varies markedly across the oceans. Moreover,  $U_{37}^K$  of flux-weighted averages in sediment traps is not always biased by seasonality but instead resembles global trends in surface sediments. Notably, approximately ninety percent of the sites compiled by Rosell-Melé and Prah (2013) are located in the northern hemisphere. Only two studies are from the southern hemisphere and only one study was performed in the Indian Ocean. According to this synthesis, our record is the second sediment trap record for alkenone from the Indian Ocean.

The ecology of GDGT producers, i.e. the seasonality of their production and/or export, and the depth of their habitat, is still poorly constrained. Thaumarchaeota occur throughout the year and the abundance of Thaumarchaeota varies seasonally (Schouten et al., 2013 and reference therein). However, there are thus far only seven seasonal  $TEX_{86}$  records from sediment traps available. To date, published records exist from the northeastern Pacific and the Arabian Sea (Wuchter et al., 2006), the Santa Barbara Basin (Huguet et al., 2007), the Mozambique Channel (Fallet et al., 2011), the western North Pacific (Yamamoto et al., 2012), the Gulf of California (McClymont et al., 2012), the Cariaco Basin (Turich et al., 2013) and Cape Blanc, Mauritania (Mollenhauer et al., 2015). In several studies it was observed that  $TEX_{86}$  temperature estimates reflect the temperature of specific seasons and were explained by either seasonality in Thaumarchaeota growth or seasonal variation in export of GDGTs (e.g., Mollenhauer et al., 2015; Turich et al., 2013; Yamamoto et al., 2012). On the other hand, some

sediment trap records suggest that the TEX<sub>86</sub>-derived temperatures reflect the temperature of subsurface water (McClymont et al., 2012; Wuchter et al., 2006). This conclusion was also reached by some recent studies investigating suspended matter samples (Nakanishi et al., 2012) and shallow water surface sediments (Xing et al., 2015). In contrast, TEX<sub>86</sub> temperature variations in the sediment trap from the Santa Barbara Basin was not coupled to changes in SST or deep-water temperatures, which was attributed to a complex contribution of GDGTs produced at different depths and hydrologic conditions (Huguet et al., 2007).

So far, there are only four published sediment trap records for both indices including the interpretation of difference between the two proxies (Fallet et al., 2011; McClymont et al., 2012; Mollenhauer et al., 2015; Turich et al., 2013). The observations made in these studies differ between the regions. While as expected alkenones in most of these studies are in close agreement with satellite SST, TEX<sub>86</sub>-based temperature estimates are more similar to subsurface temperatures or display reduced seasonal temperature amplitudes.

In this study, we present a one-year time-series record of alkenones and GDGTs from samples obtained with a sediment trap deployed in the eastern Indian Ocean off Java. The aim of this study is to investigate the seasonality of production and export of biomarkers, and to test the hypothesis of sub-surface production of GDGTs in the upwelling environment off southern Java.

### **4.3. Study area**

The Australian-Indonesian Monsoon (AIM), displaying contrasting seasonal features, is the dominating climate feature in the Eastern Indian Ocean (Fig. 4.1.), influencing wind and precipitation patterns and, consequently, surface ocean hydrography and currents. During the NW monsoon season (January-March), northwest winds from the Asian continent cause a rainy season with increased precipitation over Indonesia resulting in maximum fluvial discharge, and in low chlorophyll-a concentration

(and hence, productivity) in the adjacent ocean (Jennerjahn et al., 2004). The SE monsoon season (July-September) is associated with easterlies from Australia that carry warm and dry air over this region. In June, the easterly alongshore wind starts to intensify causing upwelling along the southern coast of Java and the Lesser Sunda Islands (LSI) leading to low SST (Susanto et al., 2001). Upwelling of nutrient-rich, cold subsurface waters results in high primary production and high particle fluxes (Rixen et al., 2006).

The hydrography in the study area is additionally affected by the El Niño-Southern Oscillation (ENSO) and the Indian Ocean Dipole (IOD) phenomena on inter-annual timescales. During the El Niño periods and positive IOD events, enhanced upwelling with higher primary productivity and decreased SST up to 4 °C relative to the mean are observed. During the strong El Niño periods, such as 1997/98, anomalous winds induced a relatively stronger and by up to three months longer upwelling period along the coast of Java with enhanced productivity (Susanto et al., 2001; Susanto and Marra, 2005). Conversely, the upwelling intensity is reduced during La Niña periods and negative IOD events.

The variable wind regime of the Eastern Indian Ocean also influences the ocean currents of the region. The South Java Current (SJC), originating from the Equatorial Counter Current (ECC) (Fig. 4.1.; Tomczak and Godfrey, 1994; Wyrтки, 1973), plays an important role in distributing freshwater into and out of the southeast Indian Ocean. It is a south-eastward flow with strong semi-annual and intraseasonal variability near the coast of Sumatra and Java. The SJC transports warm and fresh waters from the high rainfall, warm pool region into the eastern equatorial Indian Ocean (Sprintall et al., 2010 and references therein). It meets with the Leeuwin Current (LC) at the southeastern part of the Indonesian Archipelago, and feeds into the South Equatorial Current (SEC), the steady branch of the regional circulation, which flows westward between about 10° and 20° S (Donguy and Meyers, 1995; Wyrтки, 1961). In the NW monsoon season, the SEC is at its southernmost position, and the SJC flows eastward along the coast of Java. During

the SE monsoon season, the flow of the SJC reverses, flows westward along the coast of Java and feeds into the SEC without contribution of the LC (Fig. 4.1.).

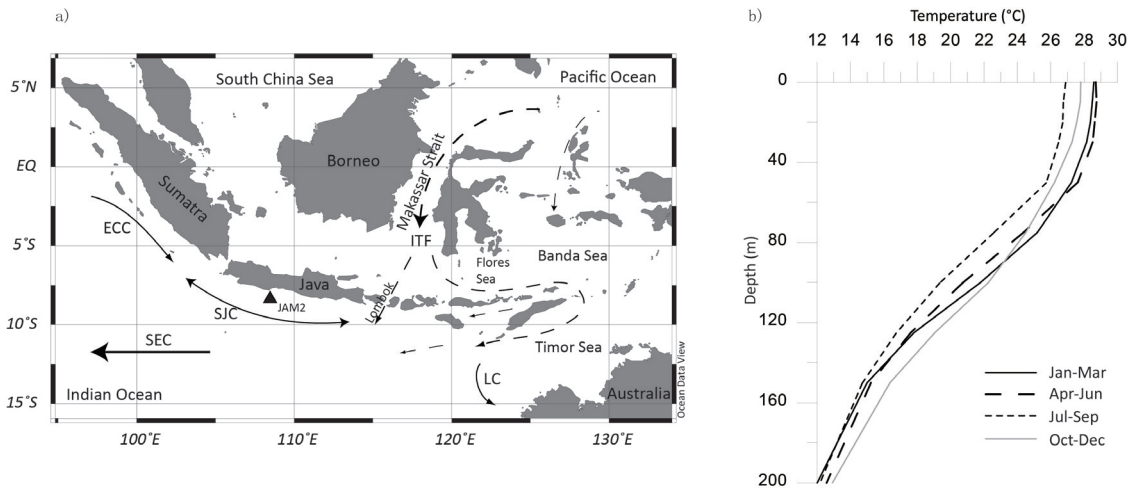


Fig. 4.1. a) Map of the study region showing the surface currents (solid arrows) and subsurface currents (dashed arrows). The black triangle shows the position of the sediment trap. Ocean currents are denoted as: ECC: Equatorial Counter Current; ITF: Indonesian Throughflow; LC: Leeuwin Current; SEC: South Equatorial Current; SJC: South Java Current. Double arrows of SJC indicate the change of direction of SJC during the NW (eastward) and SE monsoon (northwestward), respectively. b) the depth profiles of temperature in different seasons at the Jam 2 site (data extracted from World Ocean Atlas 2005 (Locarnini et al., 2006)).

The Indonesian Throughflow (ITF; Fig. 4.1.), the only low-latitude inter-ocean pathway from the Pacific to the Indian Ocean, plays an important role in global thermohaline circulation and directly impacts both the regional circulation and thermal structure of the upper water column at our study site (Qu and Meyers, 2005; Wijffels, 2001). The ITF is composed mainly of North Pacific Intermediate Water flowing through the Makassar Strait (Gordon and Fine, 1996; Fig. 4.1.). Some of the Makassar Throughflow directly enters into the Indian Ocean via the Lombok Strait, while most of the throughflow turns eastward to enter the Banda Sea. Within the Banda Sea, these water masses are modified by mixing with South Pacific Intermediate Water entering the Banda Sea, upwelling and air-sea fluxes before flowing into the Indian Ocean (Field and Gordon, 1992; Koch-Larrouy et al., 2008; Sprintall et al., 2003). From the Banda Sea,

the ITF exits to the eastern Indian Ocean through the Ombai Strait and Timor passages. During the SE monsoon season, the sea level difference between Java and the western Pacific is largest with maximum strength of the ITF, which facilitates the transfer of cooler, fresher thermocline waters of the ITF into the Indian Ocean (Gordon, 2005; Tomczak and Godfrey, 1994).

#### **4.4. Material and Methods**

##### **4.4.1 Sediment trap mooring**

The sediment trap JAM1-2 (8°17.5S, 108°02.0E) was deployed off South Java between November 2000 and November 2002 at a water depth of approximately 2200 m. The sediment trap was located about 800 m above the seafloor. Details of the sediment trap mooring are described in Mohtadi et al. (2009). We analyzed samples from JAM2 with a sampling interval of 16 days between December 2001 and November 2002.

##### **4.4.2 Lipid extraction and analysis**

Long-chain alkenones and GDGTs were extracted from freeze-dried and homogenized sediment trap material (50-330 mg). Total lipids were extracted with, successively, methanol (MeOH), MeOH:dichloromethane (DCM) 1:1 (v:v) and DCM (25 mL each, each for 5min) with an ultrasonic probe. Before extraction known amounts of C<sub>19</sub> ketone and C<sub>46</sub> GDGT were added as internal standards. After each extraction, the suspensions were centrifuged and the supernatants combined. The combined extracts were washed with 50 mL deionized water to remove salts, dried over Na<sub>2</sub>SO<sub>4</sub>, and concentrated using a rotary evaporator. The lipid extract was saponified at 80 °C for 2 h with 300 µL of 0.1M KOH in 9:1 MeOH/H<sub>2</sub>O. After saponification, each sample was separated into an apolar, a ketone and a polar fraction via silica gel column chromatography using hexane, a mixture of DCM and hexane (2:1, v:v) and MeOH, respectively.

Alkenone analyses for  $U_{37}^K$  were performed on the ketone fraction using an HP5890 series gas chromatograph (GC) equipped with a flame ionization detector. Details of alkenone analyses have been described in Chen et al. (2014).

$U_{37}^K$  was calculated as:  $U_{37}^K = (C_{37:2})/(C_{37:2}+C_{37:3})$ .  $U_{37}^K$  values were converted to temperature estimates by applying the calibration of Conte et al. (2006):

$$T = -0.957 + 54.293 \times (U_{37}^K) - 52.894 \times (U_{37}^K)^2 + 28.321 \times (U_{37}^K)^3$$

The compound concentrations ( $C_{37:2}$  and  $C_{37:3}$ ) were determined by relating chromatogram peak areas to the concentration of the internal standard. The error in quantification was less than 10%. Based on duplicate analysis, the analytical precision of determinations for alkenone unsaturation was better than 0.03  $U_{37}^K$  units (0.62 °C).

Polar fractions containing GDGTs were dissolved in a 99:1 (v:v) hexane: isopropanol solvent mixture, and filtered using a 0.45  $\mu\text{m}$  PTFE filter, before analyses using an Agilent 1200 series high performance liquid chromatography system with an Agilent 6210 mass spectrometer (HPLC-MS). Aliquots of 20  $\mu\text{L}$  were injected onto a Prevail Cyano column (2.1 x 150mm, 3  $\mu\text{m}$ ) maintained at 30 °C. GDGTs were eluted using the following gradient: 99:1 hexane: isopropanol (v:v) for 5 min followed by a linear gradient to 1.8% isopropanol for 45 min. Flow rate was 0.2 ml/min.

A surface sediment study from the eastern Indian Ocean confirmed that as recommended by Kim et al. (2010) the  $\text{TEX}_{86}^H$  corresponds best to near-surface water temperatures in our study area (Chen et al., 2014). It is calculated from the respective peak areas according to:

$$\text{TEX}_{86}^H = \log\left(\frac{[\text{GDGT-2}] + [\text{GDGT-3}] + [\text{GDGT-4}']}{[\text{GDGT-1}] + [\text{GDGT-2}] + [\text{GDGT-3}] + [\text{GDGT-4}']}\right)$$

where the numbers 1-4 indicate the number of cyclopentane rings in the isoprenoid molecules, and GDGT-4' is the regio-isomer of crenarchaeol. The  $\text{TEX}_{86}^H$  values can be

converted to temperature estimates according to the following relationship (Kim et al., 2010).

$$\text{SST} = 68.4 \times \text{TEX}_{86}^{\text{H}} + 38.6$$

Replicate analysis of samples determined that the average analytical reproducibility of this procedure is 0.01  $\text{TEX}_{86}$  units or 0.41 °C. Concentrations of GDGTs were calculated semi-quantitatively relative to the internal standard. It has to be noted, though, that no correction for differences in response factors of the individual GDGTs has been made due to the unavailability of a pure  $\text{C}_{86}$  GDGT standard at the time of the analyses.

The BIT index, a proxy for soil versus marine organic matter input to sediments (Hopmans et al., 2004), is calculated using the peak areas of branched GDGTs with 4 (branched GDGT-I), 5 (branched GDGT-II) and 6 (branched GDGT-III) methyl moieties, respectively and GDGT-4 (crenarchaeol), according to the following formula (Hopmans et al., 2004):

$$\text{BIT} = \frac{[\text{GDGT-I}] + [\text{GDGT-II}] + [\text{GDGT-III}]}{[\text{GDGT-I}] + [\text{GDGT-II}] + [\text{GDGT-III}] + [\text{GDGT-4}]}$$

## 4.5. Results

### 4.5.1. Fluxes

Alkenone and GDGT concentrations, fluxes, indices as well as temperature estimates derived from  $\text{U}_{37}^{\text{K}}$  and  $\text{TEX}_{86}^{\text{H}}$  for JAM2 are listed in Table 4.1. Concentration and flux data (both relative to dry weight and relative to TOC) are presented for total  $\text{C}_{37}$ -alkenones and isoprenoid GDGTs, including GDGT-0, GDGT-1, GDGT-2, GDGT-3, crenarchaeol and crenarchaeol regio-isomer (Table 4.1.).

The average of absolute alkenone concentrations is  $6 \mu\text{g g}^{-1}$  sediment, ranging from  $1.2 \mu\text{g g}^{-1}$  to  $22.7 \mu\text{g g}^{-1}$  sediment (Table 4.1.). However, in most samples the tri-unsaturated alkenone ( $\text{C}_{37:3}$ ) could not be quantified reliably due to small peak areas. Thus, for these samples, total alkenone concentration and flux data are expressed as concentration and flux of di-unsaturated alkenone ( $\text{C}_{37:2}$ ) (Table 4.1.). The bulk concentrations of biomarkers could be affected by high lithogenic content in this area. To compensate for this effect, we calculated the concentrations relative to TOC content determined by Rixen et al. (2006, Table 4.1.). The total alkenone concentrations vary between  $34 \mu\text{g per g C}$  and  $427 \mu\text{g per g C}$ , with an average of  $134 \mu\text{g per g C}$  (Fig. 4.2b.). The alkenone flux shows a strong seasonality with an average flux of  $2 \mu\text{g m}^{-2} \text{day}^{-1}$ , ranging from  $0.3 \mu\text{g m}^{-2} \text{day}^{-1}$  to  $8.6 \mu\text{g m}^{-2} \text{day}^{-1}$  (Fig. 4.2b.). The highest alkenone flux ( $8.6 \mu\text{g m}^{-2} \text{day}^{-1}$ ) occurred in late September during the SE monsoon. A secondary maximum in alkenone flux ( $\sim 2 \mu\text{g m}^{-2} \text{day}^{-1}$ ) is observed in March at the end of the NW monsoon.

Table 4.1. Flux measurements and summary of alkenone and GDGTs data for sediment trap JAM-2 off Java.

Cup	Trap Cup Open	days	Flux total <sup>a</sup> [mg m <sup>-2</sup> d <sup>-1</sup> ]	Carbonate <sup>a</sup> [mg m <sup>-2</sup> d <sup>-1</sup> ]	Corg <sup>a</sup> [mg m <sup>-2</sup> d <sup>-1</sup> ]	Bio Opal <sup>b</sup> [mg m <sup>-2</sup> d <sup>-1</sup> ]	Lith. <sup>a</sup> [mg m <sup>-2</sup> d <sup>-1</sup> ]	Corg <sup>a</sup> [%]	Total Alkenones (C37)		U <sup>K</sup> <sub>37</sub> [°C]	SST- U <sup>K</sup> <sub>37</sub> [°C]	SD U <sup>K</sup> <sub>37</sub>	Total GDGTs		TEX <sub>86</sub> [°C]	Temp- TEX <sup>H</sup> <sub>86</sub> [°C]	SD Temp- TEX <sup>H</sup> <sub>86</sub>	BIT		
									(μg/g dry)	(μg/g C)				(μg/g dry)	(μg/g C)					TEX <sub>86</sub>	Temp- TEX <sup>H</sup> <sub>86</sub>
D1	14/12/2001	16	239	13	10	35	173	4.2	1.8	35*	0.4*	0.83	-	-	11.2	264	3	0.67	26.8	0.2	0.04
D2	30/12/2001	16	322	25	9	45	235	2.8	1.2	36*	0.3*	0.88	-	-	6.7	235	2	0.67	26.9	0.3	0.06
D3	15/01/2002	16	349	23	10	50	259	2.8	1.6	53*	0.5*	0.95	-	-	5.7	207	2	0.67	26.6	-	0.06
D4	31/01/2002	16	289	25	9	52	195	3.2	1.8	55*	0.5*	0.95	-	-	n.d.	n.d.	n.d.	n.d.	n.d.	n.d.	n.d.
D5	16/02/2002	16	236	24	8	41	157	3.4	1.3	34*	0.3*	0.89	-	-	11.6	339	3	0.67	26.6	0.5	0.03
D6	04/03/2002	16	351	52	12	55	221	3.5	7.4	188*	2.3*	0.90	-	-	9.1	258	3	0.69	27.7	0.7	0.03
D7	20/03/2002	16	403	41	13	69	269	3.2	5.0	150*	1.9*	0.96	-	-	8.2	257	3	0.67	26.6	0.9	0.04
D8	05/04/2002	16	243	29	10	61	135	4.2	5.8	133*	1.3*	0.94	-	-	11.9	287	3	0.66	26.0	0.3	0.02
D9	21/04/2002	16	193	29	7	39	112	3.7	1.7	41*	0.3*	0.91	-	-	9.5	258	2	0.65	25.9	0.7	0.03
D10	07/05/2002	16	167	19	7	34	102	4.4	3.1	68*	0.5*	0.94	-	-	13.0	297	2	0.66	26.3	0.1	0.02
D11	23/05/2002	16	118	11	5	22	76	4.1	4.8	110*	0.5*	0.93	-	-	15.2	374	2	0.65	25.9	0.2	0.02
D12	08/06/2002	16	201	17	7	32	139	3.4	1.6	44*	0.3*	0.92	-	-	8.7	259	2	0.65	26.0	0.2	0.04
D13	24/06/2002	16	304	45	10	49	191	3.4	3.4	96*	1.0*	0.96	-	-	7.0	204	2	0.65	25.8	0.2	0.04
D14	10/07/2002	16	265	32	9	45	171	3.5	4.4	120*	1.1*	0.96	-	-	6.1	172	2	0.65	25.9	0.3	0.05
D15	26/07/2002	16	306	42	11	55	190	3.6	4.4	118*	1.3*	0.97	-	-	7.7	214	2	0.67	26.5	0.9	0.04
D16	11/08/2002	16	735	76	34	130	468	4.6	6.2	136	4.6	0.97	27.6	0.5	4.9	107	4	0.64	25.2	1.5	0.05
D17	27/08/2002	16	512	84	20	99	294	3.8	6.7	176	3.4	0.96	27.5	0.5	5.9	154	3	0.66	26.3	0.2	0.04
D18	12/09/2002	16	380	67	19	98	180	5.0	22.7	456	8.6	0.94	26.8	0.8	16.4	330	6	0.65	25.9	0.4	0.01
D19	28/09/2002	16	305	50	15	99	130	4.8	15.6	325	4.7	0.94	26.9	0.6	15.0	314	5	0.65	25.9	0.5	0.01
D20	14/10/2002	16	507	93	28	155	209	5.5	13.8	250	7.0	0.93	26.6	0.9	12.6	229	6	0.66	26.0	0.3	0.01
D21	30/10/2002	16	471	62	19	118	257	4.0	11.3	280	5.3	0.92	26.2	1.1	12.9	319	6	0.64	25.5	0.3	0.02

n.d.=not detected

a. Flux measurements published by Rixen et al., 2006.

\*. Total alkenone concentrations and flux expressed as concentration and flux of C<sub>37:2</sub>

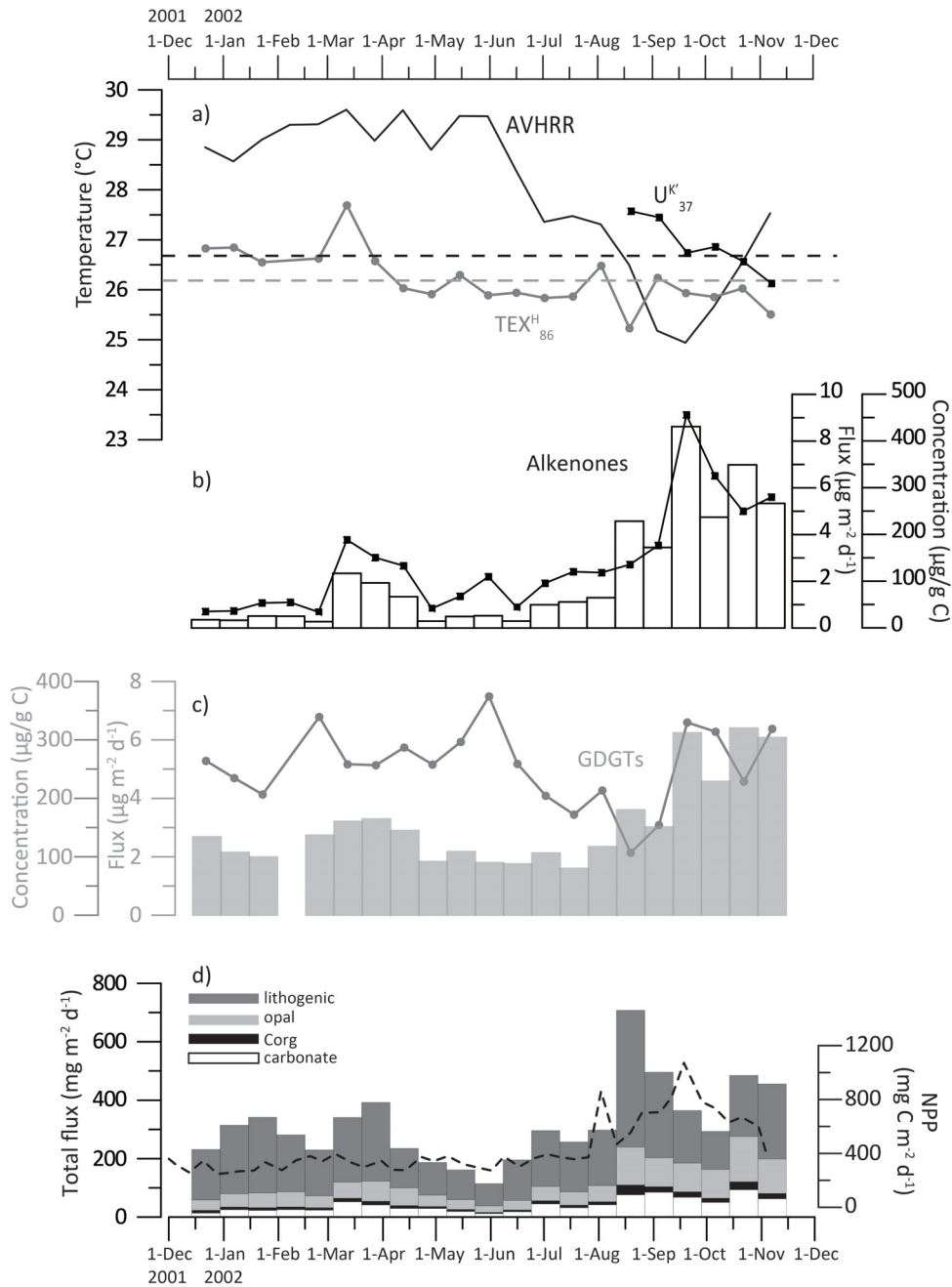


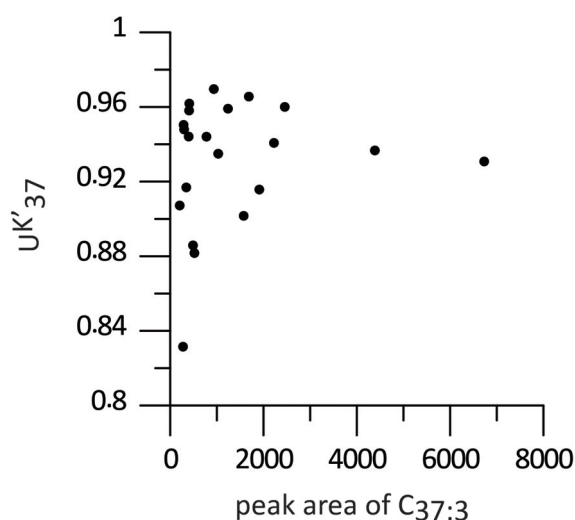
Fig. 4.2. a) local SST from AVHRR at the trap site (black) and temperature estimates from  $U^{K}_{37}$  (black squares) and  $TEX^{H}_{86}$  (grey dots). Black and grey dashed lines indicate flux-weighted average temperatures for  $U^{K}_{37}$  from the high-flux period and annual flux-weighted average temperatures for  $TEX^{H}_{86}$ , respectively; b) alkenone concentration relative to TOC ( $\mu\text{g/g C}$ , black line) and alkenone flux (white bars); c) GDGT concentration relative to TOC ( $\mu\text{g/g C}$ , grey line) and GDGTs flux (grey bars); d) satellite-based net primary production (NPP) estimates at the trap site (<http://web.science.oregonstate.edu/ocean.productivity>; blackdashed line). Flux of total mass, lithogenic, opal, organic carbon and carbonate in  $\text{mg m}^{-2} \text{day}^{-1}$  are taken from Rixen et al.2006.

The average concentration of isoprenoidal GDGTs is  $10 \mu\text{g g}^{-1}$  sediment and is dominated by crenarchaeol (GDGT-4) accounting for 52 - 58% and GDGT-0 representing 19 - 24% (Table 4.1.). The total GDGT concentration ranges from  $107 \mu\text{g per g C}$  to  $374 \mu\text{g per g C}$  (Fig. 4.2c.). The GDGT flux shows a weaker seasonality than that of the alkenones, varying between  $2 \mu\text{g m}^{-2} \text{day}^{-1}$  and  $6 \mu\text{g m}^{-2} \text{day}^{-1}$  (Fig. 4.2c.).

Branched GDGTs have also been analyzed in this study. The total concentration and flux of branched GDGTs ranges from  $63 \mu\text{g per g C}$  to  $207 \mu\text{g per g C}$  and from  $0.9 \mu\text{g m}^{-2} \text{day}^{-1}$  and  $3.5 \mu\text{g m}^{-2} \text{day}^{-1}$ , respectively (not shown). The BIT index is very low (below 0.08) throughout the entire sampling period.

#### 4.5.2. Biomarker based temperatures

Over the period from December 2001-November 2002, extremely low  $\text{C}_{37:3}$  concentrations were observed in the samples collected during the NW monsoon and intermonsoon season. As a consequence we observe a large scatter in  $U_{37}^K$  values when the amounts of  $\text{C}_{37:3}$  were below a threshold value of 2000 units (Fig. 4.3.). Therefore, no  $U_{37}^K$ -SST estimates could be obtained for the samples from the low-flux period, as the low alkenone concentrations did not permit a reliable quantification of the triple unsaturated  $\text{C}_{37}$  alkenone.



We thus only report alkenone based temperature estimates from the season where alkenone abundances allowed a reliable determination of  $C_{37:3}$  concentration, i.e., the SE monsoon season.  $U_{37}^K$ -based temperatures from the SE monsoon season vary between 26.2 °C and 27.5 °C (Table 1, Fig. 4.2a.). The analytical error based on duplicate measurements of these samples range from 0.5 to 1.1 °C (av. 0.8 °C; Table 4.1.). The flux-weighted mean for the high flux period with reliable  $U_{37}^K$ -based estimates is 26.7 °C, which is close to the average SE monsoon satellite-based SST of 26.4 °C as determined by the Advanced Very High Resolution Radiometer (AVHRR at 8°17.5S, 108°02.0E, data obtained from <http://www.ncdc.noaa.gov/oa/ncdc.html>).

The  $TEX_{86}^H$ -based temperature estimates are cooler than satellite-based temperatures throughout the entire year except during the SE monsoon (September-November). The  $TEX_{86}^H$  temperature estimates range from 25.2 °C in August to 27.7 °C in March. The annual flux-weighted average  $TEX_{86}^H$  temperature estimate is 26.2 °C, only slightly cooler than  $U_{37}^K$ -based temperatures (Table 4.1., Fig. 4.2a.). The flux-weighted average  $TEX_{86}^H$  temperature estimate of 26.2 °C is also cooler than satellite-based ma SST of 28 °C.

## 4.6. Discussion

### 4.6.1. Alkenones

#### 4.6.1.1. Fluxes

Total alkenone flux off Java as recorded in sediment trap JAM 2 is not uniform throughout the year (Fig. 4.2.). Instead, we observe a pronounced seasonality during the sampling period with an elevated flux from August to October during the SE monsoon upwelling season. The higher total alkenone flux is associated with maxima in total flux, fluxes of TOC, carbonate, lithogenic particles and opal (Rixen et al., 2006) as well as net primary productivity (NPP, Mohtadi et al., 2009). In the study area, prymnesiophyte production is dominated by *E. huxleyi* and *G. oceanica* and occurs throughout the entire year with maximum abundance during the upwelling season (Andruleit and Rogalla,

2002; Andruleit, 2007). Romero et al. (2009) observed in the same trap that maximum diatom flux occurred early in the SE monsoon upwelling season. Upwelling of cold and nutrient-rich water is the main factor promoting phytoplankton growth. Similar alkenone flux maxima associated with upwelling have also been observed in trap studies from other upwelling areas (Müller and Fischer, 2001; Turich et al., 2013).

Several published sediment trap studies reported that the seasonal variation in alkenone flux tracks seasonal variations in alkenone production (Rosell-Melé and Prah, 2013 and reference therein). Although the alkenone flux is paralleled with the mass flux, it does not mean that the highest alkenone production must occur during the period of highest primary productivity. A series of studies show that the highest alkenone flux is associated not only with their highest concentration in the particles but can be due to elevated total particle flux (e.g., Rosell-Melé and Prah, 2013). Notably, the flux of alkenones is strongly correlated with the flux of carbonate ( $r^2=0.71$ ), TOC ( $r^2=0.62$ ) and opal ( $r^2=0.77$ ) (Fig. 4.4a, b, c.). In this respect, our findings are in agreement with some sediment trap time series reporting that alkenone export varies seasonally, for instance, in the Gulf of Maine (Prah et al., 2001), in the northwestern North Pacific Ocean (Harada et al., 2006) and off Cape Blanc, Mauritania (Mollenhauer et al., 2015).

A secondary peak of alkenone flux in March during the NW monsoon occurs coevally with enhanced fluvial discharge during the rainy season. The secondary peak of alkenone flux is in accordance with elevated fluxes of lithogenic and biogenic components (opal, TOC and carbonate) (Fig. 4.2.). Romero et al. (2009) observed an elevated flux of total diatoms in the same sediment trap during the early NW monsoon season possibly due to riverine nutrient input. Diatom flux providing the bulk of opal is enhanced in late March/early April (Fig. 4.2e.), coeval with the second maximum in alkenone flux. As mentioned above, alkenone flux co-varies with the lithogenic flux, which moderately increases from late February/early March to late March/early April (Fig. 4.2e.). However, a better correlation exists between the fluxes of alkenones and carbonate, and alkenones and TOC, than alkenones and lithogenic particles ( $r^2=0.11$ , Fig.

4.4d.). The weaker correlation with lithogenic particles indicates that the lithogenic “ballasting effect” in this area likely is not the dominant control on the export of alkenones. Thus, the secondary peak of alkenones could be related to coccolithophorid blooms triggered by increased riverine nutrient discharge following the rainy season in Java (Hendiarti et al., 2004).

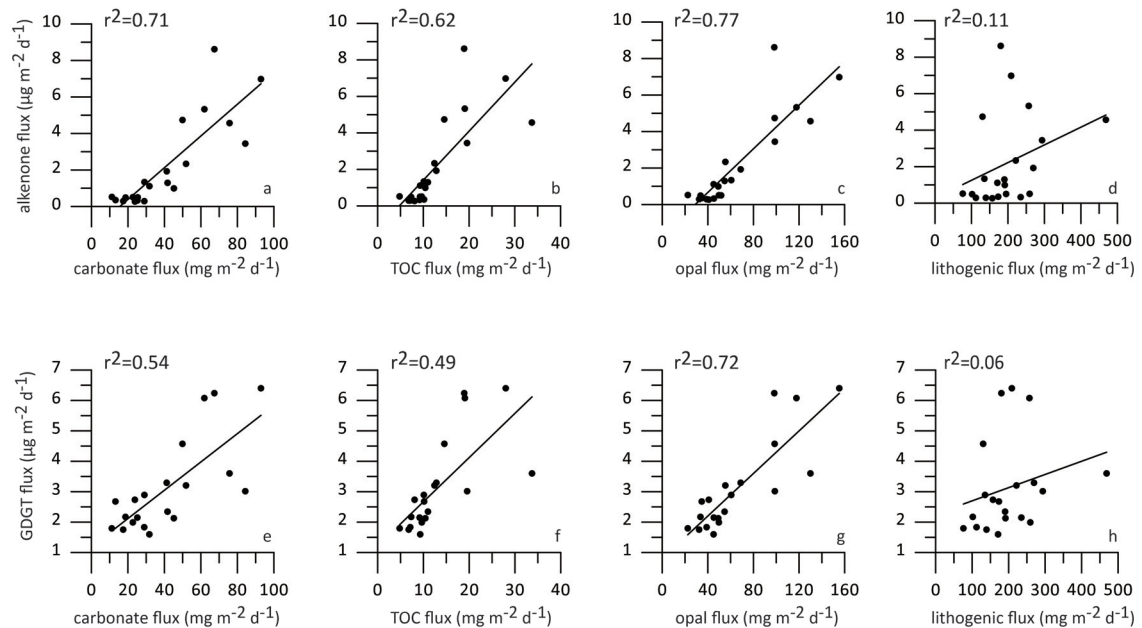


Fig. 4.4. Correlations of carbonate (a, e) flux, TOC flux(b, f), opal flux (c, g) and lithogenic flux (d, h) with lipids fluxes for trap Jam 2 and coefficients of determination.

Overall, the observation of a strong coupling between alkenone fluxes and fluxes of carbonate, opal and lithogenic particles suggests a mechanistic link between them. The export of alkenones is thus likely controlled by the formation of sinking particles, i.e., fecal pellets or aggregates, during the high flux season and does not necessarily mirror the seasonality of alkenone production. A comparison of  $U_{37}^K$  temperature estimates with observed SST at the trap site might help understand the seasonality of production.

#### 4.6.1.2. Alkenone temperature estimates

$U_{37}^K$  temperature estimates from the trap samples differ from satellite-derived SST estimates. The satellite-derived SST estimates show a large seasonal variability with

temperature minima near 25 °C during the SE monsoon, while the  $U_{37}^K$  temperature estimates are rather constant at 26.8 °C (Fig. 4.2.). Before making any interpretations from SST records, it is important to consider the reliability of the temperature estimates based on proxy data. Rosell-Melé et al. (1995) reported that the value of the  $U_{37}^K$  index could be affected by alkenone concentration, especially at extremely low  $C_{37}$  tri-unsaturated alkenone concentration. At our trap site, the concentrations of  $C_{37:3}$  alkenone for the low-flux period are extremely low (below 10 µg per g C), and peaks are therefore impossible to detect, which is likely due to the prevalent surface waters temperature of more than 26-28 °C (Pelejero and Calvo, 2003).

As discussed above, we could not obtain a full annual cycle of  $U_{37}^K$  temperature estimates. Instead, we have data for a short time period during the high flux season. The flux-weighted mean  $U_{37}^K$ -SST for the high-flux period is 26.7 °C, which is close to the satellite-derived SE SST of 26.4 °C. A hypothetical weighted mean value of 26.7 °C is also calculated from the observed alkenone flux (Table 1) assuming that during each time period, the  $U_{37}^K$ -based temperature estimate is equal to the satellite observed SST. Similarly, the alkenone-based temperature estimates in two core-tops GeoB10044 and GeoB10047 located 112 km and 158 km away from the trap site, respectively, are 26.9 °C (Chen et al., 2014). We thus infer that the total annual flux and the signals that will be recorded in the sediments are dominated by the SE monsoon season, with negligible proportions contributed during the rest of the year.

The  $U_{37}^K$  temperature estimates from the individual sediment trap cup samples collected during the high-flux period in the SE monsoon season do not, however, reflect the seasonal evolution of SST. Instead, the  $U_{37}^K$  temperature estimates are up to 2 °C higher than satellite-derived SST during the SE monsoon period in 2002.

Several potential factors may account for alkenone-based temperature estimates differing from satellite-derived SST estimates, including delayed export of particles, or lateral sediment transport by currents. In the following evaluation, we will discuss which

process most likely caused the observed temperature deviation of the  $U_{37}^K$  temperature from the satellite-derived SST.

Those samples that contained sufficient alkenones to allow for a reliable calculation of  $U_{37}^K$  were collected in the middle and at the end of upwelling period. However, the alkenone SST estimates fail to reproduce the observed minimum in SST but rather record a value similar to the average of the entire upwelling season, or to the SST observed at the onset and end of the upwelling season. It is known that alkenone producers may be outcompeted, e.g., by diatoms during the strong upwelling of silicate-rich deep water (Mitchell-Innes and Winter, 1987). A further study by Schiebel et al. (2004) reported that the coccolithophore number increased towards the more nutrient depleted areas across the upwelling area off the Oman coast to the central Arabian Sea. The coccolithophores are adapted to low turbulence and stratified surface water as well as being limited by thresholds of nitrate and phosphate (Schiebel et al., 2004). We observe that highest alkenone fluxes occur slightly after the highest total fluxes and the period of strongest upwelling (Fig. 4.2.), suggesting that the peak in alkenone production possibly occurs at the end of the upwelling season off Java. This is in agreement with previous studies suggesting that the alkenone production during the peak upwelling is reduced (e.g., Mollenhauer et al., 2015; Silva et al., 2008).

The upwelling off Java generally starts in June and reaches a maximum in July-August (Susanto et al., 2001). However, during the trap period, the weak La Niña conditions turned into weak El Niño conditions in early 2002, which cause a strengthening of the upwelling and an extension of the upwelling period until November (Susanto et al., 2001). If the peak in alkenone production occurs at the end of the upwelling season, the question is where the slightly warm alkenone temperature signal during the peak upwelling period derives from. One scenario that could lead to a warm bias in the reconstructed temperature is increased export of alkenones during the period of highest primary production due to upwelling. Those alkenones could have been produced during the early upwelling with lower nutrient conditions. Alkenone

bearing particles can remain suspended in surface waters for weeks or even months until they sink down to the seabed via scavenging by marine aggregates or within faecal pellets (e.g., Iversen and Ploug, 2010; Moran and Smith, 2003; Schmidt et al., 2002). The increased particle abundances of phytoplankton during the peak upwelling could lead to a more effective scavenging of alkenones from the surface waters, resulting in a delayed export. The relatively higher abundances of alkenones produced during the early upwelling period would effectively overprint the signal produced during the peak upwelling period when coccolithophores are not competitive and thus less abundant. Additionally, the flux-weighted temperature estimates of the available samples is 26.7 °C, which corresponds to temperatures observed at the onset and end of the upwelling season, and at the same time is similar to satellite-derived SE monsoon SST (26.4 °C). Taken together, the alkenone ratio indicates the temperature at the onset and end of upwelling season, but is still pretty close to the average temperature over the entire upwelling season.

The apparent temperature difference between satellite-derived SST and alkenone-based temperature estimates could also derive from supply of laterally transported alkenones from remote regions. Previous publications suggest that anomalously cold or warm alkenone temperatures can be caused by lateral particle and sediment transport in some settings (Benthien and Müller 2000; Müller and Fischer, 2003; Sicre et al., 2005). The offsets between  $U_{37}^K$  temperature estimates and satellite-derived SST depend on the region where advected particles derive from. In our study region, the Western Pacific Warm Pool (WPWP) and Indonesian seas are considered as the predominant water source of the eastern Indian Ocean and are thus the likely source region for potentially advected material via the ITF and/or the SJC. The average surface water temperature of the WPWP is over 28 °C, slightly warmer than the average SST of our study area, and the productivity is lower. The average of our SST- $U_{37}^K$  estimates is 26.9 °C. In addition, the main pathways of the ITF enters into the Indian Ocean are characterized by a high average SST (ca. 27.5 °C, Sprintall et al., 2003). We performed a simple mass balance calculation for the time interval from late September 2002 to mid

October 2002 (Jam-2, D19; Table 1) assuming local SST of ca. 25 °C and corresponding  $U_{37}^K$  of 0.875, and a  $U_{37}^K$  of 1 for advected particles. In order to explain the observed  $U_{37}^K$  of 0.94 by mixing of these two pools alone, the lateral contribution would amount to 48% of the total flux. If advected alkenone inputs were a dominant factor affecting the  $U_{37}^K$ -based SST estimates, a source region would be required with high productivity and a SST similar to or higher than our alkenone temperature estimates. Since productivity in the source area is rather low compared to the upwelling region we sampled in, we infer that the lateral advection is unlikely to be the main cause for the observed temperature discrepancy.

#### **4.6.2. GDGTs**

##### **4.6.2.1. Fluxes**

The GDGT flux record off Java shows less pronounced seasonality throughout the year than that of the alkenones. GDGT fluxes increased during the SE monsoon period compared to NW monsoon and intermonsoon periods (approximately 2.5 times). The highest GDGT flux occurs at the same time as the highest flux of alkenones and higher total and TOC fluxes (Fig. 4.2.). The observed seasonality of GDGT flux could thus be caused either by seasonal production, or by seasonally varying efficiency of GDGT export.

The season of GDGT production in the marine environment is still contentious. Earlier studies showed that the abundance of Thaumarchaeota varies seasonally and is mainly higher when phytoplanktonic productivity is low (Schouten et al., 2013 and references therein). Moreover, some studies suggested that the seasonal variations in GDGT fluxes might be caused by seasonal variations in the export of GDGTs, which depends on the phytoplankton productivity (e.g., Huguet et al., 2007; Wuchter et al., 2005).

Like alkenone fluxes, the flux of GDGTs to our trap correlates better with fluxes of carbonate ( $r^2=0.54$ ), TOC ( $r^2=0.49$ ), and opal ( $r^2=0.72$ ) than with lithogenic particles ( $r^2=0.06$ ) (Fig. 4.4e, f, g, h.). This indicates that GDGTs were transported to deeper

waters together with marine aggregates, in particular with opal. Variations in sinking fluxes of TOC, carbonate, opal and GDGTs are consistent with variations in chlorophyll concentration and NPP. Thus, the observed seasonality in GDGT flux might not directly be indicative of seasonal production of Thaumarchaeota. Rather, it could result from more efficient export of GDGTs during the upwelling season, which is characterized by strongly increased phytoplankton production and resulting particle flux.

Thaumarchaeota cells are neutrally buoyant, i.e., they do not sink by themselves but instead require packaging to sink through the water column (Schouten et al., 2013 and references therein). Packaging could occur in faecal pellets or by aggregation, enhanced by mineral ballasting (Passow and De La Rocha, 2006). In the Arabian Sea, Wuchter et al. (2006) observed an apparent seasonality of GDGT flux in the shallow trap (ca. 500 m), whereas the GDGT flux is insensitive to seasonality in the deeper traps at 1500 m and 3000 m. The authors concluded that the maximum in GDGT flux during the highest productivity was caused by more efficient export of the lipids rather than by higher production of Thaumarchaeota. A similar observation was made by Yamamoto et al. (2012) in the western North Pacific.

The concentrations of GDGTs in our samples are variable, but do not co-vary with GDGT flux. If the seasonality of GDGT flux was caused solely by the seasonality of total flux, we would expect decreased GDGT concentration during upwelling. In contrast, we do not observe decreased concentrations of GDGTs during high flux periods. Therefore, we infer that the elevated GDGT flux likely relates to both, the seasonal variation in the abundance of Thaumarchaeota combined with more efficient export of GDGTs by aggregation with phytoplankton detritus during the SE monsoon.

#### **4.6.2.2. $\text{TEX}_{86}^{\text{H}}$ temperature estimates**

The time series of  $\text{TEX}_{86}^{\text{H}}$  temperature estimates does not record the strong seasonal amplitude observed in the satellite-based SST (Fig. 4.2a.). The flux-weighted average  $\text{TEX}_{86}^{\text{H}}$ -based temperature of 26.2 °C is similar to that based on  $U_{37}^{\text{K}}$  and to the average SE monsoon SST. However, a hypothetical flux weighted temperature calculated

from observed SST and GDGT fluxes (see above for the alkenones), would be 27.5 °C, significantly higher than the observed temperature estimate. This results from the observed weaker seasonality in GDGT flux than that of alkenones, and argues against flux-weighted average  $\text{TEX}_{86}^{\text{H}}$  recording upwelling SST. Instead, a subsurface origin of the signal could explain the observed value.

Colder  $\text{TEX}_{86}^{\text{H}}$  temperature estimates than SST might relate to the habitat of GDGT producers. It is known that Thaumarchaeota occur throughout the water column with maximum relative abundance in the deep ocean (Karner et al., 2001). Although the  $\text{TEX}_{86}^{\text{H}}$  is expected to reflect the temperature in the upper parts of the water column, previous studies from suspended particle material (SPM) and surface sediments suggested that  $\text{TEX}_{86}^{\text{H}}$  does not record SST but rather subsurface temperature (Huguet et al., 2007; Lee et al., 2008; Lopes dos Santos et al., 2010; Nakanishi et al., 2012; Rommerskirchen et al., 2011; Schouten et al., 2002; Wuchter et al., 2006; Xing et al., 2015). Maximum GDGT concentrations in water column studies have been reported for depths of 50-200 m (e.g., Basse et al., 2014; Nakashini et al., 2012; Xie et al., 2014), and have been discussed to near the depth of the thermocline (e.g., Lopes dos Santos et al., 2010). The thermocline in the study area is observed between 40 and 70 m (Fig. 4.1.). The annual average temperature at 50m water depth for the past ~40 years (World Ocean Atlas, 2005; Locarnini et al., 2006) is 26.7 °C, similar to and well within calibration error ( $\pm 2.5$  °C, Kim et al., 2010) of the flux weighted average  $\text{TEX}_{86}^{\text{H}}$ -temperature of 26.2 °C, and, similar to our data, it shows small seasonal variations (Fig. 4.5.). Considering the analytical error, the flux-weighted GDGT temperature estimates are also similar to the  $\text{TEX}_{86}^{\text{H}}$  temperature estimates of core-tops in the vicinity (GeoB10044 and GeoB10047, 27.0 °C and 26.3 °C, respectively; Chen et al., 2014). Thus a predominant export from approximately 50 m water depth at our study site seems plausible.

This conclusion is consistent with previous studies. For instance, Lee et al. (2008) observed that  $\text{Temp-TEX}_{86}$  was colder than in-situ temperature in SPM from the Benguela upwelling system and supposed that the GDGT producers blooming below the

mixed layer (>40m) were transported upward by upwelling resulting in this cold bias. A similar depth range of approximately 75 to 100 m water depth was identified as dominant habitat of GDGT producers for the East China Sea (Nakanishi et al., 2012). Further support for our interpretation comes from the results from a sediment trap in the Arabian Sea, where  $\text{TEX}_{86}$  temperature estimates are slightly lower than SST, possibly suggesting addition of GDGTs from subsurface waters (Wuchter et al., 2006). In the Yellow Sea, a study using surface sediment and suspended particles suggested that the highest concentration of GDGTs occurred in the bottom layer, at 70 m (Xing et al., 2015). Nakanishi et al. (2012) demonstrated that the maximum GDGTs concentration appeared at 74-99 m depth in the water column at slope and shelf locations in the northern East China Sea. Our trap data are also in agreement with other settings, as discussed by Huguet et al. (2007) in the Santa Barbara Basin and by Lopes dos Santos et al. (2010) in the eastern tropical Atlantic.

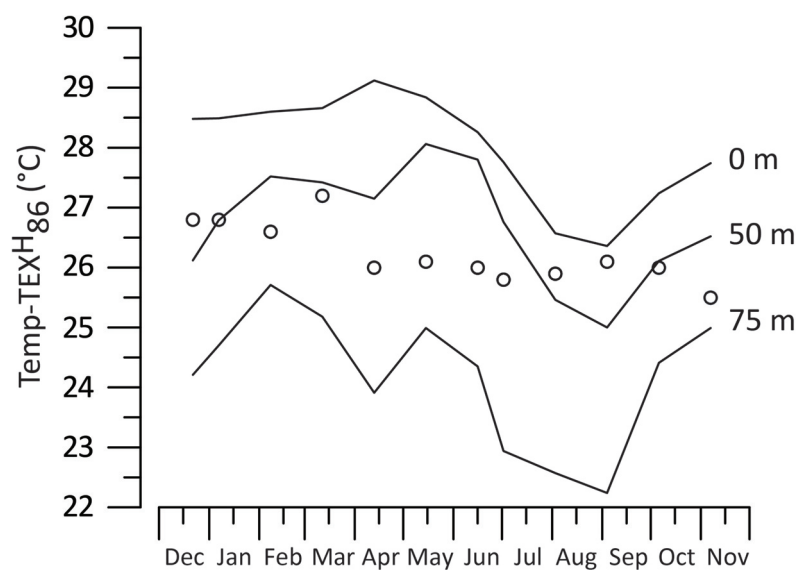


Fig. 4.5. Comparison between  $\text{TEX}_{86}^{\text{H}}$ -based temperature estimates ( $\text{Temp-TEX}_{86}^{\text{H}}$ , black circles) and the monthly mean temperatures at different depths (black lines) for the past 40 years at the sediment trap site (WOA 2005; Loncrnini et al., 2006).

TEX<sup>H</sup><sub>86</sub> temperature estimates could be influenced by fluvial input of soil-derived isoprenoid GDGTs (Weijers et al., 2006). Previous studies suggested that TEX<sub>86</sub> temperatures at sites with BIT indices lower than 0.3 are potentially reliable (Weijers et al., 2006; Zhu et al., 2011), although these values are not to be regarded globally applicable. In our sediment trap, the BIT index is extremely low and ranges between 0.01 and 0.06, suggesting a low contribution of soil organic matter. Considering these values the TEX<sup>H</sup><sub>86</sub> is unlikely biased by terrestrial input. Therefore, terrestrial GDGT input cannot explain the offset between TEX<sup>H</sup><sub>86</sub> temperature estimates and satellite-derived SST.

#### **4.7. Summary and Conclusion**

This study provides insight into seasonality and depth of production of alkenones and GDGTs in the coastal upwelling system of the eastern Indian Ocean.

Alkenone fluxes show a pronounced seasonality and their maximum flux is associated with highest primary production. A secondary alkenone flux maximum during the NW monsoon, likely related to increased production stimulated by riverine input of nutrients, does not strongly contribute to the total annual flux. The calculated flux-weighted average U<sup>K'</sup><sub>37</sub>-based temperature estimate is similar to the SE monsoon SST rather than mean annual SST. This average is based on those samples only that permitted a reliable SST estimate, i.e., mainly the samples from the SE monsoon period. Alkenone based temperature estimates yield temperatures warmer than satellite-derived temperature during the SE monsoon period. This observation suggests that the predominant alkenone production probably occurs at the onset and end of the upwelling season. The U<sup>K'</sup><sub>37</sub> signal of these samples records a value similar to the average of the entire upwelling season.

Our data show less pronounced seasonality of GDGT flux with only a small peak during the upwelling season, which may be attributed to seasonal variation in the

abundance of Thaumarchaeota or more efficient export of GDGTs by aggregation with phytoplankton detritus during the SE monsoon. The flux-weighted average  $\text{TEX}_{86}^{\text{H}}$ -based temperature estimate is cooler than ma SST and in agreement with water temperature at around 50m depth. Our results show no pronounced seasonal cycle in  $\text{TEX}_{86}$ , suggesting that the  $\text{TEX}_{86}$  in sediments reflects an integrated mean annual upper thermocline temperature at 50 m depth.

### **Acknowledgements**

We are grateful to the captain, crew and scientists of the two cruises (MARK VII and SONNE 184) for their help in collecting the samples. Tim Rixen is thanked for providing the samples. We wish to thank Ralph Kreutz for technical support. This research was supported by the German Federal Ministry of Education and Research through funding of the projects 03G0184A "PABESIA" and 03F0440A, the Helmholtz Association through a Young Investigators Group Award to GM and the China Scholarship Council (CSC) with support to WC. Data are archived in PANGAEA ([www.Pangaea.de](http://www.Pangaea.de)).

### **4.8. References**

- Andrulleit, H., Rogalla, U., 2002. Coccolithophores in surface sediments of the Arabian Sea in relation to environmental gradients in surface waters. *Marine Geology*, 186, 505–526.
- Andrulleit, H., 2007. Status of the Java upwelling area (Indian Ocean) during the oligotrophic northern hemisphere winter monsoon season as revealed by coccolithophores. *Marine Micropaleontology*, 64(1), 36-51.
- Basse, A., Zhu, C., Versteegh, G.J.M., Fischer, G., Hinrichs, K.-U., Mollenhauer, G., 2014. Distribution of intact and core tetraether lipids in water column profiles of

- suspended particulate matter off Cape Blanc, NW Africa. *Organic Geochemistry*, 72, 1-13.
- Benthien, A., Müller, P.J., 2000. Anomalously low alkenone temperatures caused by lateral particle and sediment transport in the Malvinas Current region, western Argentine Basin. *Deep-Sea Research I*, 47, 2369-2393.
- Brochier-Armanet, C., Boussau, B., Gribaldo, S., Forterre, P., 2008. Mesophilic crenarchaeota: proposal for a third archaeal phylum, the Thaumarchaeota. *Nature Reviews Microbiology*, 6, 245-252.
- Conte, M.H., Thompson, A., Lesley, D., Harris, R. P., 1998. Genetic and physiological influences on the alkenone/alkenoate versus growth temperature relationship in *Emiliana huxleyi* and *Gephyrocapsa oceanic*. *Geochimica et Cosmochimica Acta*, 62, 51-68.
- Conte, M.H., Sicre, M.-A., Rühlemann, C., Weber, J.C., Schulte, S., Schulz-Bull, D., Blanz, T., 2006. Global temperature calibration of the alkenone unsaturation index ( $U_{37}^K$ ) in surface water and comparison with surface sediments. *Geochemistry Geophysics Geosystems*, 7, Q02005, doi: 10.1029/2005GC001054.
- Chen, Wenwen., Mohtadi, M., Schefuß, E., Mollenhauer, G., 2014. Organic-geochemical proxies of sea surface temperature in surface sediments of the tropical Eastern Indian Ocean. *Deep-Sea Research I*, 88, 17-29.
- Donguy, J.R., Meyers, G., 1995. Observations of geostrophic transport in the western tropical Indian Ocean. *Deep-Sea Research*, 42(6), 1007-1028.
- Fallet, U., Ullgren, J.E., Castañeda, I.S., van Aken, H.M., Schouten, S., Ridderinkhof, H., Brummer, G.J.A., 2011. Contrasting variability in foraminiferal and organic paleotemperature proxies in sedimenting particles of the Mozambique Channel (SW Indian Ocean). *Geochimica et Cosmochimica Acta*, 75(20), 5834-5848.
- Ffield, A., Gordon, A., 1992. Vertical mixing in the Indonesian Thermocline. *Journal of Physical Oceanography*, 22, 184-195.
- Fischer, G., Karakas, G., Blaas, M., Ratmeyer, V., Nowald, N., Schlitzer, R., Helmke, P., Davenport, R., Donner, B., Neuer, S., Wefer, G., 2009. Mineral ballast and particle

- settling rates in the coastal upwelling system off NW Africa and the South Atlantic. *International Journal of Earth Sciences*, 98(2), 281-298, doi: 10.1007/s00531-007-0234-7.
- Gordon, A.L., Fine, R.A., 1996. Pathways of water between the Pacific and Indian oceans in the Indonesian seas. *Nature*, 379, 146-149.
- Gordon, A.L., 2005. Oceanography of the Indonesian seas and their throughflow. *Oceanography*, 18(4), 14-28.
- Harada, N., Sato, M., Shiraishi, A., Honda, M.C., 2006. Characteristics of alkenone distributions in suspended and sinking particles in the northwestern North Pacific. *Geochimica et Cosmochimica Acta*, 70, 2045-2062.
- Hendiarti, N., Siegel, H., Ohde, T., 2004. Investigation of different coastal processes in Indonesian water using SeaWiFS data. *Deep Sea Research II*, 51, 85-97.
- Herfort, L., Schouten, S., Boon, J.P., Sinninghe Damsté, J.S., 2006. Application of the TEX<sub>86</sub> temperature proxy to the southern North Sea. *Organic Geochemistry*, 37(12), 1715-1726.
- Hopmans, E.C., Weijers, J.W.H., Schefuß, E., Herfort, L., Sinninghe Damsté, J.S., Schouten, S., 2004. A novel proxy for terrestrial organic matter in sediments based on branched and isoprenoid tetraether lipids. *Earth and Planetary Science Letters*, 224, 107-116.
- Huguet, C., Kim, J.-H., Sinninghe Damsté, J.S., Schouten, S., 2006. Reconstruction of sea surface temperature variations in the Arabian Sea over the last 23 kyr using organic proxies (TEX<sub>86</sub> and U<sup>K</sup><sub>37</sub>). *Paleoceanography*, 21, PA3003.
- Huguet, C., Schimmelmann, A., Thunell, R., Lourens, L.J., Sinninghe Damsté, J.S., Schouten, S., 2007. A study of the TEX<sub>86</sub> paleothermometer in the water column and sediments of the Santa Barbara Basin, California. *Paleoceanography*, 22, PA3202.
- Iversen, M.H., Ploug, H., 2010. Ballast minerals and the sinking carbon flux in the ocean: carbon-specific respiration rates and sinking velocity of marine snow aggregates. *Biogeosciences*, 7(9), 2613-2624.

- Jennerjahn, T.C., Ittekkot, V., Klöpper, S., Adi, S., PurwoNugroho, S., Sudiana, N., Yusma, A., Gaye-Haake, B., 2004. Biogeochemistry of a tropical river affected by human activities in its catchment: Brantas River estuary and coastal waters of Madura Strait, Java, Indonesia. *Estuarine, Coastal and Shelf Science*, 60(3), 503-514.
- Jia, G., Zhang, J., Chen, J., Peng, P., Zhang, C.L., 2012. Archaeal tetraether lipids record subsurface water temperature in the South China Sea. *Organic Geochemistry*, 50, 68-77.
- Karner, M.B., DeLong, E.F., Karl, D.M., 2001. Archaeal dominance in the mesopelagic zone of the Pacific Ocean. *Nature*, 409, 507-510.
- Kim, J.-H., Schouten, S., Hopmans, E.C., Donner, B., Sinninghe Damsté, J.S., 2008. Global sediment core-top calibration of the TEX<sub>86</sub> paleothermometer in the ocean. *Geochimica et Cosmochimica Acta*, 72, 1154-1173.
- Kim, J.-H., van der Meer, J., Schouten, S., Helmke, P., Willmott, V., Sangiorgi, F., Koç, N., Hopmans, E.C., Sinninghe Damsté, J.S., 2010. New indices and calibrations derived from the distribution of crenarchaeal isoprenoid tetraether lipids: implications for past sea surface temperature reconstructions. *Geochimica et Cosmochimica Acta*, 74, 4639-4654.
- Kim, J.-H., Romero, O.E., Lohmann, G., Donner, B., Laepple, T., Haam, E., SinningheDamsté, J.S., 2012. Pronounced subsurface cooling of North Atlantic waters off Northwest Africa during Dansgaard–Oeschger interstadials. *Earth and Planetary Science Letters*, 339-340, 95-102.
- Koch-Larrouy, A., Madec, G., Iudicone, D., Atmadipoera, A., Molcard, R., 2008. Physical processes contributing to the water mass transformation of the Indonesian Throughflow. *Ocean Dynamics*, 58(3), 275-288.
- Lee, K.E., Kim, J.-H., Wilke, I., Helmke, P., Schouten, S., 2008. A study of the alkenones, TEX<sub>86</sub>, and planktonic foraminifera in the Benguela Upwelling System: Implication for past sea surface temperature estimates. *Geochemistry Geophysics Geosystems*, 9, Q10019, doi: 10.1029/2008GC002056.

- Leduc, G., Schneider, R., Kim, J.-H., Lohmann, G., 2010. Holocene and Eemian sea surface temperature trends as revealed by alkenone and Mg/Ca paleothermometry. *Quaternary Science Reviews*, 29, 989-1004.
- Leider, A., Hinrichs, K.-U., Mollenhauer, G., Versteegh, G.J.M., 2010. Core-top calibration of the lipid-based  $U^{K}_{37}$  and  $TEX_{86}$  temperature proxies on the southern Italian shelf (SW Adriatic Sea, Gulf of Taranto). *Earth and Planetary Science Letters*, 300, 112-124.
- Locarnini, R.A., Mishonov, A.V., Antonov, J.I., Boyer, T.P., Garcia, H.E., Levitus, S., 2006. *World Ocean Atlas 2005 Volume 1: Temperature*, NOAA Atlas NESDIS, 61(1). NOAA: [s.l.]. 182 pp.
- Lopes dos Santos, R., Prange, M., Castaneda, I.S., Schefuß, E., Mulitza, S., Schulz, M., Niedermeyer, E.A., Sinninghe Damsté, J.S., Schouten S., 2010. Glacial-interglacial variability in Atlantic Meridional Overturning Circulation and thermocline adjustment in the tropical North Atlantic. *Earth and Planetary Science Letters*, 300, 407-414.
- Marlowe, I.T., Brassell, S.C., Eglinton, G., Green, J.C., 1984. Long chain unsaturated ketones and esters in living algae and marine sediments. *Organic Geochemistry*, 6, 135-141.
- McClymont, E.L., Ganeshram, R.S., Pichevin, L.E., Talbot, H.M., van Dongen, B.E., Thunell, R.C., Haywood, A.M., Singarayer, J.S., Valdes, P.J., 2012. Sea-surface temperature records of Termination 1 in the Gulf of California: Challenges for seasonal and interannual analogues of tropical Pacific climate change. *Paleoceanography*, 27, PA2202, doi: 10.1029/2011PA002226.
- Mitchell-Innes, B.A., Winter, A., 1987. Coccolithophores: A major phytoplankton component in mature upwelled waters off the Cape Peninsula, South-Africa in March, 1983. *Marine Biology*, 5(1), 25-30, doi:10.1007/BF00447481.
- Mohtadi, M., Steinke, S., Groeneveld, J., Fink, H.G., Rixen, T., Hebbeln, D., Donner, B., Herunadi, B., 2009. Low-latitude control on seasonal and interannual changes in

- planktonic foraminiferal flux and shell geochemistry off south Java: A sediment trap study. *Paleoceanography*, 24, PA1201, doi:10.1029/2008PA001636.
- Mollenhauer, G., Basse, A., Kim, J.-H., Sinninghe Damsté, J.S., 2015. A four-year record of  $U^{K}_{37}$  and TEX<sub>86</sub>-derived sea surface temperature estimates from sinking particles in the filamentous upwelling region off Cape Blanc, Mauritania. *Deep-Sea Research I*, 97, 67-79.
- Moran, S.B., Smith, J.N., 2000.  $^{234}\text{Th}$  as a tracer of scavenging and particle export in the Beaufort Sea. *Continental Shelf Research*, 20(2), 153-167.
- Müller, P.J., Kirst, G., Ruhland, G., von Storch, I., Rosell-Melé, A., 1998. Calibration of the alkenone paleotemperature index  $U^{K}_{37}$  based on core-tops from the eastern South Atlantic and the global ocean (60°N-60°S). *Geochimica et Cosmochimica Acta*, 62, 1757-1772.
- Müller, P.J., Fischer, G., 2001. A 4-year sediment trap record of alkenones from the filamentous upwelling region off Cape Blanc, NW Africa and a comparison with distributions in underlying sediments. *Deep-Sea Research I*, 48(8), 1877-1903.
- Müller, P.J., Fischer, G., 2003. C<sub>37</sub>-alkenones as paleotemperature tool: fundamentals based on sediment traps and surface sediments from the south atlantic ocean. From Wefer G., Mulitza, A., Ratmeyer, V (eds), *The South Atlantic in the late Quaternary: Reconstruction of material budgets and current system*, Springer-Verlag Berlin Heidelberg New York Tokyo, pp 167-193.
- Nakanishi, T., Yamamoto, M., Irino, T., Tada, R., 2012. Distribution of glycerol dialkyl glycerol tetraethers, alkenones and polyunsaturated fatty acid in suspend particulate organic matter in the East China Sea. *Journal of Oceanography*, 68, 959-970, doi:10.1007/s10872-012-0146-4.
- Passow, U., De La Rocha, C.L., 2006. Accumulation of mineral ballast on organic aggregates. *Global Biogeochemical Cycles*, 20(1).
- Pelejero, C., Calvo, E., 2003. The upper end of the  $U^{K}_{37}$  temperature calibration revisited. *Geochemistry Geophysics Geosystems*, 4(2), doi:10.1029/2002GC000431.

- Prahl, F.G., Wakeham, S.G., 1987. Calibration of unsaturation patterns in long-chain ketone compositions for palaeotemperature assessment. *Nature*, 330, 367-369.
- Prahl, F.G., Pilskaln, C.H., Sparrow, M.A., 2001. Seasonal record for alkenones in sedimentary particles from the Gulf of Maine. *Deep-Sea Research I*, 48, 515-528.
- Prahl, F.G., Popp, B.N., Karl, D.M., Sparrow, M.A., 2005. Ecology and biogeochemistry of alkenone production at Station ALOHA. *Deep-Sea Research I*, 52, 699-719.
- Qu, T., Meyers, G., 2005. Seasonal characteristics of circulation in the southeastern tropical Indian Ocean. *Journal of Physical Oceanography*, 35(2), 255-267.
- Rommerskirchen, F., Condon, T., Mollenhauer, G., Dupont, L., Schefuss, E., 2011. Miocene to Pliocene development of surface and subsurface temperatures in the Benguela Current system. *Paleoceanography*, 26, PA3216, doi:10.1029/2010PA002074.
- Rixen, T., Ittekkot, V., Herunadi, B., Wetzel, P., Maier-Reimer, E., Gaye-Haake, B., 2006. ENSO-driven carbon sea saw in the Indo-Pacific. *Geophysical Research Letters*, 33, L07606, doi:10.1029/2005GL024965.
- Romero, O.E., Rixen, T., Herunadi, B., 2009. Effects of hydrographic and climate forcing on diatom production and export in the tropical southeastern Indian Ocean. *Marine Ecology Progress Series*, 384, 69-82.
- Rosell-Melé, A., Carter, J.F., Parry, A.T., Eglinton, G., 1995. Determination of the  $U^{K}_{37}$  index in geological samples. *Analytical Chemistry*, Vol.67, No. 7.
- Rosell-Melé, A., Prahl, F.G., 2013. Seasonality of  $U^{K}_{37}$  temperature estimates as inferred from sediment trap data. *Quaternary Science Reviews*, 72, 128-136.
- Schiebel, R., Zeltner, A., Treppke, U.F., Waniek, J.J., Bollmann, J., Rixen, T., Hemleben, C., 2004. Distribution of diatoms, coccolithophores and planktic foraminifers along a trophic gradient during SW monsoon in the Arabian Sea. *Marine Micropaleontology*, 51, 345-371.
- Schmidt, S., Chou, L., Hall, I.A., 2002. Particle residence times in surface waters over the north-western Iberian Margin: Comparison of pre-upwelling and winter periods. *Journal of Marine Systems*, 32, 3-11.

- Schneider, B., Leduc, G., Park, W., 2010. Disentangling seasonal signals in Holocene climate trends by satellite-model-proxy integration. *Paleoceanography*, 25, PA4217.
- Schouten, S., Hopmans, E.C., Schefuß, E., Sinninghe Damsté, J.S., 2002. Distributional variations in marine crenarchaeotal membrane lipids: a new tool for reconstructing ancient sea water temperatures? *Earth and Planetary Science Letters*, 204, 265-274.
- Schouten, S., Hopmans, E.C., Sinninghe Damsté, J.S., 2013. The organic geochemistry of glycerol dialkyl glycerol tetraether lipids: A review. *Organic Geochemistry*, 54, 19-61.
- Seki, O., Nakatsuka, T., Kawamura, K., Saitoh, S.-I., Wakatsuchi, M., 2007. Time-series sediment trap record of alkenones from the western Sea of Okhotsk. *Marine Chemistry*, 104, 253-265.
- Sicre, M.A., Labeyrie, L., Ezat, U., Duprat, J., Turon, J.L., Schmidt, S., Mazaud, A., Michel, E., 2005. Mid-latitude Southern Indian Ocean response to Northern Hemisphere Heinrich events. *Earth and Planetary Science Letters*, 240, 724-731.
- Silva, A., Palma, S., Moita, M.T., 2008. Coccolithophores in the upwelling waters of Portugal: Four years of weekly distribution in Lisbon bay. *Continental Shelf Research*, 28, 2601-2613.
- Sinninghe Damsté, J.S., Schouten, S., Hopmans, E.C., van Duin, A.C.T., Geenevasen, J.A.J., 2002. Crenarchaeol: the characteristic core glycerol dibiphytanyl glycerol tetraether membrane lipid of cosmopolitan pelagic crenarchaeota. *Journal of Lipid Research*, 43, 1641-1651.
- Sprintall, J., Potemra, J.T., Hautala, S.L., Bray, N.A., Pandoe, W.W., 2003. Temperature and salinity variability in the exit passages of the Indonesian Throughflow. *Deep-Sea Research II*, 50(12), 2183-2204.
- Sprintall, J., Wijffels, S., Molcard, R., Jaya, I., 2010. Direct evidence of the south Java current system in Ombai Strait. *Dynamics of Atmospheres and Oceans*, 50(2), 140-156.

- Susanto, R. D., Gordon, A.L., Zheng, Q., 2001. Upwelling along the coasts of Java and Sumatra and its relation to ENSO. *Geophysical Research Letters*, 28(8), 1599-1602.
- Susanto, R. D., Marra, J., 2005. Effect of the 1997/98 El Niño on chlorophyll a variability along the southern coasts of Java and Sumatra. *Oceanography*, 18, 124-127, doi:10.5670/oceanog.2005.13.
- Tomczak, M., Godfrey, J.S., 1994. *Regional oceanography: an introduction*. Elsevier, New York.
- Tolar B.B., King, G.M., Hollibaugh, J.T., 2013. An analysis of Thaumarchaeota populations from the Northern Gulf of Mexico. *Frontiers in Microbiology*, 4, doi: 10.3389/fmicb.2013.00072.
- Turich, C., Schouten, S., Thunell, R.C, Varela, R., Astor, Y., Wakeham, S.G., 2013. Comparison of TEX<sub>86</sub> and U<sup>K</sup><sub>37</sub> temperature proxies in sinking particles in the Cariaco Basin. *Deep-Sea Research I*, 78, 115-133.
- Volkman, J.K., Eglinton, G., Corner, E.D.S., Forsberg, T.E.V., 1980. Long-chain alkenes and alkenones in the marine coccolithophorid *Emiliana huxleyi*. *Phytochemistry*, 19, 2619-2622.
- Wang, Y.V., Leduc, G., Regenberg, M., Andersen, N., Larsen, T., Blanz, T., Schneider, R.R., 2013. Northern and southern hemisphere controls on seasonal sea surface temperatures in the Indian Ocean during the last deglaciation. *Paleoceanography*, 28, 1-14, doi:10.1002/palo.20053.
- Weijers, J.W.H., Schouten, S., Spaargaren, O.C., Sinninghe Damsté, J.S., 2006. Occurrence and distribution of tetraether membrane lipids in soil: Implications for the use of the TEX<sub>86</sub> proxy and the BIT indeed. *Organic Geochemistry*, 37, 1680-1693.
- Wijffels, S.E., 2001. Ocean transport of freshwater, in *Ocean Circulation and Climate*, edited by G. Siedler, J. Church, and J. Gould, Elsevier, New York.
- Wuchter, C., Schouten, S., Wakeham, S.G., Sinninghe Damsté, J.S., 2005. Temporal and spatial variation in tetraether membrane lipids of marine Crenarchaeota in

- particulate organic matter: implications for TEX<sub>86</sub> paleothermometry. *Paleoceanography*, 20, PA3013, doi: 10.1029/2004PA001110.
- Wuchter, C., Schouten, S., Wakeham, S.G., Sinninghe Damsté, J.S., 2006. Archaeal tetraether membrane lipid fluxes in the northeastern Pacific and the Arabian Sea: implications for TEX<sub>86</sub> paleothermometry. *Paleoceanography*, 21, PA4208, doi: 10.1029/2006PA001279.
- Wyrski, K., 1961: Physical oceanography of Southeast Asian waters. NAGA Rep. 2, Scripps Institution of Oceanography, University of California, San Diego, 195 pp.
- Wyrski, K., 1973: An equatorial jet in the Indian Ocean. *Science*, 181, 262-264.
- Xie, S., Liu, X.-L., Schubotz, F., Wakeham, S. G., Hinrichs, K.-U., 2014. Distribution of glycerol ether lipids in the oxygen minimum zone of the Eastern Tropical North Pacific Ocean. *Organic Geochemistry*, 71, 60-71, doi: 10.1016/j.orggeochem.2014.04.006.
- Xing, L., Sachs, J.P., Gao, W., Tao, S., Zhao, X., Li, L., Zhao, M., 2015. TEX<sub>86</sub> paleothermometer as an indication of bottom water temperature in the Yellow Sea. *Organic Geochemistry*, 86, 19-31.
- Yamamoto, M., Shimamoto, A., Fukuhara, T., Naraoka, H., Tanaka, Y., Nishimura, A., 2007. Seasonal and depth variations in molecular and isotopic alkenone composition of sinking particles from the western North Pacific. *Deep Sea Research I*, 54(9), 1571-1592.
- Yamamoto, M., Shimamoto, A., Fukuhara, T., Tanaka, Y., Ishizaka, J., 2012. Glycerol dialkyl glycerol tetraethers and TEX<sub>86</sub> index in sinking particles in the western North Pacific. *Organic Geochemistry*, 53, 52-62.
- Zhu, C., Weijers, J.W.H., Wagner, T., Pan, J.-M., Chen, J.-F., Pancost, R.D., 2011. Sources and distributions of tetraether lipids in surface sediments across a large river-dominated continental margin. *Organic Geochemistry*, 42 (4), 376-386.

## **Chapter 5 Sea surface and subsurface temperature variations in the upwelling area of the eastern Indian Ocean during the last 22,000 years**

Wenwen Chen<sup>1</sup>, Mahyar Mohtadi<sup>2</sup>, Enno Schefuß<sup>2</sup>, Gesine Mollenhauer<sup>1,2,3</sup>

<sup>1</sup> Department of Geosciences, University of Bremen, Bremen, Germany

<sup>2</sup> MARUM-Center for Marine Environmental Sciences, University of Bremen, Bremen, Germany

<sup>3</sup> Alfred-Wegener Institute for Polar and Marine Research, Bremerhaven Germany

In preparation for Earth and Planetary Science Letters

## 5.1 Abstract

We present a multi proxy study of sea-water temperatures based on  $U^{K'}_{37}$  (alkenones unsaturation index) and  $TEX^H_{86}$  (tetraether index of GDGTs with 86 carbon atoms) in sediment core GeoB10053-7, which provides new insights into the variability of the sea surface and subsurface temperatures off south Java covering the past 22,000 years. Our results show that  $TEX^H_{86}$  temperature estimates are consistently warmer than  $SST-U^{K'}_{37}$  up to 2°C in most of the records except during the last glacial maximum (LGM) and late Holocene. A previous study suggested that the  $U^{K'}_{37}$ -based temperature estimates represent past changes in the SE monsoon SST in the upwelling region off south Java, while  $TEX^H_{86}$  reflects mean annual temperature at 50 m depth. In comparing the two temperature indices, we consider the potential for upwelling intensity to be recorded. In addition, the initial timing for the deglacial warming of GDGT temperature estimates started at ~18 ka, whereas the lowest  $U^{K'}_{37}$  temperature estimates appeared in the middle of the Younger Dryas period (YD, ca. 12 ka) and the late Heinrich Stadial 1 period (HS1, ca. 15 ka). Our data reveal that the seasonal SSTs and mean annual subsurface temperatures are closely linked to climate changes occurring in both hemispheres. Thus, by combining  $U^{K'}_{37}$  and  $TEX^H_{86}$  records and their difference allow a more comprehensive reconstruction of sea-water temperature developments and its controls in the tropical eastern Indian Ocean.

## 5.2. Introduction

The tropical oceans provide the main source of heat and water vapor transfer to the high-latitudes and play a crucial role in modulating centennial- to millennial-scale global climate change (e.g., Cane and Clement, 1999; Clement et al., 2001; Lea et al, 2000; Visser et al., 2003). Reconstructing sea surface temperatures (SSTs) is essential to understand the mechanisms behind the climate changes in the past from the glacial to interglacial terminations. The last deglaciation is characterized by abrupt climate changes of millennial duration such as Heinrich Stadial 1 (HS1) and the Younger Dryas (YD) cold events, the Bølling-Allerød (B-A) warm phase in the north hemisphere, and the

Antarctic Cold Reversal (ACR) cold event in the southern hemisphere (e.g., Alley and Clark, 1999; Jouzel et al., 1995). Two different mechanisms, i.e., the so-called bipolar seesaw, and increased atmospheric CO<sub>2</sub> concentration, are invoked in interpreting SST reconstructions. The so-called bipolar seesaw hypothesis is typically attributed to changes in reorganizations of the ocean's thermohaline circulation. The changes in Atlantic meridional overturning circulation (AMOC) strength is responsible for much of total oceanic heat redistribution in the Atlantic and thus cause the bipolar seesaw behavior (e.g., Broecker, 1998; Clark et al., 2002). In contrast, the other hypothesis focuses on changes in tropical atmosphere-ocean dynamics, such as increased atmospheric CO<sub>2</sub> concentration (e.g., Stott et al., 2007; Visser et al., 2003). This hypothesis is also supported by Shakun et al. (2010; 2012), who synthesized archive proxy temperature records and model simulations.

The Indonesian Archipelago is a climate-sensitive location and is of major importance to atmospheric state, not only over the region itself, but globally (Qu et al., 2005). Previous studies demonstrate that the small variability in SSTs results in an important influence on Indonesia's marine hydrological systems (e.g., Neale and Slingo, 2003). However, recent studies of past SST changes in and around Indonesia show obvious discrepancies of last deglacial SST records based on different proxies. Some studies argue that the SST estimates based on Mg/Ca and  $\delta^{18}\text{O}$  co-vary with Antarctic temperature (e.g., Lea et al., 2000; Levi et al., 2007; Mohtadi et al., 2010a; Visser et al., 2003; Xu et al., 2008). Some studies suggest that  $U_{37}^K$  temperature estimates from south of Sumatra are related to strengthening of upwelling during periods of increased boreal summer insolation over the past 300 ka and 140 ka (Lückge et al., 2009; Mohtadi et al., 2010b). Mohtadi et al., (2011) inferred that upwelling intensity and hence, the Australian-Indonesian austral winter monsoon variation was closely linked to northern hemispheric summer insolation. Hence, establishing the timing of climate changes in different proxies for surface or subsurface temperature is necessary for understanding of controls over the Indonesian region climate change.

Here we present a high-resolution record of sea water temperature estimates from the eastern Indian Ocean based on  $U_{37}^K$  and  $TEX_{86}^H$  from a marine sediment core (GeoB10053-7) retrieved off south Java and covering the last 22 ka. The temperature variability in the past 22 ka is compared with the deglacial temperature evolution in the northern and southern hemispheres in order to assess the linkage between  $U_{37}^K$  ( $TEX_{86}^H$ ) and northern (southern) hemisphere climate change.

### **5.3. The Java Upwelling System (JUS)**

Climate conditions in the eastern Indian Ocean south of Java display a strong, monsoon-related seasonal variability. The mean annual SST off Java ranges from 26 to 28°C (WOA 09, Locarnini et al., 2010). During the austral summer (from January to March, henceforth summer), the predominant winds are northwest trades (Fig. 5.1.), which force the South Java Current (SJC, originated from the Equatorial Counter Current (ECC)) to move towards the southeast to meet the Leeuwin Current (LC), which carries warm and saline water transported from the eastern part of the Indonesian Archipelago (e.g., Tapper, 2002; Tomczak and Godfrey, 1994). The mixing of the SJC with the LC gives origin to the South Equatorial Current (SEC) that flows towards the west. In this season, the NW monsoon carries warm and moist air from the Asian continent and is associated with a southerly position of Intertropical Convergence Zone (ITCZ), causing heavy rainfall over Indonesia. The rainfall offshore off south Java is over 30 cm per month (<http://trmm.gsfc.nasa.gov>). In contrast, in the SE monsoon season (austral winter, from July to September, henceforth winter), the strong southeast trade winds cause the SJC to flow in an opposite direction and join the SEC. The ITCZ is located in a northerly position. In this season, the winds induce upwelling along the coast of south Java (Wyrtki, 1961). The upward movement brings cool, high-nutrient water from the thermocline into the euphotic layers where phytoplankton develops. Compared with the surrounding eastern Indian Ocean, i.e., Timor and Banda Sea, where the amplitude of the seasonal temperature variability exceeds 4°C, a smaller range of SST variability of depression of SSTs (~2 °C) is found off Java (Qu et al., 2005). Two mechanisms are

proposed to explain the small SST depression in the JUS. One is the so-called barrier layer, representing an intermediate layer that separates the base of the mixed layer from the top of the thermocline (Lukas and Lindstrom, 1991). It can prevent the thermocline water from entering the mixed layer (Qu and Meyers, 2005; Sprintall and Tomczak, 1992). The other potential mechanism is related to the Indonesian Throughflow (ITF), which transfers a large amount of water from the Pacific to the Indian Ocean through several passages of the Indonesian Archipelago (Fig. 5.1., Gordon and Fine, 1996; Gordon, 2005). It has been suggested that the cooling of the sea surface due to upwelling is counterbalanced by intrusion of the relatively warm ITF (Sprintall et al., 2009).

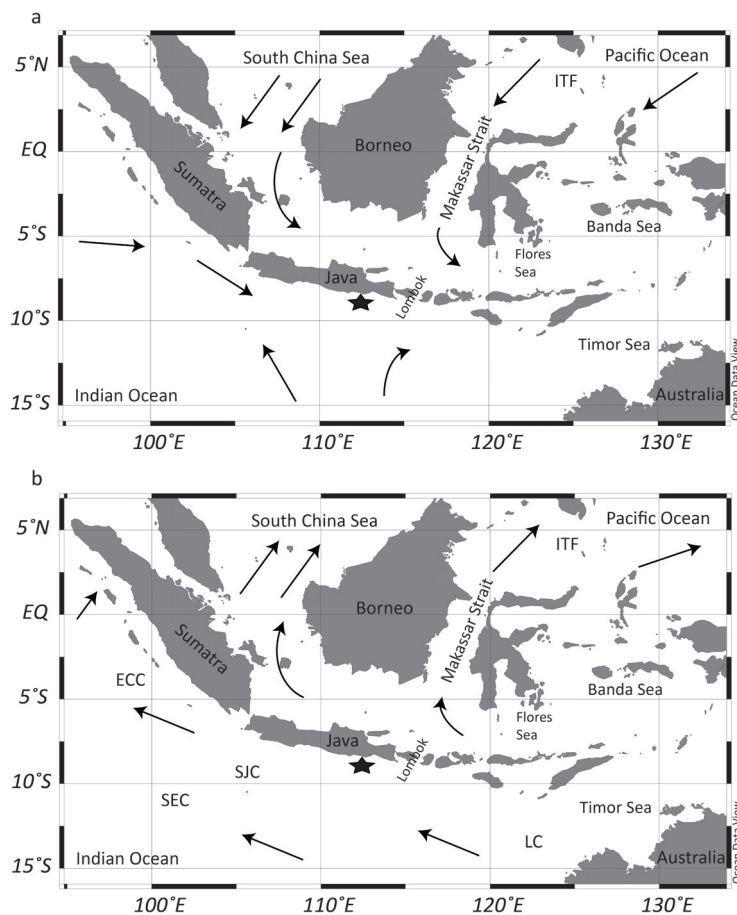


Fig. 5.1. Location of sediment core GeoB10053-7 (Black star). Arrows show the winds direction in the austral summer (a) and the austral winter (b).

In addition to the monsoon, at least two other inter-annual climate phenomena, i.e., the El Niño-Southern Oscillation (ENSO) and the Indian Ocean Dipole (IOD) could strongly affect the hydrography of the equatorial Indian Ocean (e.g., Gordon, 2005; Meyers et al., 2007; Susanto et al., 2001). The El Niño episodes and positive IOD years are characterized by an intensified SE monsoon with strong SST depressions that can reach as much as 5°C and an increased primary production off Java and Sumatra. In contrast, during La Niña and negative IOD years, the pattern of SST is reversed, including enhanced westerly winds, and increased precipitation in the study area.

## **5.4. Material and Methods**

### **5.4.1. Sediment Core**

Gravity core GeoB10053-7 (8°40.56'S, 112°50.33'E, at 1372m water depth, 760 cm core length) was collected off Java during the PABESIA Cruise SO-184 with R/V Sonnein 2005 (Hebbeln et al., 2005; Fig. 5.1.). The core was sampled at 5 cm intervals. The age model was established by Mohtadi et al., (2011) using nineteen accelerator mass spectrometry (AMS) <sup>14</sup>C dates from mixed planktonic foraminifera.

### **5.4.2. Analytical Methods**

Aliquots of 3 g of freeze-dried and homogenized samples were ultrasonically extracted three times with successively methanol (MeOH), MeOH: dichloromethane (DCM) 1:1 (v:v) and DCM (25 mL each), and all extracts were combined. Before extraction, a known amount of C<sub>19</sub> ketone and C<sub>46</sub> GDGT were added as internal standards. The total lipid extract was saponified for 2 hours at 80 °C with 300 µL of 0.1M KOH in 90:10 MeOH/H<sub>2</sub>O. The neutral fraction was recovered by liquid-liquid extraction using hexane and separated into apolar, intermediate polarity and polar fractions via silica gel column chromatography, eluting with hexane, DCM: hexane 2:1 (v:v) and MeOH, respectively.

Seventeen marine sediment standard subsamples were extracted independently and measured at regular intervals during the analysis of our samples.

#### 5.4.2.1. Alkenone analysis and $U_{37}^K$ SST

The alkenone fraction was re-dissolved in 25  $\mu$ l MeOH: DCM 1:1 (v:v) prior to capillary gas chromatography (GC). For quantification of alkenones, samples were analysed using an HP5890 series GC equipped with a flame ionization detector, using Helium as carrier gas with a constant flow rate of 2.0 ml/min. The oven temperature initiated at 60 °C, was held for 1 min, subsequently increased to 150 °C at a rate of 10 °C/min, then raised to 310 °C at a rate of 4 °C/min with a total run-time of 75 min. Lipid concentrations were calculated with reference to the internal standard  $C_{19}$  ketone. The  $U_{37}^K$  index was defined as the relative concentration of the di- and tri-unsaturated  $C_{37}$  alkenones:

$$U_{37}^K = (C_{37:2}) / (C_{37:2} + C_{37:3})$$

$U_{37}^K$  values were converted to temperature values by applying the calibration of Conte et al. (2006):

$$T = 29.876 * (U_{37}^K) - 1.334$$

The reproducibility of the analysis is 0.27 °C based on repeated analyses of the marine bulk sediment standard.

#### 5.4.2.2. GDGT analysis and $TEX_{86}$ temperature

The polar fraction containing the GDGTs for  $TEX_{86}$  and BIT was dried under  $N_2$  and re-dissolved in mixture of 99:1 (v:v) *n*-hexane and isopropanol with a concentration of 2 mg/ml (Schouten et al., 2013), and filtered through 0.45  $\mu$ m PTFE filters prior to analysis as described by Hopmans et al. (2000; 2004).

GDGT fractions were analyzed using an Agilent 1200 Series high performance liquid chromatography mass spectrometry system (HPLC-MS). Procedures described by Leider et al. (2010) were applied. HPLC-MS analyses were conducted using a Prevail

Cyano column (2.1×150 mm, 3 μm; Alltech, Grace) maintained at 30 °C. GDGTs were eluted using the mixture of solvent A (*n*-hexane) and solvent B (5% isopropanol in *n*-hexane): 80% A: 20% B for 5 min, linear gradient to 36% B in 45 min. Flow rate was 0.2 ml/min. After each analysis the column was cleaned by back-flushing with *n*-hexane: isopropanol 90:10 (v/v) at 0.2 ml/min for 8 min. GDGTs were identified using single ion mode (SIM) as described in Schouten et al. (2007).

The TEX<sub>86</sub> index was calculated based on the peak areas of the respective GDGTs. The TEX<sub>86</sub> is defined as follows (Schouten et al., 2002):

$$\text{TEX}_{86} = (\text{GDGT2} + \text{GDGT3} + \text{cren}') / (\text{GDGT1} + \text{GDGT2} + \text{GDGT3} + \text{cren}')$$

where GDGT1, GDGT2, GDGT3 and cren' indicate GDGTs containing 1, 2, 3 cyclopentane moieties and the crenarchaeol regio-isomer, respectively. TEX<sup>H</sup><sub>86</sub> is the log-transformed original TEX<sub>86</sub> and has been introduced by Kim et al. (2010) for reconstruction of SSTs in (sub) tropical oceans (>15°C):

$$\text{TEX}_{86}^{\text{H}} = \log(\text{TEX}_{86})$$

A surface sediment study in the eastern Indian Ocean confirmed that TEX<sup>H</sup><sub>86</sub> is the appropriate index for our study area (Chen et al., 2014). The TEX<sup>H</sup><sub>86</sub> values relate to temperature according to the following calibration equation (Kim et al., 2010):

$$\text{SST} = 68.4 * \text{TEX}_{86}^{\text{H}} + 38.6$$

Based on standard sediment extracts that were independently measured along with our samples, the standard deviation of TEX<sup>H</sup><sub>86</sub> is better than 0.6 °C.

The BIT index (Branched and Isoprenoid Tetraether) is a measure of the relative terrestrial organic matter input to marine sediments of branched GDGTs from soil bacteria (Hopmans et al., 2004) and was calculated according to the relative concentrations of the branched GDGTs and crearchaeol as defined by Hopmans et al. (2004).

## 5.5. Results

### 5.5.1. Alkenone temperature estimates

$U_{37}^K$  SST estimates range from 22.2 °C to 27.1 °C for the past 22,000 years (Fig. 5.2b.). The SST- $U_{37}^K$  varies between 22.9 °C and 24.9 °C during the LGM (22-19 ka) and 22.9 °C and 24.9 °C during the early deglaciation (19-17.5 ka), respectively. SST decreased from 23.9 °C to 22.2 °C during HS1 period (17.3-14.7 ka) followed by a gradual increase of  $U_{37}^K$ -SST estimates from 22.3 °C to 23.6 °C during the B-A period (14.7-12.9 ka). The  $U_{37}^K$ -derived temperature estimates decrease rapidly from 23.6 °C to 22.2 °C during the older part of the YD, (12.9-11.5 ka; older part ca.12.9-12.0 ka), followed by a warming during the younger part of the YD period. Subsequently, SST- $U_{37}^K$  increased gradually from ~22.9 °C at 11.5 ka towards the present-day with the core top value of ~26.9 °C. The overall amplitude of SST- $U_{37}^K$  amounts to about 5 °C.

### 5.5.2. GDGT temperature estimates and BIT index

The  $TEX_{86}^H$ -based temperature estimates (Temp- $TEX_{86}^H$ ) vary between 20.9 °C and 27.8 °C (Fig. 5.2b.). The Temp- $TEX_{86}^H$  range from 20.9 °C to 22.9 °C between 22 ka BP and 17.5 ka BP, about 2.5 °C lower compared to the SST- $U_{37}^K$  during the same period. Subsequently, the value increased rapidly from 22.1 °C to 24.9 °C during the HS1 period, remain constant during the B-A period, and increased from 24.7 °C to 25.8 °C during the YD period until 6 ka. After 6 ka, the temperatures based on  $TEX_{86}^H$  remained rather constant until the present-day. The total amplitude of Temp- $TEX_{86}^H$  data amounts to about 7°C, generally larger than that of the  $U_{37}^K$ .

The BIT index is extremely low, recording values of 0.03-0.11 (not shown) with highest values in the latest Holocene (1.5 ka BP to modern).

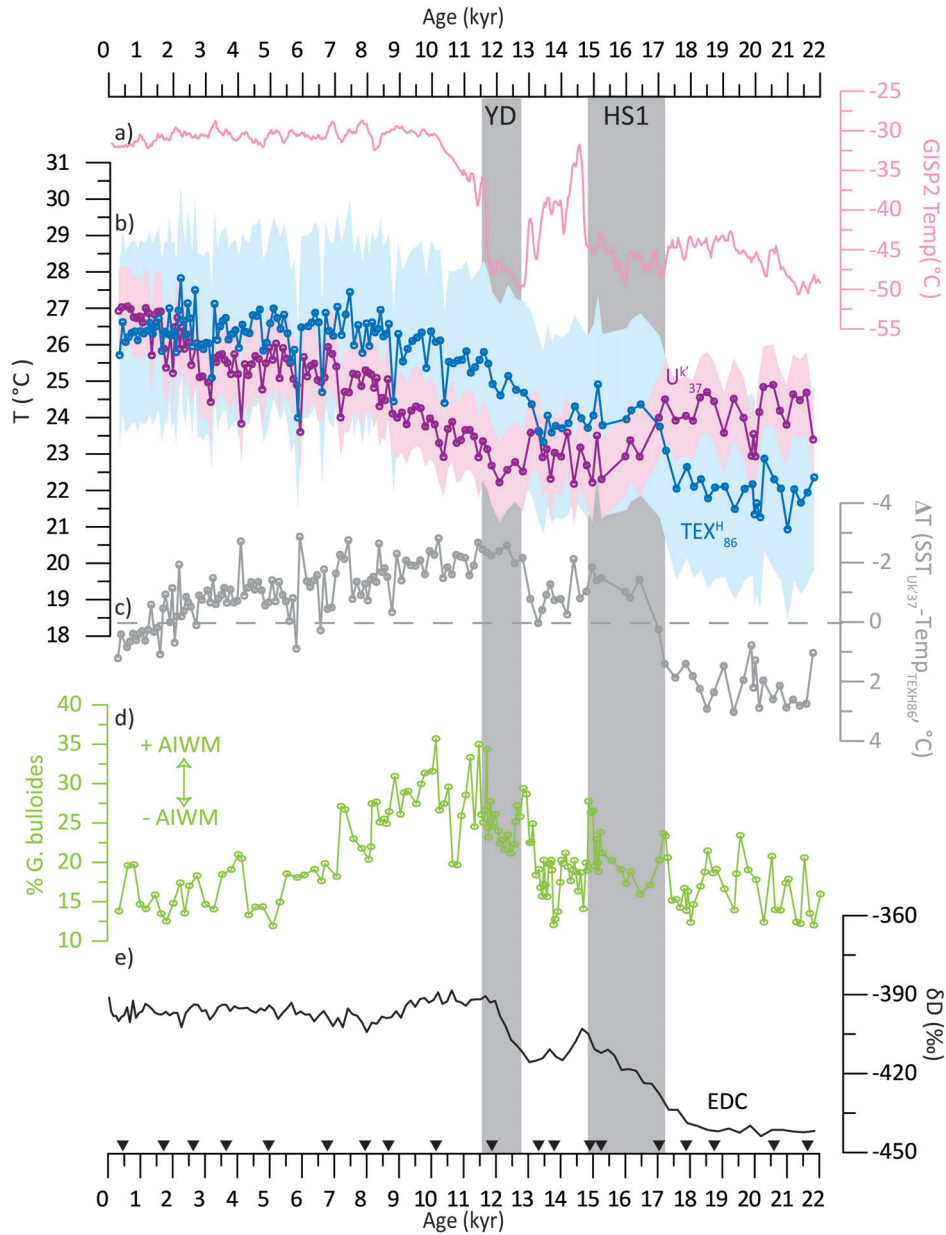


Fig. 5.2. a) temperature reconstruction of GISP 2 ice core (Greenland, Alley, 2004, pink); b)  $U^K_{37}$  and  $TEX^H_{86}$  index estimated temperatures in this study, the blue and purple areas correspond to the errors of the temperature calibration equations for  $U^K_{37}$  ( $\pm 1.1$  °C) and  $TEX^H_{86}$  ( $\pm 2.5$  °C); c)  $\Delta T$  calculated by  $SST-U^K_{37}$  minus  $Temp-TEX^H_{86}$  (grey); d) relative contribution of *G. bulloides* (Mohtadi et al., 2011, green); e)  $\delta D$  record of EPICA Dome C ice core (Antarctic; EPICA, 2004, black). The grey bars correspond to the HS1 and YD period. Triangles denote AMS  $^{14}C$  dating points (Mohtadi et al., 2011).

## 5.6. Discussion

### 5.6.1. Temperature Proxy Implication

Two different approaches are used to estimate the magnitude of temperature changes across the last glacial-interglacial transition. Although both the proxies seem to record mean annual SST, the discrepancy between the two indicates are commonly reported in previous studies (e.g., Huguet et al., 2006; McClymont et al., 2012; Wang et al., 2013).

A one-year sediment trap and a surface sediment study of  $U^{K'}_{37}$  and  $TEX^H_{86}$  in this region have revealed that  $U^{K'}_{37}$  records the upwelling season, while  $TEX^H_{86}$  is inferred to represent mean annual (ma) temperature at 50 m depth (i.e., the top of the thermocline; Chen et al., 2014 and submitted). The  $U^{K'}_{37}$  and  $TEX^H_{86}$  based temperature for surface sediment at the core location are 26.9 °C and 25.6 °C, respectively, which agree with SE monsoon SST (26.5 °C) and ma temperature at 50 m depth (26.0 °C) from World Ocean Atlas 2009 (WOA 09, Locarnini et al., 2010), supporting this interpretation. Therefore, we infer that the  $U^{K'}_{37}$  in this core reflects past changes in the SE monsoon SST in the upwelling region off south Java, while  $TEX^H_{86}$  records ma temperature at 50 m depth.

### 5.6.2. Overall temperature changes

The magnitude of temperature variations and absolute temperature values between the two indices are different in the study area. The average  $U^{K'}_{37}$ -based SST and  $TEX^H_{86}$ -based temperature estimates during the LGM (defined according to EPILOG as 19-22 ka; Mix et al., 2001) are 24.0 °C and 21.9 °C, respectively, showing cooling of 2.9 °C and 3.8 °C compared to present-day temperature based on alkenone and GDGT, respectively. In accordance with our estimates, the MARGO project reconstruction suggested an approximate 2 °C cooling for the LGM in the eastern Indian Ocean (MARGO Project Members, 2009) and Barrows and Juggins (2005) inferred up to 4°C cooling in the on Mg/Ca ratios of planktonic foraminifera in the eastern Indian Ocean. In addition, Analyses of Mg/Ca ratios of planktonic foraminifera in the eastern Indian

Ocean show 2° - 3 °C cooler SSTs during the LGM than during the Holocene (Mohtadi et al., 2010). Taken together, the amplitudes of last glacial-interglacial temperature variations in our records are in good agreement with those of published records from the eastern Indian Ocean.

#### 5.6.2.1 U<sup>K</sup><sub>37</sub> SST changes

As aforementioned, the U<sup>K</sup><sub>37</sub> temperature estimates reflect SE monsoon SST. In the study area, visual comparison of variations in alkenone-based SST estimates and the *G. bulloides* percentages as a proxy for upwelling intensity which shows that the two records covary well, indicating that wind-driven upwelling was an important factor for SST variability during last 22,000 years. Similar observations were made in the southern Sumatra approximately located 1000 km away from our site over the past 300,000 years and 130,000 years, respectively, where the authors hypothesized that alkenone-based SST changes were related to the monsoon-controlled seasonal upwelling (Lückge et al., 2009; Mohtadi et al., 2010).

The U<sup>K</sup><sub>37</sub> record shows pronounced decreasing trends during the HS1 and the YD periods and a slow rate of temperature rise during the B-A period, respectively (Fig. 5.2.). The lowest U<sup>K</sup><sub>37</sub> temperature estimates appeared in the middle of the YD (ca. 12 ka) and the late HS1 (ca. 15 ka). These events were nearly synchronous with important palaeoclimate changes recorded in the Greenland isotope records, possibly implying a coupling to the deglacial development of the North Atlantic region (Fig. 5.2.). What are the broader implications of our findings concerning the seasonal SST change in this region during the last glacial-interglacial transition?

The tropical SSTs are sensitive to Northern hemisphere high-latitude climate changes has been documented in several paleoclimate records (e.g., Kienast et al., 2006; Muller et al., 2012). Two basic scenarios may have contributed to these variations, including: (1) a slowdown or potentially a shutdown of the AMOC with a southward

displacement of the ITCZ (e.g., Chiang and Bitz, 2005; McManus et al., 2004; Zhang and Delworth, 2005); (2) variations in cross-equatorial surface winds.

There is a widespread paleoclimatic evidence for the variability of the tropical climate in the Indian Ocean responds to the North Atlantic deglacial climate oscillations that were accompanied by the variations in the AMOC (e.g., Naidu et al., 1996). A series of abrupt events occurred vgenerally through the ocean by a slowdown or potentially a shutdown of the AMOC and through the atmospheric circulation (e.g., Griffiths et al., 2009; McManus et al., 2004). Several studies suggest that a reduction AMOC in the past including a southward shift of the ITCZ during the HS1 and the YD events (e.g., Griffiths et al., 2009; McManus et al., 2004). It is well known that the position of the ITCZ is closely tied to hemispheric energy budgets through its role in cross-equatorial atmospheric heat transport. Changes in ITCZ position provide insight into the past changes in heat transport by the AMOC. Regards to HS1 as an example, a southward shift of the ITCZ during the HS1 would increase atmosphere heat transport into the northern hemisphere, compensating for a reduction or shutdown of the AMOC (McGee et al., 2014 and reference therefore). Moreover, a simulation experiment in the study area recently, which suggested that the northern hemisphere cooling by generating anomalous heat transport from the southern hemisphere to the northern hemisphere is driven by a reorganization of the Hadley circulation (Mohtadi et al., 2014).

Several studies on the wind field and SST of the Indian Ocean suggested that the intensity of the trade winds in the Indian Ocean is significantly correlated to the inter-hemispheric temperature gradients (e.g., Naidu et al., 1996 and reference therein). Previous studies demonstrated that increased evaporation (latent heat flux from ocean to atmosphere), increased southern hemisphere trade winds, increased cross-equatorial transport of latent heat and strong austral summer monsoon winds over the eastern Indian Ocean (Clemens et al., 1991 and reference therein). Furthermore, results by Clemens et al. (1991) based on biological, biogeochemical and lithogenic evidence over

the past 350,000 years corroborated the mechanisms of the inter-hemispheric pressure gradients in the Indian Ocean.

Our data suggest that a weak SE monsoon during the LGM and a strong SE monsoon during the YD and HS1 periods. An increased cross-equatorial heat transport is accompanied by increased southern trade winds would be expected during times of northern hemisphere cooling, such as the HS1 and the YD periods, indeed the SE monsoon was strong, vice versa. This mode of explanation has recently been proven by a modeling study (McGee et al., 2014). The authors suggested that a small ITCZ shifts is associated with relatively large changes in northward cross-equatorial atmospheric heat transport due to a weakened AMOC during the HS1, indicating modestly stronger SE monsoon.

In summary, the last glacial-interglacial variations of  $U_{37}^K$ -based temperature estimates provide strong evidence that they reflect variations in the strength of large-scale cross-equatorial winter monsoon winds, probably in response to ocean-atmosphere heat transport owing to changes to AMOC.

#### 5.6.2.2. $TEX_{86}^H$ temperature changes

As discussed above,  $TEX_{86}^H$  likely reflects shallow subsurface water temperatures (i.e., the top of thermocline). During the last glacial-interglacial cycle, temperature fluctuations were much more pronounced at the thermocline depth (up to 6°C, Fig. 5.2a.). The  $TEX_{86}^H$  record shows a continuous deglacial warming, starting at around 18 ka, but punctuated by a decreasing temperature during the B-A period, coeval with the ACR found in the Antarctic ice cores (EPICA, 2004; Fig. 5.2.). An early onset of sea-water temperature increase at about 18-19 ka has been observed in several records from the eastern Indian Ocean and the Western Pacific Warm Pool region (Lea et al., 2000; Levi et al., 2007; Mohtadi et al., 2010a; Rosenthal et al., 2003; Stott et al., 2007; Visser et al., 2003; Xu et al., 2006;). These records point to uniform, stable and warm deglacial SST variations in the low latitude, which is roughly coincide

with southern high latitude climate changes and the rising global CO<sub>2</sub> level, suggesting that the warming of surface waters in these regions during the deglaciation would be attributed to the flux of CO<sub>2</sub> into the atmosphere (e.g., Shakun et al., 2010; Stott et al., 2007; Visser et al., 2003). Although there is similarity in the timing and magnitude of subsurface water temperature changes compared to previous SSTs in the eastern Indian Ocean and the Western Pacific Warm Pool region, the relationship between CO<sub>2</sub> concentration and subsurface water temperature changes is not obvious.

In general, thermocline temperatures are controlled by two factors. One is that the upwelling intensity during the SE monsoon that injects cooler waters from deeper depths. Our data show that a strong SE monsoon during the HS1 and the YD periods. Cooler TEX<sub>86</sub><sup>H</sup> temperature estimates would be expected during the two periods. Contrary to this assumption, however, warmer TEX<sub>86</sub><sup>H</sup>-based temperatures are not observed. Moreover, warmer TEX<sub>86</sub><sup>H</sup>-based temperatures reflect mean annual temperatures that could probably be compensated by the temperature signals from other seasons. Thus, our data suggest that an overall insignificant impact of upwelling intensity on mean annual conditions.

Alternatively, our study area is an upwelling area, feeding by subsurface and intermediate waters originated in the Southern Ocean. Another important factor is that changes in the subsurface temperatures are remotely forced by changes in the temperature of the source. Deep-water temperatures reflect a globally average record of Earth's radiative-heat balance. Based on benthic foraminiferal δ<sup>18</sup>O, Stott et al. (2007) documented that the increased austral-spring insolation over the Southern Ocean is responsible for deglacial warming and atmospheric CO<sub>2</sub> increase around 18.5 ka. Our records show that the warming subsurface waters began at around 18 ka, indicating ~500 years lag between the high and low latitudes. A study by Matsumoto and key (2004) using conventional <sup>14</sup>C ages of dissolved carbon showed that the transport of Southern Ocean intermediate and deep water to the eastern tropical Indian Ocean takes approximately ~300-400 years. Considering to this time lag, our data suggest the

changes in subsurface waters are related to the changes in atmospheric CO<sub>2</sub> concentration. This finding is in agreement with the thermocline temperature reconstruction based on Mg/Ca ration in the Timor Sea during the Termination I by Xu et al. (2008). Therefore, the variation of temperature estimates based on GDGT that represents subsurface water temperature during the last glacial-interglacial period is presumably attributed to CO<sub>2</sub> forcing.

Our results suggest that the U<sub>37</sub><sup>K'</sup> and TEX<sub>86</sub><sup>H</sup> temperatures are closely linked to climate changes in both hemispheres due to their response to seasonal and mean annual temperature, respectively (Fig. 5.2.). The same pattern has been observed in other parts of the tropical Indian Ocean, i.e., in the western Indian Ocean, in the Arabian Sea, between different proxies, suggesting seasonal effect on SSTs is a prevailing picture during terminations (e.g., Saher et al., 2009; Wang et al., 2013).

### 5.6.3. Difference between U<sub>37</sub><sup>K'</sup> and TEX<sub>86</sub><sup>H</sup> records

Our U<sub>37</sub><sup>K'</sup> and TEX<sub>86</sub><sup>H</sup> temperature estimates show a different pattern for the entire period: The Temp-TEX<sub>86</sub><sup>H</sup> record shows an overall warming trend, whereas the SST-U<sub>37</sub><sup>K'</sup> record decreases from 22 ka BP to 14 ka BP and increases from 12 ka BP to the present-day (Fig. 5.2b.).

We observe a positive  $\Delta T$  (SST-U<sub>37</sub><sup>K'</sup> minus Temp-TEX<sub>86</sub><sup>H</sup>) during the LGM (22 ka BP to 19 ka BP), the early deglaciation (19 ka BP to 17.5 ka BP) and late Holocene (2 ka BP to present-day), while  $\Delta T$  is negative during the rest of the record (Fig. 5.2c.). Offsets between both indices have previously been observed in several regions (Huguet et al., 2006; Li et al., 2013; Lopes dos Santos et al., 2010; McClymont et al., 2012; Rommerskirchen et al., 2011) and are commonly attributed to the differences in seasonal occurrence and habitat depth of source organisms. As introduced above, the U<sub>37</sub><sup>K'</sup> (TEX<sub>86</sub><sup>H</sup>) represent past changes in the SE monsoon SST (sea temperature at 50 m depth) in the upwelling region off south Java.

The temporal evolution of the temperature difference is paralleled with *G. bulloides* percentages that are identified as a proxy for winter upwelling and monsoon intensity (Fig. 5.2., Mohtadi et al., 2011). Moreover, the temporal evolution of the  $\Delta T$  is also paralleled by difference in  $\delta^{18}\text{O}$  ( $\Delta\delta^{18}\text{O}$ ) of two foraminiferal species thriving throughout the year and predominantly in winter, respectively, whereby a greater difference implies stronger upwelling (Mohtadi et al., 2011). This indicates that the difference between the two organic proxy based temperature reconstructions is likewise tied to the upwelling strength. This is consistent with previous studies showing that the temperature offset depends on the degree of marine primary productivity (Chen et al., 2014; Rommerskirchen et al., 2011). The positive temperature offsets during the latest Holocene match the modern conditions as observed in surface sediments (Chen et al., 2014). Similar conditions likely prevailed during the LGM period.

In surface sediments, no modern analogue situation exists for negative  $\Delta T$  between SE monsoon SST ( $U_{37}^K$  estimate) and mean annual subsurface waters ( $\text{TEX}_{86}^H$  estimate) as observed in our records during the last deglacial and early Holocene (Chen et al., 2014). In the study area, the mixed layer varies seasonally under the Australian Indonesian monsoon. The mean annual thickness of the mixed-layer is generally 40-50 m (Qu and Meyers, 2005). The mixed-layer shoals during the SE monsoon and thickest during the NW monsoon (Fig. 5.3.). Mohtadi et al. (2011) suggested a weaker Australian-Indonesian austral winter monsoon (AIWM) during LGM and late Holocene, strongest AIWM during early Holocene, and a relatively strong AIWM during HS1 and the YD. As illustrated in Fig. 5.3b, when the AIWM is strong off Java, the surface water is cooler and nutrient supply is increased, which likely results in low  $U_{37}^K$  temperature estimates. On the other hand, when Australian-Indonesian austral summer monsoon (AISM) is strong and the mixed-layer is deep, a small vertical temperature gradient would be expected. The cooler  $\text{TEX}_{86}^H$  temperature estimates expected during the strongest AIWM are possibly compensated by warmer  $\text{TEX}_{86}^H$  signals from AISM, resulting in warmer mean temperature at 50 m depth ( $\text{Temp-TEX}_{86}^H$ ) than SST during SE monsoon ( $\text{SST-U}_{37}^K$ ) (Fig. 5.3b.). In previous studies, it has been postulated that the AISM was generally strongest

during warm phases and weakest during cool phases of the Late Quaternary (Kershaw and Nanson, 1993). However, the AISM was not stronger enough during the last deglacial as implied by the Ti/Ca records of our core as proxy for NW monsoon intensity (Mohtadi et al., 2011). The average  $\text{TEX}_{86}^{\text{H}}$ -based temperature estimates is 26.1 °C range from 17.5 ka BP to 2 ka BP, which agrees with the core-top data (25.9 °C, Chen et al., 2014) as well as modern mean annual temperature at 50 m depth (26.0 °C). The relatively constant warm mean annual temperature at 50 m depth we concerned is probably less affected by the intensity of NW monsoon. This implies that the coolest SE monsoon SST associated with strongest upwelling strength is the dominant factor in the negative  $\Delta T$  scenario during the last deglacial and early Holocene. A similar observation was made in same upwelling area, such as the South China Sea and the Gulf of California, where the authors noted that the offset between  $U_{37}^{\text{K}}$  and  $\text{TEX}_{86}^{\text{H}}$  based temperature estimates can be used to reconstruct upwelling intensity (e.g., Li et al., 2013; McClymont et al., 2012). Therefore, the offset between the two proxies off south Java in the eastern Indian Ocean can be explained through the variations in the strength of the austral winter upwelling.

### 5.7. Summary and Conclusions

$U_{37}^{\text{K}}$  and  $\text{TEX}_{86}^{\text{H}}$  records covering the last 22 ka were obtained from a sediment core (GeoB10053-7) in the upwelling area off south Java. The  $U_{37}^{\text{K}}$  and  $\text{TEX}_{86}^{\text{H}}$  records reveal different temperature variations spanning the past 22 ka. Temp- $\text{TEX}_{86}^{\text{H}}$  record shows an overall warming tendency during the whole time period, whereas SST- $U_{37}^{\text{K}}$  record is punctuated by two abrupt cooling events during HS1 and the YD. Our results reveal that the tropical eastern Indian Ocean seasonal and mean annual temperatures are closely linked to climate changes in both hemispheres. The  $U_{37}^{\text{K}}$ -SST is controlled by upwelling strength, which in turn reflects northern hemisphere climate variations (cold HS1 and the YD). Temperature estimates based on  $\text{TEX}_{86}^{\text{H}}$  reflecting mean annual conditions at 50 m depth show a trend closely resembling the southern hemisphere continuous warming pattern. Temp- $\text{TEX}_{86}^{\text{H}}$  is up to 2 °C warmer than SST- $U_{37}^{\text{K}}$  during the

last deglacial and early Holocene, whereas lower  $\text{TEX}_{86}^{\text{H}}$  temperature estimates are observed during LGM and late Holocene. The offset between two temperature proxies can be used to reconstruct the upwelling intensity in the study area.

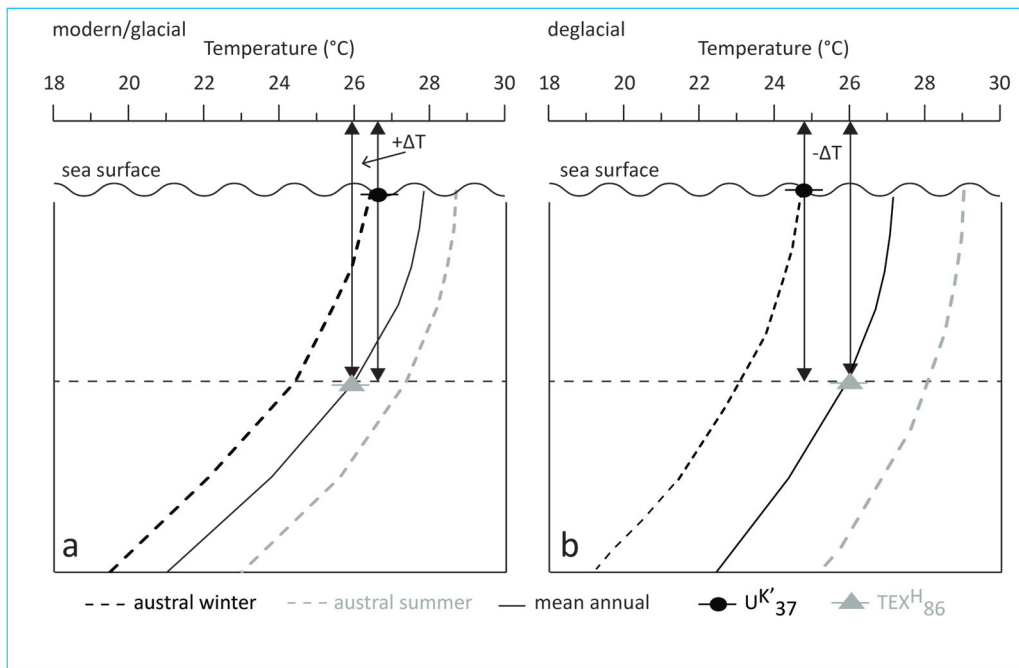


Fig. 5.3. Schematic illustration of the relationship between temperature difference and intensity of upwelling: a) modern/glacial conditions; b) deglacial conditions. Temperature profiles in the core site from WOA 09, Solid black lines: mean annual temperature; dashed black lines: austral winter temperature; dashed grey lines: austral summer temperature; black dots and grey triangles represent flux-weighted  $U^{K'}_{37}$  temperature estimates and  $\text{TEX}_{86}^{\text{H}}$  temperature estimates, respectively (Chen et al., submitted).

### Acknowledgements

We thank the participating crews and scientific party of the PABESIA expedition (RV Sonne Cruise SO-184) for core collection. We thank Ralph Kreutz for laboratory assistance. We are grateful to German Bundesministerium für Bildung und Forschung (PABESIA) and China Scholarship Council (CSC) for funding support.

## 5.8. References

- Alley, R.B., Clark, P.U., 1999. The deglaciation of the northern hemisphere: a global perspective. *Annual Review of Earth and Planetary Sciences*, 27(1), 149-182.
- Alley, R.B., 2004. GISP2 ice core temperature and accumulation data, <http://www.ncdc.noaa.gov/paleo/metadata/noaa-icecore-2475.html>, World Data Center for Paleoclimatology, Boulder, Colo.
- Barrows, T.T., Juggins, S., 2005. Sea-surface temperatures around the Australian margin and Indian Ocean during the Last Glacial Maximum. *Quaternary Science Reviews*, 24, 1017-1047.
- Broecker, W.S., 1998. Paleocean circulation during the last deglaciation: A bipolar seesaw? *Paleoceanography*, 13(2), 119-121.
- Cane, M.A., Clement, A.C., 1999. A Role for the tropical Pacific coupled ocean-atmosphere system on Milankovitch and millennial time- scales. part II: Global impacts, in *Mechanisms of Global Climate Change at Millennial Time Scales*, Geophys. Monogr. Ser., vol. 112, edited by P. U. Clark, R. S. Webb, and L. D. Keigwin, pp. 373 – 383, AGU, Washington D. C.
- Chen, W., Mohtadi, M., Schefuß, E., Mollenhauer, G., 2014. Organic-geochemical proxies of sea surface temperature in surface sediments of the tropical Eastern Indian Ocean. *Deep-Sea Research I*, 88, 17-29.
- Chen, W., Mohtadi, M., Schefuß, E., Mollenhauer, G. Concentrations and abundance ratios of long-chain alkenones and glycerol dialkyl glycerol tetraether in sinking particles south off Java. Submitted.
- Chiang, J.C.H., Bitz, C.M., 2005. Influence of high latitude ice cover on the marine Intertropical Convergence Zone. *Climate Dynamics*, 25, 477-496.
- Clark, P.U., Pisias, N.G., Stocker, T.F., Weaver, A.J., 2002. The role of the thermohaline circulation in abrupt climate change. *Nature*, 415(6874), 863-869.
- Clement, A.C., Cane, M.A., Seager, R., 2001. An orbitally driven tropical source for abrupt climate change. *Journal of Climate*, 14, 2369-2375.

- Clemens, S., Prell, W., Murray, D., Shimmield, G., Weedon, G., 1991. Forcing mechanisms of the Indian Ocean Monsoon. *Nature*, 353, 720-725.
- Conte, M.H., Sicre, M.-A., Rühlemann, C., Weber, J.C., Schulte, S., Schulz-Bull, D., Blanz, T., 2006. Global temperature calibration of the alkenone unsaturation index ( $U'_{37}$ ) in surface waters and comparison with surface sediments. *Geochemistry Geophysics Geosystems*, 7, doi: 10.1029/2005GC001054.
- EPICA community members, 2004. Eight glacial cycles from an Antarctic ice core. *Nature*, 429 623-628.
- Gordon, A.L., Fine, R.A., 1996. Pathways of water between the Pacific and Indian oceans in the Indonesian seas. *Nature*, 379, 146-149.
- Gordon, A.L., 2005. Oceanography of the Indonesian seas and their throughflow. *Oceanography*, 18 (4), 14-28.
- Griffiths, M.L., Drysdale, R.N., Gagan, M.K., Zhao, J.-x., Ayliffe, L.K., Hellstrom, J.C., Hantoro, W.S., Frisia, S., Feng, Y.-x., Cartwright, I., Pierre, E.St., Fischen, M.J., Suwargadi, B.W., 2009. Increasing Australian-Indonesian monsoon rainfall linked to early Holocene sea-level rise. *Nature Geoscience*, 2(9), 636-639, doi: 10.1038/NGEO0605.
- Hebbeln, D., et al. 2005. Report and preliminary results of RV SONNE cruise SO-184, PABESIA, Durban (South Africa)-Cilacap (Indonesia)-Darwin (Australia), July 8th-September 13th, 2005, Rep. 246, 142 pp., Univ. Bremen, Bremen, Germany.
- Hopmans, E.C., Schouten, S., Pancost, R.D., van der Meer, M.T.J., Sinninghe Damsté, J.S., 2000. Analysis of intact tetraether lipids in archaeal cell material and sediments by high performance liquid chromatography/atmospheric pressure chemical ionization mass spectrometry. *Rapid Communications in Mass Spectrometry*, 14, 585-589.
- Hopmans, E.C., Weijers, J.W.H., Schefuß, E., Herfort, L., Sinninghe Damsté, J.S., Schouten, S., 2004. A novel proxy for terrestrial organic matter in sediments based on branched and isoprenoid tetraether lipids. *Earth Planetary Science Letter*, 224, 107-116.

- Huguet, C., Cartes, J.E., Sinninghe Damsté, J.S., Schouten, S., 2006. Marine crenarchaeotal membrane lipids in decapods: implications for the TEX<sub>86</sub> paleothermometer. *Geochemistry Geophysics Geosystems*, 7(11), Q11010.
- Jouzel, J., Vaikmae, R., Petit, J.R., Martin, M., Duclos, Y., Stievenard, M., Lorius, C., Toots, M., Mélières, M.A., Burckle, L.H., Barkov, N.I., Kotlyakov, V.M., 1995. The two-step shape and timing of the last deglaciation in Antarctica. *Climate Dynamics*, 11 (3), 151-161.
- Kershaw, A.P., Nanson, G.C., 1993. The last full glacial cycle in the Australian region. *Global and Planetary Change*, 7, 1-9.
- Kienast, M., Kienast, S.S., Calvert, S.E., Eglinton, T. I., Mollenhauer, G., François, R., Mix, A. C., 2006. Eastern Pacific cooling and Atlantic overturning circulation during the last deglaciation. *Nature*, 443(7113), 846-849.
- Kim, J.-H., van der Meer, J., Schouten, S., Helmke, P., Willmott, V., Sangiorgi, F., Koç, N., Hopmans, E.C., Sinninghe Damsté, J.S., 2010. New indices and calibrations derived from the distribution of crenarchaeal isoprenoid tetraether lipids: implications for past sea surface temperature reconstructions. *Geochimica et Cosmochimica Acta*, 74, 4639-4654.
- Lea, D. W., Pak, D. K., Spero, H. J., 2000. Climate impact of late Quaternary equatorial Pacific sea surface temperature variations. *Science*, 289 (5485), 1719-1724.
- Levi, C., Labeyrie, L., Bssinot, F., Guichard, F., Cortijo, E., Waelbroeck, C., Caillon, N., Duprat, J., de Garidel-Thoron, T., Elderfield, H., 2007. Low-latitude hydrological cycle and rapid climate changes during the last deglaciation. *Geochemistry, Geophysics, Geosystems*, 8, Q02007.
- Li, D., Zhao, M., Tian, J., Li, L., 2013. Comparison and implication of TEX<sub>86</sub> and U<sup>K'</sup><sub>37</sub> temperature records over the last 356 kyr of ODP Site 1147 from the northern South China Sea. *Palaeogeography, Palaeoclimatology, Palaeoecology*, 376, 213-223.

- Locarnini, R.A., Mishonov, A.V., Antonov, J.I., Boyer, T.P., Garcia, H.E., Baranova, O.K., Zweng, M.M., Johnson, D.R., 2010, World Ocean Atlas 2009, Volume 1: Temperature, 184.
- Lukas, R., Lindstrom, E., 1991. The mixed layer of the western equatorial Pacific Ocean. *Journal of Geophysical Research*, 96, 3343-3357.
- Lückge, A., Mohtadi, M., Rühlemann, C., Scheeder, G., Vink, A., Reinhardt, L., Wiedicke, M., 2009. Monsoon versus ocean circulation controls on paleoenvironmental conditions off southern Sumatra during the past 300,000 years. *Paleoceanography*, 24(1).
- MARGO Project Members, 2009. Constraints on the magnitude and patterns of ocean cooling at the Last Glacial Maximum. *Nature Geoscience*, 2, doi:10.1038/NGEO0411.
- Matsumoto, K., Key, R.M., 2004. Natural radiocarbon distribution in the deep ocean. In: Shiyomi, et al. (Ed.), *Global Environmental Change in the Ocean and on Land*, pp. 45–58.
- Meyers, G., Mcintosh, P., Pigot, L., Pook, M., 2007. The years of El Niño, La Niña, and Interactions with the tropical Indian Ocean. *Journal of Climate*, 20, 2872-2880.
- McClymont, E.L., Ganeshram, R.S., Pichevin, L.E., Talbot, H.M., Dongen, B.E., Thunell, R.C., Haywood, A.M., Singarayer, J.S., Valdes, P.J., 2012. Sea-surface temperature records of Termination 1 in the Gulf of California: Challenges for seasonal and interannual analogues of tropical Pacific climate change. *Paleoceanography*, 27, PA2202, doi: 10.1029/2011PA002226.
- McGee, D., Donohoe, A., Marshall, J., Ferreira, D., 2014. Changes in ITCZ location and cross-equatorial heat transport at the Last Glacial Maximum, Heinrich Stadial 1, and the mid-Holocene. *Earth and Planetary Science Letters*, 390, 69-79.
- McManus, J.F., Francois, R., Gherardi, J.M., Keigwin, L.D., Brown-Leger, S., 2004. Collapse and rapid resumption of Atlantic meridional circulation linked to deglacial climate changes. *Nature*, 428(6985), 834-837.

- Mix, A.C., Bard, E., Schneider, R., 2001. Environmental processes of the ice age: Land, oceans glaciers (EPILOG). *Quaternary Science Reviews*, 20, 627-657.
- Mohtadi, M., Steinke, S., Lückge, A., Groeneveld, J., Hathorne, E.C., 2010a. Glacial to Holocene surface hydrography of the tropical eastern Indian Ocean. *Earth and Planetary Science Letters*, 292, 89-97.
- Mohtadi, M., Lückge, A., Steinke, S., Groeneveld, J., Hebbeln, D., Westphal, N., 2010b. Late Pleistocene surface and thermocline conditions of the eastern tropical Indian Ocean. *Quaternary Science Reviews*, 29, 887-896.
- Mohtadi, M., Oppo, D. W., Steinke, S., Stuut, J. B. W., De Pol-Holz, R., Hebbeln, D., Lückge, A., 2011. Glacial to Holocene swings of the Australian-Indonesian monsoon. *Nature Geoscience*, 4(8), 540-544.
- Mohtadi, M., Prange, M., Oppo, D.W., De Pol-Holz, R., Merkel, U., Zhang, X., Steinke, S., Lückge, A., 2014. North Atlantic forcing of tropical Indian Ocean climate. *Nature*, 509(7498), 76-80, doi:10.1038/nature13196.
- Muller, J., McManus, J.F., Oppo, D.W., Francois, R., 2012. Strengthening of the Northeast Monsoon over the Flores Sea, Indonesia, at the time of Heinrich event 1. *Geology*, 40, 635-638, doi:10.1130/G32878.
- Naidu, P.D., Malmgren, B.A., 1996. A high-resolution record of late Quaternary upwelling along the Oman Margin, Arabian Sea based on planktonic foraminifera. *Paleoceanography*, 11(1), 129-140.
- Neale, R., Slingo, J., 2003. The maritime continent and its role in the global climate: A GCM study. *Journal of Climate*, 16(5), 834-848.
- Qu, T., Du, Y., Strachan, J., Meyers, G., Slingo, J. M., 2005. Sea surface temperature and its variability in the Indonesian region. *Oceanography*, 18, 50-61.
- Qu, T., Meyers, G., 2005. Seasonal characteristics of circulation in the southeastern tropical Indian Ocean, *Journal of Physical Oceanography*, 35(2), 255-267.
- Rommerskirchen, F., Condon, T., Mollenhauer, G., Dupont, L., Schefuss, E., 2011. Miocene to Pliocene development of surface and subsurface temperatures in the Benguela Current system. *Paleoceanography*, 26, 3216.

- Rosenthal, Y., Oppo, D.W., Linsley, B.K., 2003. The amplitude and phasing of climate change during the last deglaciation in the Sulu Sea, western equatorial Pacific. *Geophysical Research Letters*, 30 (8), 1428.
- Saher, M.H., Rostek, F., Jung, S.J.A., Schneider, R.R., Greaves, M., Ganssen, G.M., Elderfield, H., Kroon, D., 2009. Western Arabian sea SST during the penultimate interglacial: A comparison of  $U^{K'}_{37}$  and Mg/Capaleothermometry. *Paleoceanography*, 24, PA2212, doi: 10.1029/2007PA001557.
- Schouten, S., Hopmans, E.C., Schefuss, E., Sinninghe Damsté, J.S., 2002. Distributional variations in marine crenarchaeotal membrane lipids: a new tool for reconstructing ancient sea water temperatures? *Earth and Planetary Science Letters*, 204, 265-274.
- Schouten, S., Huguet, C., Hopmans, E.C., Kienhuis, M.V.M., Sinninghe Damsté, J.S., 2007. Analytical methodology for TEX<sub>86</sub> paleothermometry by High-Performance Liquid Chromatography/Atmospheric Pressure Chemical Ionization-Mass Spectrometry. *Analytical Chemistry*, 79, 2940-2944.
- Schouten, S., Hopmans, E.C., Rosell-Melé, A., Pearson, A., Adam, P., Bauersachs, T., Bard, E., Bernasconi, S.M., Bianchi, T.S., Brocks, J.J., Carlson, L.T., Castañeda, I.S., Derenne, S., Selver, A.D., Dutta, K., Eglinton, T., Fosse, C., Galy, V., Grice, K., Hinrichs, K.-U., Huang, Y., Huguet, A., Huguet, C., Hurley, S., Ingalls, A., Jia, G., Keely, B., Knappy, C., Kondo, M., Krishnan, S., Lincoln, S., Lipp, J., Mangelsdorf, K., Martínez-García, A., Ménot, G., Mets, A., Mollenhauer, G., Ohkouchi, N., Ossebaar, J., Pagani, M., Pancost, R.D., Pearson, E.J., Peterse, F., Reichert, G.-J., Schaeffer, P., Schmitt, G., Schwark, L., Shah, S.R., Smith, R.W., Smittenberg, R.H., Summons, R.E., Takano, Y., Talbot, H.M., Taylor, K.W.R., Tarozo, R., Uchida, M., van Dongen, B.E., Van Mooy, B.A.S., Wang, J., Warren, 957 C., Weijers, J.W.H., Werne, J.P., Woltering, M., Xie, S., Yamamoto, M., Yang, H., Zhang, C.L., Zhang, Y., Zhao, M., Damsté, J.S.S., 2013. An interlaboratory study of TEX<sub>86</sub> and BIT analysis of sediments, extracts, and standard mixtures. *Geochemistry Geophysics Geosystems*, 14 (12), 5263-5285.

- Shakun, J.D., Carlson, A.E., 2010. A global perspective on Last Glacial Maximum to Holocene climate change. *Quaternary Science Reviews*, 29(15), 1801-1816.
- Shakun, J.D., Clark, P.U., He, F., Marcott, S.A., Mix, A.C., Liu, Z., Bard, E., 2012. Global warming preceded by increasing carbon dioxide concentrations during the last deglaciation. *Nature*, 484(7392), 49-54.
- Sprintall, J., Tomczak, M., 1992. Evidence of the barrier layer in the surface layer of the tropics. *Journal of Geophysical Research*, 97, 7305-7316.
- Sprintall, J., Wijffels, S.E., Molcard, R., Jaya, I., 2009. Direct estimates of the Indonesian Through flow entering the Indian Ocean: 2004-2006. *Journal of Geophysical Research*, 114, doi:10.1029/2008JC005257.
- Stott, L., Timmermann, A., Thunell, R., 2007. Southern Hemisphere and deep-sea warming led deglacial atmospheric CO<sub>2</sub> rise and tropical warming. *Science*, 318, 435-438.
- Susanto, R.D., Gordon, A.L., Zheng, Q., 2001. Upwelling along the coasts of Java and Sumatra and its relation to ENSO. *Geophysical Research Letters*, 28, 1599-1602.
- Tapper, N. J., 2002. Climate, climatic variability and atmospheric circulation patterns in the maritime continent region, in *Bridging Wallace's Line: The Environmental and Cultural History and Dynamics of the Southeast Asian-Australian Region*, edited by P. Kershaw et al., pp. 5-28, Catena, Reiskirchen, Germany.
- Tomczak, M., Godfrey, J.S., 1994. *Regional oceanography: an introduction*. Elsevier, New York.
- Xu, J., Kuhnt, W., Holbourn, A., Andersen, N., Bartoli, G., 2006. Changes in the vertical profile of the Indonesian Throughflow during Termination II: Evidence from the Timor Sea. *Paleoceanography*, 21, doi: 10.1029/2006PA001278.
- Xu, J., Holbourn, A., Kuhnt, W., Jian, Z., Kawamura, H., 2008. Changes in the thermocline structure of the Indonesian outflow during Termination I and II. *Earth and Planetary Science Letters*, 273, 152-162.
- Visser, K., Thunell, R.C., Stott, L.D., 2003. Magnitude and timing of temperature change in the Indo-Pacific warm pool during deglaciation. *Nature* 421(9), 152-155.

- Wang, Y. V., G. Leduc, M. Regenberg, N. Andersen, T. Larsen, T. Blanz, R. R. Schneider, 2013. Northern and southern hemisphere controls on seasonal sea surface temperatures in the Indian Ocean during the last deglaciation. *Paleoceanography*, 28, 1-14, doi: 10.1002/palo.20053.
- Weijers, J.W.H., Schouten, S., Spaargaren, O.C., Sinninghe Damsté, J.S., 2006. Occurrence and distribution of tetraether membrane lipids in soil: Implications for the use of the TEX<sub>86</sub> proxy and the BIT indeed. *Organic Geochemistry*, 37, 1680-1693.
- Wyrtki, K., 1961. *Physical oceanography of Southeast Asian waters*, NAGA Rep.2, Scripps Institution of Oceanography, University of California, San Diego, 195pp.
- Zhang, R., Delworth, T. L., 2005. Simulated tropical response to a substantial weakening of the Atlantic thermohaline circulation. *Journal of Climate*, 18(12), 1853-1860.

## Chapter 6 Conclusions and Outlook

### 6.1. Summary and Conclusions

In this thesis, the seasonality, depth habitats of source organism and the application of two commonly used organic-geochemical SST reconstruction proxies ( $U_{37}^{K'}$  and  $TEX_{86}^H$ ) in the eastern Indian Ocean for modern and last glacial-interglacial timescale were investigated. Additionally, a detailed study in the Java upwelling area was carried out. In the following sections the major findings are summarized.

In the sediment core-top study, the temperatures based on the  $U_{37}^{K'}$  and  $TEX_{86}^H$  proxies deviate from the mean annual temperature of the World Ocean Atlas 2009 (WOA09), particularly for the samples from the upwelling regions off south of Java and the Lesser Sunda Islands. Variations in these lipid biomarker proxies could be attributed to differences in seasonal production and/or spatial distribution of the water column. In the upwelling regions, alkenone-based temperature estimates are up to 2 °C lower than mean annual SST, but are in agreement with SE monsoon SST. This indicates that the SST- $U_{37}^{K'}$  reflects the SE monsoon SST consistent with previous studies demonstrating maximum alkenone production during the colder season associated with higher marine primary productivity (e.g. Leider et al., 2010). Further support for this interpretation is given by the results from the sediment trap. Highest alkenone flux (4.3  $\mu\text{g}/\text{m}^2/\text{day}$ ) is measured in late September during the SE monsoon, coincident with high total organic carbon fluxes as well as high net primary productivity. The flux-weighted average  $U_{37}^{K'}$ -SST of 26.8 °C for the high flux period is also similar to the satellite-based SE monsoon SST (26.4 °C), which is consistent with the findings in the core-top study. This average is based on those samples only that permitted a reliable SST estimate, i.e. mainly the samples from the SE monsoon period. The surface sediment SST- $U_{37}^{K'}$  of core GeoB10044, which is located 112 km away from our trap site, is 26.9 °C, which is similar to the flux-weighted average  $U_{37}^{K'}$ -SST. Furthermore, a secondary flux maximum during the NW monsoon, likely related to increased production stimulated by riverine input of nutrients, does not strongly contribute to the total annual flux. On the other hand, the

sediment trap results show less pronounced seasonality of GDGT flux with only a small peak during the upwelling season, which may be attributed to more efficient export of GDGTs by aggregation with phytoplankton during austral winter. The flux-weighted average  $\text{TEX}_{86}^{\text{H}}$ -based temperature estimates is 26.2 °C, cooler than mean annual SST (28.0 °C), but in better agreement with the water temperature at 50 m depth (26.7 °C). Lower  $\text{TEX}_{86}^{\text{H}}$ -temperatures than the mean annual SST were also observed in the core-top study. The different performance of both temperature proxies resulted in a temperature offset ( $\Delta T$ ) off Lesser Sunda Islands, which could be interpreted by either one or a combination of the following factors: the  $\text{TEX}_{86}^{\text{H}}$  signal is derived from subsurface water at 50 m depth with lower temperatures and/ or highest archaeal and alkenone production occurs at different times, with alkenones-based temperatures not representing the coldest upwelling SSTs whereas the lower  $\text{TEX}_{86}^{\text{H}}$  signal might derive from times of peak upwelling associated with the highest export flux. Furthermore, alkenone-based temperature estimates probably underestimate tropical SST due to reduced sensitivity of the  $U_{37}^{\text{K}}$  proxy at SST beyond 28 °C in the equatorial non-upwelling area off western Sumatra. In contrast, GDGT-based temperature estimates are in agreement with mean annual SST, implying that the Temp- $\text{TEX}_{86}^{\text{H}}$  reflects the mean annual SST in the non-upwelling region.

Subsequently, the retrieved knowledge about  $U_{37}^{\text{K}}$  and  $\text{TEX}_{86}^{\text{H}}$  from surface sediments and sediment trap was applied to a sediment core off south of Java in the eastern Indian Ocean spanning the past 22,000 years. SST- $U_{37}^{\text{K}}$  records fluctuated between 22.2 °C and 27.1 °C, with a glacial-interglacial difference of 3.0 °C.  $\text{TEX}_{86}^{\text{H}}$ -temperature records fluctuated between 20.9 °C and 27.8 °C, with a glacial-interglacial difference of 3.8 °C. The records show two apparent temperature discrepancy phases,  $\text{TEX}_{86}^{\text{H}}$ -temperature records are up to 2 °C warmer than SST- $U_{37}^{\text{K}}$  records during the last deglacial, whereas lower  $\text{TEX}_{86}^{\text{H}}$  temperature estimates are observed during LGM and late Holocene. The  $\Delta T$  is paralleled by *G. bulloides* percentage as a proxy for upwelling and monsoon intensity, indicating the difference is tied to the upwelling strength. This is coincident with previous findings in the surface sediments study, showing that the  $\Delta T$

depends on the degree of marine primary productivity. Furthermore, the data documents the contrasting cooling and warming trends record in alkenones and GDGTs during the abrupt climate changes phases, e.g., the HS1, the ACR and the YD. I hypothesize that this may be caused by different mechanisms, i.e. bipolar seesaw and increased greenhouse gases. Depressed alkenone-based temperature estimates during HS1 and the YD could possibly be controlled by upwelling strength. On the other hand,  $\text{TEX}^{\text{H}}_{86}$ -temperatures are likely mediated by climate changes occurring in the southern hemisphere with respect to increased atmospheric  $\text{CO}_2$  concentration.

## 6.2. Outlook

This thesis provides valuable insights to understanding the two lipids biomarkers temperature proxies ( $\text{U}^{\text{K}}_{37}$  and  $\text{TEX}^{\text{H}}_{86}$ ) in tropical upwelling regions. However, some open questions remain and need to be addressed in future work.

Although global calibrations of marine core-tops studies reveal a strong relationship between  $\text{U}^{\text{K}}_{37}$  and mean annual SST (e.g. Müller et al., 1998; Conte et al., 2006), several studies observed that  $\text{U}^{\text{K}}_{37}$  may be biased towards a certain season due to seasonality in production of alkenone (e.g. Herbert et al., 2003 and reference therein; Leider et al., 2010). Conte et al. (2006) documented the global production temperature calibration, suggesting that the regional bias in temperature estimates using this calibration is insignificant. However, there are no surface sediments and surface water samples from the eastern Indian Ocean included in the datasets of Conte et al. (2006). Only five surface water samples which are located in Indian Ocean and the Arabian Sea in the whole datasets with 629 samples are available (Conte et al., 2006). The sediment trap study reveals a pronounced seasonality in production of alkenone. The SST- $\text{U}^{\text{K}}_{37}$  reflects seasonal SST rather than mean annual SST. Thus, a regional calibration for the tropical Indian Ocean is required in order to reconcile the differences between different proxy-based temperatures and real temperatures.

In the sediment trap, as the low alkenone concentration do not permit a reliable quantification of the triple unsaturated  $\text{C}_{37}$  alkenone ( $\text{C}_{37:3}$ ), however, only those  $\text{U}^{\text{K}}_{37}$ -

SST estimates from the high flux period where alkenone abundance allowed a determination of  $C_{37:3}$  concentration can be reported instead of the all samples for the one-year time series. This leads to lack of information for the low flux period. On the other hand, for further studies it would be interesting to gain more information about sinking particles, to calculate more realistic particle sinking rates, and to examine the particle residence time in the surface water not only for alkenones but also for GDGTs. Therefore, a long-time series and shallow/deep trap should be deployed in the study area.

As discussed thoroughly in the previous chapters, consistent temperature estimates on the proxy applicability could be inferred from core-top data, sediment trap data and downcore records, suggesting that both indices might be valid in the past off Java. Our records reveal that the seasonal SSTs and mean annual subsurface temperatures (i.e. the top of the thermocline) are closely linked to climate changes occurring in both hemispheres during the last glacial-interglacial cycle. The obvious deviations between the two indices are observed. However, no modern analogue situation exists for negative  $\Delta T$  ( $SST-U_{37}^K$  minus  $Temp-TEX_{86}^H$ ) during strong upwelling season, which is further needed to investigate. Additionally, our data provide evidence for synchronous change in subsurface temperatures in the southern high latitudes and tropical eastern Indian Ocean, which is probably related to globally rising  $CO_2$  levels. On the other hand, thermocline waters in the eastern Indian Ocean are dominated by two water masses: the North Indian Water (NIW) and the ITF. The NIW is originated from the Indian Central Water (ICW) that forms in latitudes 40-45°S during the late winter convective overturning and northward propagation of the Subantarctic Mode Water (Mohtadi et al., 2010 and reference therein). At this point it would be of interest to assess how meridional shifts in southern hemisphere front systems resulting in impact of the mean annual subsurface temperatures in the tropics. More locations to detect the pathway and modeling study are needed.

### 6.3. References

- Conte, M.H., Sicre, M.-A., Rühlemann, C., Weber, J.C., Schulte, S., Schulz-Bull, D., Blanz, T., 2006. Global temperature calibration of the alkenone unsaturation index ( $U_{37}^K$ ) in surface waters and comparison with surface sediments. *Geochemistry Geophysics Geosystems*, 7, Q02005, doi: 10.1029/2005GC001054.
- Herbert, T.D., 2003. Alkenone Paleotemperature Determinations. In: *Treatise on Geochemistry*, pp. 391-432. Pergamon, Oxford.
- Leider, A., Hinrichs, K.-U., Mollenhauer, G., Versteegh, G.J.M., 2010. Core-top calibration of the lipid-based  $U_{37}^K$  and  $TEX_{86}$  temperature proxies on the southern Italian shelf (SW Adriatic Sea, Gulf of Taranto). *Earth Planetary Science Letter*, 300, 112-124.
- Mohtadi, M., Lückge, A., Steinke, S., Groeneveld, J., Hebbeln, D., Westphal, I., 2010. Late Pleistocene surface and thermocline conditions of the eastern tropical Indian Ocean. *Quaternary Science Reviews*, 29, 887-896.
- Müller, P.J., Kirst, G., Ruhland, G., Von Storch, I., Rosell-Melé, A., 1998. Calibration of the alkenone paleotemperature index  $U_{37}^K$  based on core-tops from the eastern South Atlantic and the global ocean (60°N-60°S). *Geochimica et Cosmochimica Acta* 62, 1757-1772.

## Acknowledgements

How times fly! Six years PhD journey should be completely ended in Germany. One of the joys of completion is to look over the journey past and remember all the friends and family who have helped and supported me along this long but fulfilling road.

First of all, the deepest thanks certainly go to my supervisor, Prof. Dr. Gesine Mollenhauer, whose expertise, understanding and patience. I never forget when we first met in Qingdao in 2009. I was attracted by a series of interesting lectures which she gave. I really thank her to give me the opportunity to enter the exciting organic geochemistry world, although I have no experience in this field. Thanks for her guidance by inspiring ideas and fruitful discussion. I particularly appreciate her for encouraging me when I was depressed even when I had gave up, for teaching patiently me a lot of things on the way.

I would like to thank my thesis committee Dr. Torsten Bickert, Prof. Dr. Gesine Mollenhauer, Dr. Mahyar Mohtadi, Dr. Jürgen Pätzold and Dr. Enno Schefuß (in alphabetical order). With their individual expertise, they greatly contributed to the completion of this thesis. Although they are busy scheduled, they always took their time to answer my questions, to discuss about scientific questions and to teach me how to write a real scientific manuscript. I especially thank to Dr. Mahyar Mohtadi to provide samples for my PhD work, to share ideas, suggestions and advices. Thanks to Dr. Tim Rixen for providing sediment trap samples, without which the project would have not been possible.

A great thank-you goes to Ralph Kreutz for teaching me the basic lab working procedures when I first started to work in the lab. I would like to thank to Andreas, Katja and Maria, who share the office with me, you have brought me great work times in Bremen. And very warm thanks to Maria Winterfeld for improving my thesis and helping me submitting my thesis when I am in China.

I am especially grateful for the lectures, seminars and travelling funds for the international conferences provided by the Glomar organized by Prof. Dr. Dierk Hebbeln.

The detailed administrative documentation and arrangements of funding applications in the Glomar are carried out by Dr. Christina Klose, Jutta Bülten and Carmen Murken. Many warm thanks to them.

I would like to thank to my friends, Hui Min, Li Mingming, Shao Xiwen, Shu Liping, Sun shuwen, Yang Yiran, Xiang Yixian, Zhang Chenjian, Zhu Rong and so on (in alphabetic order), you have brought great fun after work times. Special thanks go to Liang Chen. I will never forget the things that he helped us, e.g. searching an apartment, picking us up at the airport, carrying our heavy luggages, and inviting us to his place for dinner when we just arrived at Bremen.

And of course, I am indebted to my mother for her unconditional support and for encouraging me to pursue my passion for science, even if it would mean that she have to be thousands of miles away from me and get to see me three times in the past four years.

Many thanks to Shuwen Sun, who provided essential help for submitting my dissertation.

I am very thankful to my motherland - China and Ocean University of China for providing me this opportunity to study in Germany.

Last but not least, I cannot thank my husband, Junhui Xing enough. Fortunately, we have the same memories in Bremen. Thank for your support and invaluable help for my PhD work. Thank you to listen to my incessant complaints with endless patience. Thank you for sharing happiness and sadness in our life. Thank you for taking good care of me every day.

感谢祖国，感谢国家留学基金委（CSC），感谢母校中国海洋大学，给我提供了这个留学深造的机会以及四年的奖学金。感谢妈妈、公公、婆婆一直对我求学路的支持，没有你们的支持，不可能有今天的我。

最后，特别感谢我亲爱的老公邢军辉，感谢你对我的爱，感谢你陪我一路走过，一起生活，一起学习，一起欢笑，一起苦恼，希望五六十年后再回忆起这段德国生活的时候，依旧那样甜蜜。